Application of multi-criteria analysis for the introduction of green port management practices: an evaluation of energy efficient mobility in nautical ports

Ukić Boljat, Helena; Vilke, Siniša; Grubišić, Neven; Maglić, Livia

Source / Izvornik: **Scientific journals of the Maritime University of Szczecin, 2021, 65, 72 - 83**

Journal article, Published version
Rad u časopisu, Objavljena verzija rada (izdavačev PDF)

https://doi.org/10.17402/462

Permanent link / Trajna poveznica: https://urn.nsk.hr/urn:nbn:hr:187:802007

Rights / Prava: In copyright / Zaštićeno autorskim pravom.

Download date / Datum preuzimanja: **2024-08-31**

Sveučilište u Rijeci, Pomorski fakultet
University of Rijeka, Faculty of Maritime Studies

Repository / Repozitorij:

Repository of the University of Rijeka, Faculty of Maritime Studies - FMSRI Repository

UNIRI DIGITALNA KNJIŽNICA

dabar
DIGITALNI AKADEMSKI ARHIVI I REPOZITORIJI

ResearchGate

See discussions, stats, and author profiles for this publication at: https://www.researchgate.net/publication/350897248

Scientific Journals of the Maritime University of Szczecin Zeszyty Naukowe Akademii Morskiej w Szczecinie, ZN AM 65(137)

Book · March 2021

CITATIONS
0

READS
434

18 authors, including:

Izabela Dembińska
Maritime University of Szczecin
64 PUBLICATIONS **171** CITATIONS
SEE PROFILE

Pawel Michal Kacprzak
Maritime University of Szczecin
2 PUBLICATIONS **0** CITATIONS
SEE PROFILE

Valerii Kuznetsov
Admiral Makarov National University of Shipbuilding
5 PUBLICATIONS **4** CITATIONS
SEE PROFILE

Parviz Ghadimi
Amirkabir University of Technology
191 PUBLICATIONS **1,605** CITATIONS
SEE PROFILE

Some of the authors of this publication are also working on these related projects:

Trimaran hull optimization View project

Marine incydent analysis View project

All content following this page was uploaded by Izabela Dembińska on 16 April 2021.

The user has requested enhancement of the downloaded file.

Scientific Journals

of the Maritime University of Szczecin ● 65 (137) 2021

Zeszyty Naukowe Akademii Morskiej w Szczecinie

Quarterly

Szczecin, March 2021

Editor-in-Chief

Dr hab. Izabela Dembińska, Associate Professor, Maritime University of Szczecin, Poland

Editorial Secretary

Mgr inż. Katarzyna Biniek, Editor, Maritime University of Szczecin, Poland

Assistant Editors

Marine Technology and Innovation

Dr hab. inż. Cezary Behrendt, Associate Professor, Maritime University of Szczecin, Poland
Dr hab. inż. Sławomir Żółkiewski, Silesian University of Technology, Poland

Navigation and Maritime Transport

Dr hab. inż. Jarosław Artyszuk, Associate Professor, Maritime University of Szczecin, Poland
Dr hab. inż. Jakub Montewka, Aalto University and Finnish Geospatial Research Institute, Finland

Transportation Engineering

Dr hab. inż. Cezary Behrendt, Associate Professor, Maritime University of Szczecin, Poland
Prof. Srećko Krile, Dr. Sc., University of Dubrovnik, Croatia
Dr inż. Bogusz Wiśnicki, Maritime University of Szczecin, Poland

Scientific Board

Dr hab. Izabela Dembińska, Associate Professor, Maritime University of Szczecin, Poland – chairman
Dr hab. inż. Leszek Chybowski, Associate Professor, Maritime University of Szczecin, Poland
Dr hab. inż. Jarosław Artyszuk, Associate Professor, Maritime University of Szczecin, Poland
Dr hab. inż. Cezary Behrendt, Associate Professor, Maritime University of Szczecin, Poland
Prof. Andrzej Cwirzen, Docent, D.Sc., Luleå University of Technology, Sweden
Prof. Sören Ehlers, DSc., NTNU Trondheim, Norway & Hamburg University of Technology, Germany
Prof. Niksa Fafandjel, Dr.Sc., University of Rijeka, Croatia
Prof. dr. ir. Pieter van Gelder, Delft University of Technology, The Nederlands
Prof. Hassan Ghassemi, Ph.D., Amirkabir University of Technology, Iran
Prof. Kazuhiko Hasegawa, Ph.D., Osaka University, Japan
Doc. Ing. František Helebrant, CSc., VŠB – Technical University of Ostrava, The Czech Republic
Dr inż. Robert Jasionowski, Maritime University of Szczecin, Poland
Prof. Srećko Krile, Dr. Sc., University of Dubrovnik, Croatia
Prof. Pentti Kujala, D.Sc., Aalto University, Finland
Dr hab. inż. Andrzej Miszczak, Associate Professor, Gdynia Maritime University, Poland
Prof. Piotr Moncarz, Ph.D., Stanford University, USA
Dr hab. inż. Jakub Montewka, Aalto University and Finnish Geospatial Research Institute, Finland
Prof. Dr. Junmin Mou, Wuhan University of Technology, China
Prof. dr. Tea Munjishvili, Ivane Javakhishvili Tbilisi State University, Georgia
Habil. Dr., Prof. Vytautas Paulauskas, Klaipeda University, Lithuania
Prof. dr inż. Andrzej M. Pawlak, prezes Vortex, LLC., USA
Dr hab. inż. Zbigniew Piotrowski, Associate Professor, Military University of Technology, Poland
Dr.-Ing. habil. Dirk Proske, University of Natural Resources and Applied Life Sciences, Austria
Prof. Jin Wang, Ph.D., Liverpool John Moores University, UK
Prof. Dr.-Ing. Holger Watter, Flensburg University of Applied Sciences, Germany
Dr inż. Bogusz Wiśnicki, Maritime University of Szczecin, Poland
Prof. Tsz Leung Yip, Ph.D., MBA, The Hong Kong Polytechnic University, Hong Kong
Dr hab. inż. Sławomir Żółkiewski, Silesian University of Technology, Poland

Statistical Editors

Dr hab. Lech Kasyk, Associate Professor, Maritime University of Szczecin, Poland
Prof. dr hab. Zenon Zwierzewicz, Maritime University of Szczecin, Poland

Editorial Staff

Publishing House Manager – mgr Barbara Tatko
Translation and Proofreading – dr hab. Mark J. Hunt
Editor – mgr inż. Katarzyna Biniek
Computer Typesetting – mgr inż. Irena Hajdasz
Layout Design – tech. Tomasz Kwiatkowski

© Copyright by Maritime University of Szczecin, Szczecin 2021

Scientific Journals of the Maritime University of Szczecin
Zeszyty Naukowe Akademii Morskiej w Szczecinie
ISSN 1733-8670 (Printed)
ISSN 2392-0378 (Online)

The Scientific Journals of the Maritime University of Szczecin printed version is primary
Wersja drukowana Zeszytów Naukowych Akademii Morskiej w Szczecinie jest wersją pierwotną wydawanego czasopisma

Editorial office: ul. T. Starzyńskiego 8, 70-506 Szczecin, Poland
tel. +48 91 480 96 45, +48 91 480 96 16, e-mail: journals@am.szczecin.pl, http://scientific-journals.eu/

First Edition. 150 copies. 5.375 publishing sheets (ark. wyd.)

Printed by Volumina.pl Daniel Krzanowski, ul. Ks. Witolda 7–9, 71-063 Szczecin, Poland

CONTENTS

Scientific Journals
of the Maritime University of Szczecin

Zeszyty Naukowe
Akademii Morskiej w Szczecinie

2021, 65 (137), 5–6
ISSN 1733-8670 (Printed)
ISSN 2392-0378 (Online)
DOI: 10.17402/455

Editorial preface

Izabela Dembińska

Maritime University of Szczecin
11 Henryka Pobożnego St., 71-899 Szczecin, Poland
e-mail: i.dembinska@am.szczecin.pl
https://orcid.org/0000-0001-7618-0018

Dear Readers,

We are pleased to present this year's first issue (No. 65) of the Scientific Journals of the Maritime University of Szczecin. This year will bring many new challenges, also for the journal, where we continually focus on improved quality. We would like to thank the authors, reviewers and readers for their contribution to our journal. I hope that we will continue to develop this path together.

This issue presents the research results and authors' views in seven articles organized into three thematic sections: Civil Engineering and Transport, Mechanical Engineering, and Economics, Management and Quality Science.

The Civil Engineering and Transport section features two articles. The first article presents an analysis of internal forces and roll motion during a nodule loading simulation for a ship at sea. The study carried out a full assessment of a ship's behaviour during loading, which took into account wave height and period around the Clarion–Clipperton Zone by the use of an operational efficiency index. The second article addresses the International Convention for the Safety of Life at Sea (SOLAS). The Convention aims to improve the safety of life at sea by laying down rules and regulations for the construction of ships and providing models for the documents created.

The Mechanical Engineering section consists of three articles. In the first article, the authors analysed the special configuration of a multi-role moving-column machining centre by the finite element method. In the second article, a CFD-based numerical approach was developed and applied to a trimaran hull in the presence of regular and irregular waves. According to the authors, the proposed CFD method reduces the simulation time and calculation resources needed to determine a ship's motion. The third article presents the results of the testing of long-distance heat transfer surfaces in marine diesel engines, including elliptical and flat-oval tubes. The study used mathematical models that involved equations from conservation of energy, equations of motion, continuity and state, where the RSM of turbulence was also used to complete the equation system.

The Economics, Management and Quality Science section includes two articles. The first article analyses the factors affecting the performance of VTS operators. Its general conclusion is that the effective work of VTS operators, combined with a specific maritime environment and vessel traffic management support system, are the key determinants for ensuring the reliability and safety of the entire system. The second article's authors wanted to see if a multi-criteria analysis was appropriate for the evaluation and implementation of energy-efficient mobility in seaports. The multi-criteria model for the selection of the most appropriate energy-efficient mobility solution was tested for two Croatian private marinas.

The articles featured in this issue reflect the authors' theoretical and practical inspirations, contributing to important and state-of-the-art scientific research. We believe that these findings will become the basis for further reflection, discussion, and broader research.

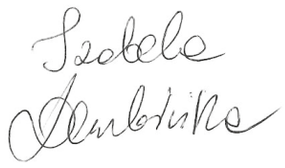

dr hab. Izabela Dembińska, Associate Professor
Editor-In-Chief
Szczecin, 31.03.2021

Civil Engineering and Transport

Scientific Journals
of the Maritime University of Szczecin

Zeszyty Naukowe
Akademii Morskiej w Szczecinie

2021, 65 (137), 9–20
ISSN 1733-8670 (Printed)
ISSN 2392-0378 (Online)
DOI: 10.17402/456

Received: 07.07.2020
Accepted: 24.03.2021
Published: 31.03.2021

An analysis of shear forces, bending moments and roll motion during a nodule loading simulation for a ship at sea in the Clarion–Clipperton Zone

Paweł Kacprzak

https://orcid.org/0000-0002-0917-3827

Maritime University of Szczecin, Faculty of Navigation
1-2 Wały Chrobrego St., 70-500 Szczecin, Poland
e-mail: p.m.kacprzak@gmail.com

Keywords: nodule loading, ship, shear force, bending moment, wave, roll

JEL Classification: C6, C69, L9, L99, L7, L79

Abstract

This article presents an analysis of internal forces and roll motion during a nodule loading simulation for a ship at sea. The study carried out a full assessment of ship behavior during loading, which took into account wave height and period occurrence around the Clarion–Clipperton Zone by the use of an operational efficiency index. One of the aims was to verify whether waves have an influence on excessive ship motion and internal forces during nodule loading. Two alternative loading sequences were developed and compared by taking loading time, shear forces, bending moments, roll motion and waving into account. The research shows that loading is only possible during specific sea weather conditions for the selected bulk carrier.

Introduction

Deep-sea polymetallic nodules found deep on the seabed are conglomerates consisting of various elements, such as manganese, iron, nickel, cobalt and copper, as well as rare earth elements. For this reason, polymetallic nodules are a promising source of metallic raw materials. These nodules are located on the ocean seabed at a depth of 4000–6000 m. Various mining systems have been designed to collect these polymetallic nodules. These systems should perform the following functions (Abramowski & Szelangiewicz, 2011):

- collect nodules from the seabed,
- mine them from the ocean's surface (per mining unit),
- perform preliminary cleaning,
- periodically store the nodules in the mining unit hold,
- load nodules into bulk carrier holds on the ocean surface.

The implementation of these tasks requires the resolution of a number of technical problems relating to the impact of the marine environment on the mining system. One of these problems involves the loading of nodules onto a ship at open sea. Polymetallic nodules are characterized by their high density, from 2 to 3 t/m^3. Thus, while loading the ship with such a substantial cargo, large vertical shear forces and bending moments can occur.

There are no current publications in scientific literature describing the loading of polymetallic nodules onto a vessel at sea. Current publications have only focused on the problems of ship design and the environmental impact on the underwater section of the mining system. Bortnowska (Bortnowska, 2008) presented a design study on the preliminary concept of ship dimensions and ship spatial arrangement

for the collection of polymetallic nodules from the sea bed. In this study an appropriate mathematical model was applied to ship winning system optimization. Sharma (Sharma, 2011) selected a number of technical, technological and environmental issues that only influence the design and operation of the underwater section of the mining system. This work did not discuss the problems of loading the nodules onto a ship on the surface of the sea. Abramowski and Cepowski (Abramowski & Cepowski, 2013) presented some initial considerations which could be used in the development of the design of a polymetallic nodule mining ship. A concept for the discharge of the nodules to a shuttle transport ship via self-unloading was proposed in their article. Nishi (Nishi, 2012) theoretically examined the two-dimensional static mechanics of axially moving cables to be used in a mining nodule system.

Standard bulk carriers loaded with heavy cargo are designed under the assumption that the loading takes place in the port. Where, typical loading/unloading sequences are developed to ensure safe loading at the port. However, guidelines have yet to be created to develop a heavy cargo loading sequence at sea.

Polymetallic nodules can be transported in small or large bulk carriers. In the case of small bulk carriers, the following considerations are required for the loading and transportation of nodules:

- shorter loading time and good longitudinal strength are key advantages;
- lower transport capacity, greater ship motion and poorer stability are the main associated disadvantages.

In contrast, when a large bulk carrier is used:

- high transport capacity, small ship motion and good stability are the main advantages;
- longer loading time and lower longitudinal strength are clear disadvantages.

The selection of the optimal size of a bulk carrier should be carried out with the use of a transport study, which has to take into account the loading of the nodules at sea, among other concerns.

The nodule cargo can be loaded into one or several holds simultaneously. With the increase in the number of concurrent loaded holds, the loading time will decrease, but more internal forces may arise.

Any nodule mining system design should assume that the trans-shipment of the nodules to the transport units would take place at sea, often under adverse weather conditions. Where, ship motion and secondary phenomena, such as vertical shear force and bending moments, are caused by the high waves present under these conditions.

Considering the aforementioned aspects, the aim of this research was to compare nodule loading sequences onto a ship, which takes vertical shear forces, bending moments, ship motion and sea waves into account. An additional goal was to check whether waves could have an influence on the occurrence of excessive ship motion and vertical shear forces and bending moments, and whether it would disrupt nodule loading operation at sea. Therefore, to achieve this aim, the following objectives were defined: 1) determine the maximum wave height at which the loading operation can be carried out, and 2) estimate peak wave period at which a nodule loading operation should be stopped.

Research method

Ship motion and cross-sectional forces on the seaway may be calculated using the following numerical methods:

- linear strip theory method based on two-dimensional potential flow theory, where the solution is simulated only in the domain of wave frequency;
- a non-linear method based on three-dimensional potential flow theory, where the solution is most often simulated in the time domain.

An advantage of using the non-linear method is a better phenomenon model is produced, whereas the disadvantage of a more complicated numerical model is its complex nature, as well as difficulties with verification. The use of the non-linear method to calculate internal forces is necessary in some cases. Where this method of calculating internal forces is primarily required for ships with a low block coefficient value, i.e., for container ships. Jensen and Pedersen (Jensen and Pedersen, 1981) noted that there are large nonlinearities of vertical shear forces and bending moments in the case of container ships. Soares et al. (Soares, Fonseca & Pascoal, 2004) noted that for ships with a small block coefficient (i.e., container ship), the wave induced structural loads are highly non-linear. McTaggart et al. (McTaggart et al., 1997) showed that the use of a linear model for the calculation of internal forces for a frigate with a low block coefficient value can lead to an overestimation of extreme wave bending moments of around 10%.

However, for vessels with a high block coefficient value, such as bulk carriers and tankers, the use of a linear model is sufficiently accurate and effective. Jensen and Pedersen (Jensen & Pedersen,

1981) noted that the effects of wave non-linearities induced a bending moment and shear force in the case of a VLCC carrier sailing were small in a moderate sea.

Therefore, the linear strip theory method is often used to determine internal forces in ship design. For example, Parunov and Senjanović (Parunov & Senjanović, 2004) applied linear strip theory to calculate the vertical wave bending moments in an unconventional oil product tanker design.

In this study, a linear strip method was used both to calculate internal forces and ship motion. According to this theory, a ship on waves may be considered a linear dynamic system with coefficients dependent on frequency and linear applied forces. All coefficients and forces were calculated by the use of the method presented in (Karppinen, 1987; McTaggart et al., 1997; Phelps, 1997; Kukkanen, 2012). The hydrodynamic coefficients were calculated by the use of two-dimensional hydrodynamic potential coefficients. The Frank pulsating source (Frank, 1967) method was used to calculate these two-dimensional coefficients. The Ikeda et al. (Ikeda, Himeno & Tanaka, 1978) empirical method was used for the estimation of additional roll damping parts. Wave loads were calculated by the use of the diffraction method detail presented in (Jensen & Pedersen, 1981).

In linear strip theory, the harmonic vertical shear force SF(x_1) and bending moment BM(x_1) in a wave's cross section, x_1, may be obtained from the longitudinal and vertical load q_1 and q_3 by the following integrals (Jensen & Pedersen, 1981):

$$\mathrm{SF}(x_1) = -\int_{x_0}^{x_1} q_3(x_b)\cdot dx_b \tag{1}$$

$$\mathrm{BM}(x_1) = +\int_{x_0}^{x_1} q_1(x_b)\cdot \overline{bG}(x_b)\cdot dx_b + \int_{x_0}^{x_1} q_3(x_b)\cdot x_b \cdot dx_b - x_1\int_{x_0}^{x_1} q_3(x_b)\cdot dx_b \tag{2}$$

where:

x_b – ship section,

$\overline{bG}$ – the vertical distance of the ship's gravitational center G above the centroid b of the local submerged sectional area,

q_1, q_3 – the harmonic longitudinal and vertical dynamic loads per unit length on the unfastened disk calculated by the use of Newton's second law of dynamics, and surge and heave motions as follows (Jensen & Pedersen, 1981):

$$q_1(x_b) = +X'_{h_1}(x_b) + X'_{\omega_1}(x_b) - m'(x_b)\cdot\left(\ddot{x} - \overline{bG}\cdot\ddot{\theta}\right) \tag{3}$$

$$q_3(x_b) = +X'_{h_3}(x_b) + X'_{\omega_3}(x_b) - m'(x_b)\cdot\left(\ddot{z} - x_{b\cdot}\cdot\ddot{\theta}\right) \tag{4}$$

where:

$\ddot{x}$ – surge,

$\ddot{z}$ – heave,

θ – pitch,

$X'_{h_1}(x_b)$ – the sectional hydromechanical load for surge,

$X'_{h_3}(x_b)$ – the sectional hydromechanical load for heave,

$X'_{\omega_1}(x_b)$, $X'_{\omega_3}(x_b)$ – the sectional wave loads for surge and heave.

The solution for the strip method is a combination of ship motion, vertical shear forces and bending moment transfer functions. Statistical ship motion and internal forces can then be calculated on the basis of these transfer functions and the energy spectrum of the wave.

The energy spectrum of a sailing ship in motion on irregular waves is calculated by multiplying the squared motion transfer functions with the wave energy spectrum. A common ITTC spectrum based on Bretschneider wave energy spectrum was used here.

In ship theory, a short- or long-term wave model should be taken into account. In the case of design issues related to wave loads encountered throughout the intended life of the ship, the long-term loading is usually selected. In this case 20-, 50- or 100-year wave parameters should be considered.

In contrast, short-term loading usually relates to loads encountered throughout ship operation for a period of time lasting from around half an hour to 10 hours. This depends on the time period when the wave parameters remain constant on a given sea area. In this study, a short-term wave model was applied due to a short loading operation period.

Statistical parameters, such as significant height or characteristic wave period are time independent in a short-term wave model. In these studies, these parameters were calculated through the use of the Rayleigh distribution.

In the first part of the research, the effect of wave parameters on internal forces was investigated. To this purpose, the following work plan was used:

1. Development of still water loading sequences into one and two holds simultaneously without taking into account the effects of waves;

2. Selection of loading phase and cross-section in which the maximum vertical shear force and bending moment occur;
3. Analysis of the relationship between the vertical shear force and bending moment at this stage and the following wave parameters:
   a) Characteristic period for a constant wave height and variable wave directions;
   b) Wave direction for a constant wave height and peak wave period.

In all loading phases, ship motion was also investigated.

In the second part of the study, an assessment of ship behavior on the Clarion–Clipperton Zone, was carried out. The operational effectiveness index presented in (Karppinen, 1987; Szelangiewicz, 2000; Cepowski, 2007), was applied to assess internal forces and ship motion in all loading phases. This index enables the assessment of the quantitative sea-keeping performance of a given ship operation. The operational effectiveness index, E_T, usually expresses the probability (P) that a ship's response for given wave conditions (i.e., significant wave height H_S and characteristic period T) will not exceed the limit level. This E_T index may be calculated as follows:

$$E_T = \sum_{H_S,T} P(\Gamma = 1) \tag{5}$$

where:
E_T – operational effectiveness index,
H_S – significant height of wave,
T – characteristic period of the wave,
P – probability that ship motion does not exceed limited level,
Γ – bivalent function that has only two values in given wave conditions:
"0" when ship motion exceeds the acceptable level or
"1" when ship motion does not exceed the acceptable level.

Index E_T is the sum of the occurrence probability of such wave conditions in which the ship motion will not exceed the acceptable level. Hence, index E_T takes values between the interval of 0 to 1. The higher the index value, the better predicted sea-keeping performance. Figure 1 shows a general scheme for the calculation of the operational effectiveness index, E_T.

In this study, the loading sequences were compared by using index E_T. Thus, taking into account the limited values of vertical shear force, bending moment and roll motion.

The permissible values of internal forces for sea-going conditions, determined on the basis of classification requirements, were assumed as an acceptable limit for the vertical shear force and bending moment. However, the problem is that these permissible values have been developed by classification societies for sea conditions and do not take the loading of the nodules at sea into account. But these permissible values were assumed as there are no other standards.

Another difficulty is that strip theory does not differentiate between hogging and sagging bending moments. Therefore, a smallest absolute bending moment value has been assumed as the limit value regardless of whether the hull is sagged or hogged.

The operative-limiting criteria for ship operations were presented in (Karppinen, 1987). Table 1 shows criteria for acceleration and roll depending on work performed on the ship.

Table 1. Criteria for accelerations and roll (Karppinen, 1987)

Description	RMS Vertical Acceleration	RMS Lateral Acceleration	RMS Roll Motion
Light Manual Work	0.20 g	0.10 g	6.0°
Heavy Manual Work	0.15 g	0.07 g	4.0°
Intellectual Work	0.10 g	0.05 g	3.0°
Transit Passenger	0.05 g	0.04 g	2.5°
Cruise Liner	0.02 g	0.03 g	2.0°

In this study, the criterion for roll, as presented in Table 1, which refers to heavy manual work, was

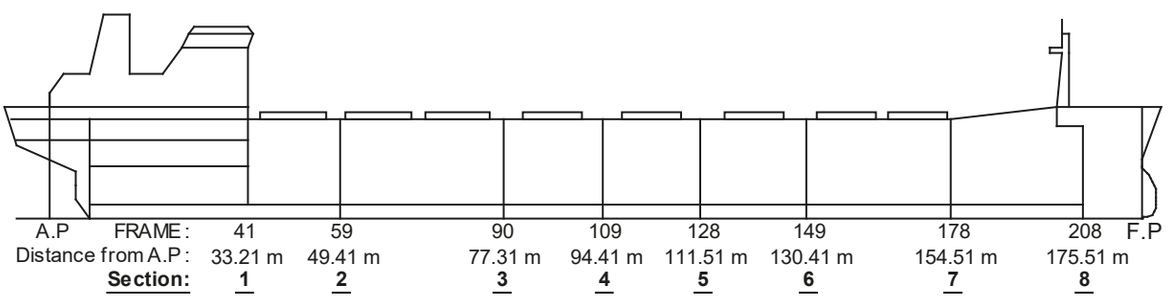

Figure 1. Sections used for the internal force analysis

Table 2. Acceptable values of vertical shear force (SF), bending moment (BM) and roll motion

	Section							
	1	2	3	4	5	6	7	8
SF (kN)	28 822	32 530	36 434	38 337	38 210	31 784	43 929	55 004
BM	934 795 kNm							
Roll	4° (RMS)							

selected as the acceptable limit value for the investigated ship motion.

The study was performed for a bulk carrier design with the following characteristics:

- length between perpendiculars: LBP = 185 m,
- breadth: B = 24.4 m,
- design draught: T_D = 11 m,
- deadweight: DWT = 32 000 t.

Table 2 shows the acceptable values of vertical shear force, bending moment and roll motion used in this study.

Vertical shear force, bending moment and roll values were determined through the use of SEAWAY software. SEAWAY is a frequency-domain ship motion computer program, based on linear strip theory, to calculate wave-induced loads, motion, added resistance and internal loads for the six degrees of freedom for the displacement of ships sailing over regular and irregular waves (Journee, 2001).

Vertical shear force and bending moment values in still water were calculated through the use of the author's software.

Loading simulation in still water

Initially, checks were made to ascertain whether loading sequences available in the loading manual could be used for loading polymetallic nodules at sea. It has been assumed that the loading sequence would be characterized by:

- the lowest number of loading stages to minimize loading time and to avoid the negative influence of the sea environment on the ship during loading operations;
- the lowest internal forces in sections No. 1–8 (according to Figure 1).

The internal forces of the ship were compared with the acceptable values of internal forces for a seagoing ship. It was noted that the shear forces which exceeded the limit values in the 3rd stage were the cross-sections 3 and 6 (Figure 2). Simulation and any further analysis were suspended in this case.

This means that the sequence from the loading instruction cannot be used to load a ship at sea. The reason for this non-compliance is that the all

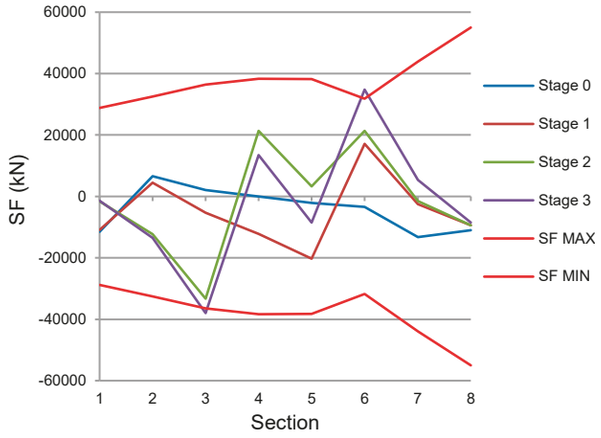

Figure 2. Shear forces during loading in accordance with the loading manual

sequences were developed in relation to still water conditions at port.

Therefore, it was decided to develop new loading sequences, in which internal forces would not exceed seagoing condition limit values.

The following two loading methods were assumed:

- Method A – where each cargo hold is loaded separately;
- Method B – where two cargo holds are loaded simultaneously.

Table 3. Loading sequence in which each cargo hold is loaded separately (Method A), where GM – metacentric height, *D* – mass of displacement

Stage	Hold No. / Cargo loaded (t)							GM (m)	*D* (t)
	7	6	5	4	3	2	1		
0								3.27	22 369
1					+5000			3.53	22 713
2			+5000					3.55	26 275
3							+4000	3.34	27 208
4	+3000							3.32	28 168
5					+3500			3.24	31 668
6	+2500							3.08	34 168
7			+3650					2.76	37 818
8							+2950	2.65	40 768
9	+1150							2.62	41 818
Total	**6550**		**8650**		**8500**		**6950**		**41 818**

Additional factors to be taken into consideration were:

- Prior to loading, the ship is in heavy ballast condition;
- During loading all de-ballasting operations were carried out in the currently loaded compartment.

In Tables 3 and 4, the developed loading sequences are shown. Figures 3 and 4 show the internal forces during the loading process under the developed loading sequences.

Table 4. Loading sequence in which two cargo holds are loaded simultaneously (Method B)

Stage	Hold No. / Cargo loaded (t)							GM (m)	*D* (t)
	7	6	5	4	3	2	1		
0								3.27	22 369
1			+5000		+5000			3.67	26 071
2	+5500					+4000		3.15	34 607
3			+3650		+3500			2.78	38 721
4	+1150					+2950		2.61	41 818
Total	**6550**		**8650**		**8500**	**6950**			**41 818**

The influence of waves on the internal forces of the ship at key loading stages

In this part, sectional forces considering the influence of waves were analyzed. To restrict the scope of analysis, only stages with maximum internal forces in conditions of still water were taken into account, which were:

- During the loading of a ship using method A:
  - Stage 7 section 3 due to shear forces,
  - Stage 0 section 4 due to bending moments,
- During the loading of a ship using method B:
  - Stage 4 section 7 due to shear forces,
  - Stage 2 section 5 due to bending moments.

The purpose of these studies was to analyze the impact of waves on internal forces, taking into account:

- characteristic wave period T – assuming constant wave height of 1 m and varying wave direction,
- wave direction β – assuming constant wave height 1 m and adverse peak wave period.

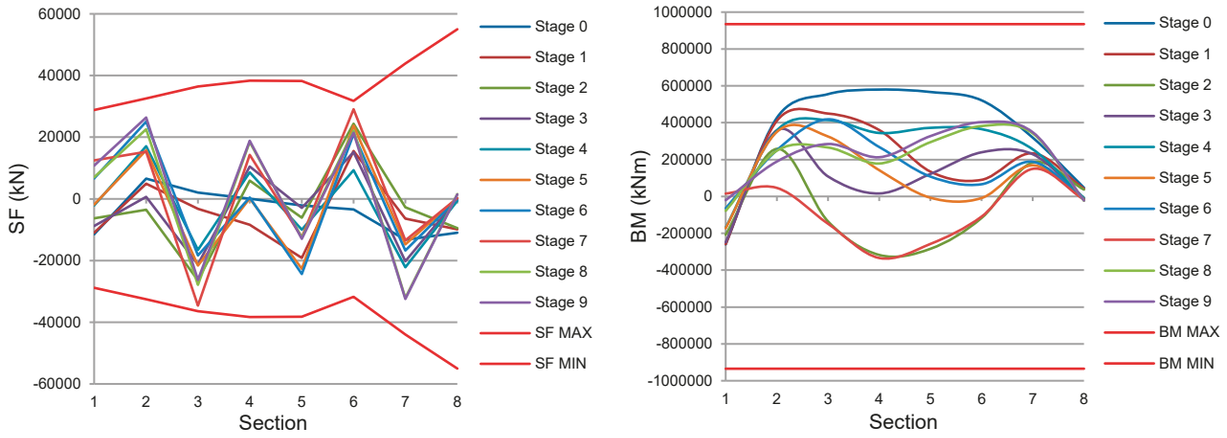

Figure 3. Internal forces when loading by the use of method A

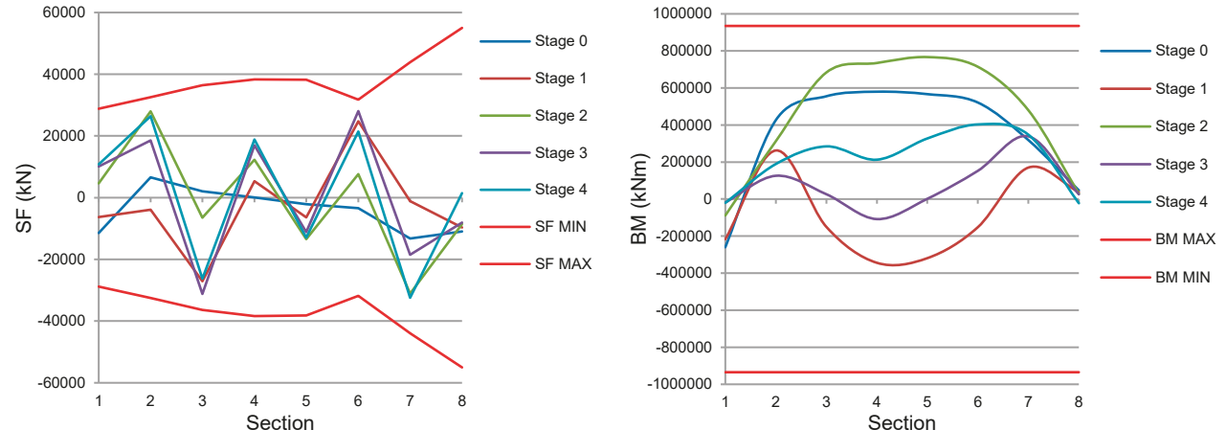

Figure 4. Internal forces when loading by the use of method B

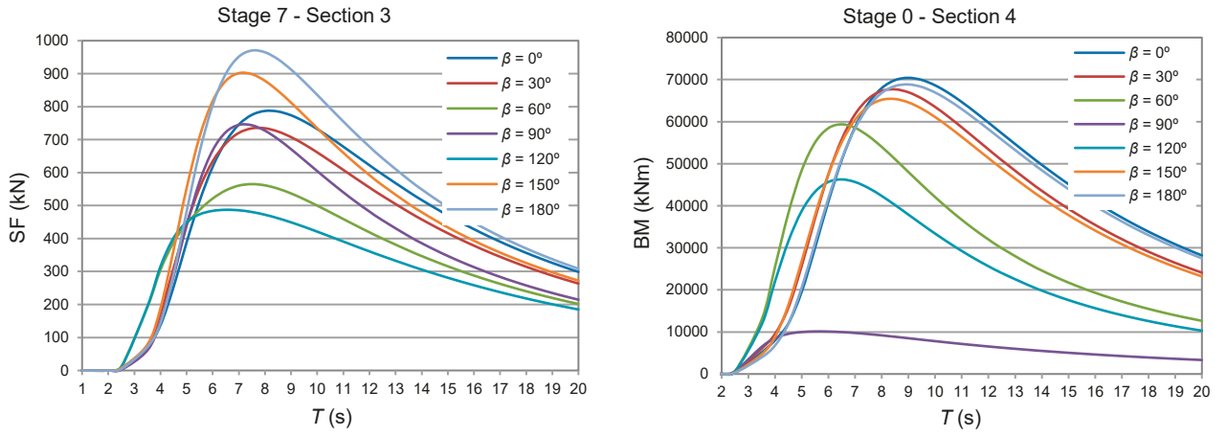

Figure 5. The influence of characteristic wave period *T* on shear forces and bending moments, Significant wave height H_S = 1 m, different waves angles *β* = var, via loading method A

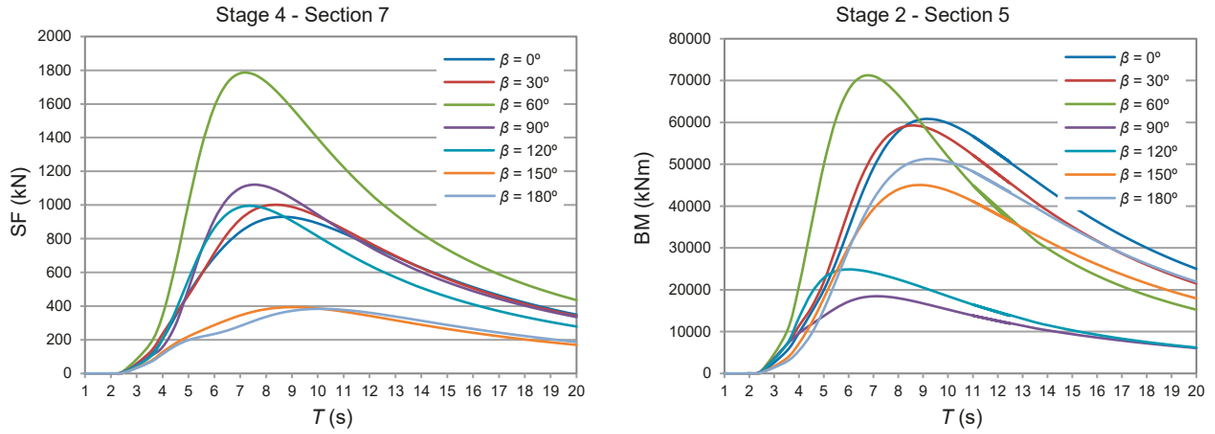

Figure 6. The influence of characteristic wave period *T* on shear forces and bending moments, significant wave height H_S = 1 m, different wave angles *β* = var, via loading method B

Internal forces, which were calculated by an adopted calculation method, are linear to wave height. Therefore, the influence of wave height on internal forces was not investigated in this study.

Figures 5 and 6 show the influence of characteristic wave period on shear forces and bending moments, assuming a constant significant wave height (H_S = 1 m) and variable wave direction by using "A" and "B" loading methods. Wave directions are defined by any value between 0° and 180° in this study, where following waves are at 0° and head waves are at 180°.

Ship motion during loading operations

Figure 7 shows RAO roll functions on a regular side wave at key loading stages by the use of loading methods "A" and "B". Figure 8 shows the significant amplitudes of roll on an irregular side wave at the loading stages.

An assessment of ship behavior on the Clarion–Clipperton Zone through the use of an operational effectiveness index

In the previous sections, the influence of selected wave parameters on internal forces and motion was taken into account. In this part, vessel behavior was comprehensively analyzed, taking into account the probability of wave height and period occurrence around the Clarion–Clipperton Zone throughout the year based on 1,000,000 waves. On the basis of this distribution, the probability of wave height and period occurrence was calculated, the results are presented in Table 5. In this study, extreme waves greater than 8 m have been omitted, due to the probability of their occurrence is close to zero.

First, the values of the internal forces and roll motion were calculated for every wave parameter from Table 5. These result values were then compared to the limit values in accordance with Table 2.

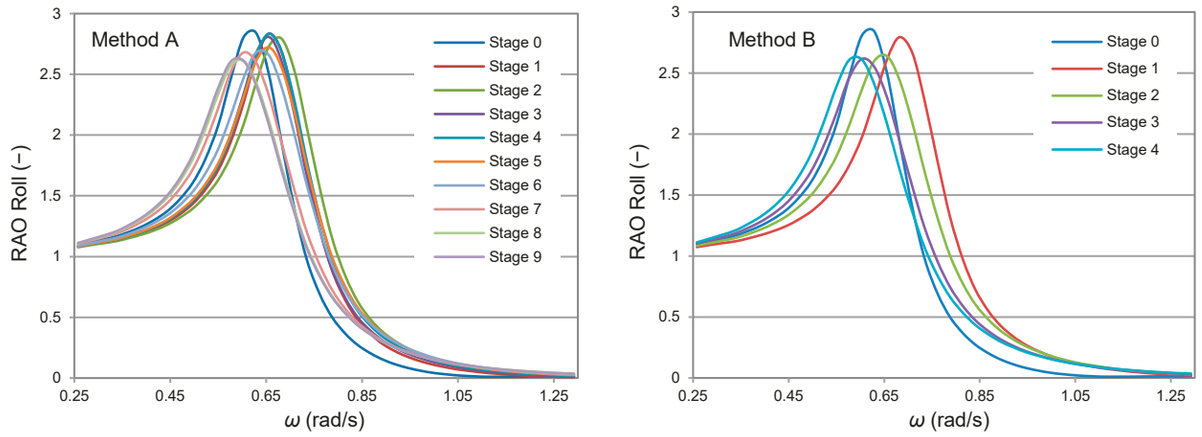

Figure 7. RAO Roll functions of a ship on a regular wave at key loading stages by the use of "A" and "B" loading methods, wave direction $\beta = 90°$

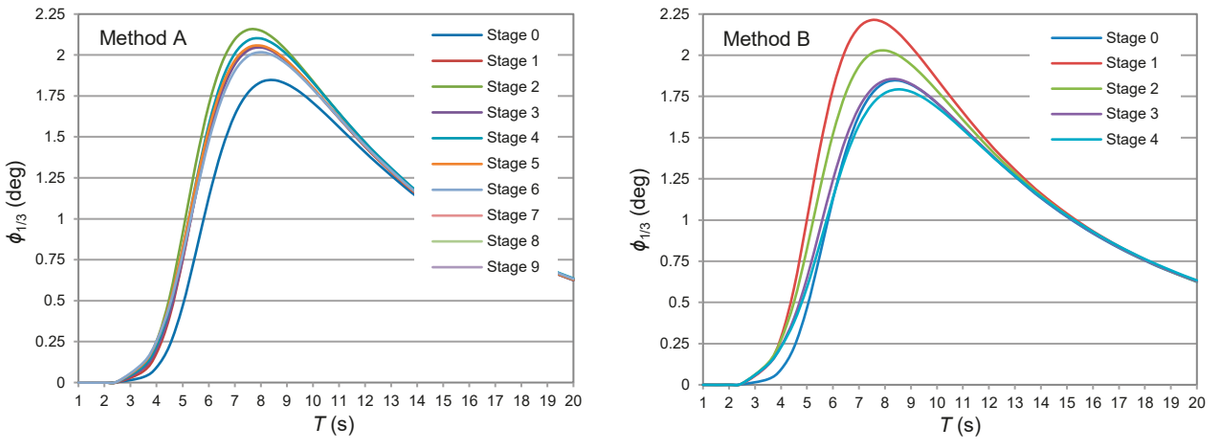

Figure 8. The significant amplitudes of roll motion on an irregular side wave at key loading stages through the use of "A" and "B" loading methods, wave direction $\beta = 90°$, significant wave height $H_S = 1$ m

Finally, an assessment was made as to whether the ship's behavior is safe on the waves with parameters from Table 5.

Tables 6–11 show the results of this comparison. In these tables, wave ranges for which the internal forces or roll motion exceed the limit values are marked in red. These are dangerous wave ranges, for which the function Γ according to the formula (5) reaches the value "0". In contrast, safe wave parameters are marked in green. For these wave parameters, function Γ has the value "1".

Table 5. The probability of significant wave height and characteristic wave period occurrence throughout the year around the Clarion–Clipperton Zone calculated on the basis of Nimmo (Nimmo, 2012), where H_S – significant height of wave, T – characteristic period of a wave

H_S (m)	T (s)										
	< 4	4 to 5	5 to 6	6 to 7	7 to 8	8 to 9	9 to 10	10 to 11	11 to 12	12 to 13	> 13
7 to 8				6E-06	3.5E-05	9.4E-05	0.00014	0.00014	9.7E-05	5.4E-05	2.5E-05
6 to 7			3E-06	4.4E-05	0.00022	0.0005	0.00066	0.00057	0.00036	0.00018	7.6E-05
5 to 6			2.9E-05	0.00034	0.00141	0.00272	0.00306	0.00231	0.00129	0.00058	0.00022
4 to 5		6E-06	0.00027	0.00248	0.00813	0.01286	0.01205	0.00769	0.00369	0.00143	0.00047
3 to 4		7.7E-05	0.00225	0.01501	0.03702	0.04545	0.0339	0.01761	0.00701	0.00229	0.00065
2 to 3	5E-06	0.00081	0.01432	0.06225	0.10541	0.09277	0.0514	0.02043	0.00639	0.00168	0.00039
1 to 2	8.9E-05	0.0057	0.04737	0.11003	0.10918	0.06052	0.02235	0.0062	0.0014	0.00027	4.8E-05
0 to 1	0.00048	0.00637	0.0191	0.01849	0.00817	0.00213	0.00039	5.7E-05	7E-06	1E-06	

Table 6. The range of safe and dangerous wave conditions for shear forces, $\beta = 180°$, stage 7, Section 3, Method A, where those figures marked green mean safe wave conditions and red means dangerous wave conditions

H_S (m)	T (s)										
	< 4	4 to 5	5 to 6	6 to 7	7 to 8	8 to 9	9 to 10	10 to 11	11 to 12	12 to 13	> 13
7 to 8				6E-06	3.5E-05	9.41E-05	0.00014	0.000137	9.71E-05	5.4E-05	2.5E-05
6 to 7			3E-06	4.4E-05	0.00022	0.000503	0.00066	0.000571	0.000363	0.000182	7.61E-05
5 to 6			2.9E-05	0.000342	0.001406	0.002723	0.003063	0.002309	0.001291	0.000576	0.000216
4 to 5		6E-06	0.00027	0.002484	0.008133	0.012862	0.012046	0.00769	0.003693	0.001433	0.000473
3 to 4		7.71E-05	0.00225	0.015006	0.037017	0.045451	0.033903	0.017607	0.007008	0.002291	0.000647
2 to 3	5E-06	0.000812	0.014324	0.062251	0.105412	0.092766	0.051397	0.020427	0.006386	0.001676	0.000387
1 to 2	8.91E-05	0.005701	0.047369	0.110025	0.109182	0.060523	0.022345	0.006195	0.0014	0.000273	4.8E-05
0 to 1	0.000475	0.00637	0.019102	0.018486	0.008173	0.002133	0.000391	5.7E-05	7.01E-06	1E-06	

Table 7. The range of safe and dangerous wave conditions for bending moments, $\beta = 180°$, stage 0, Section 4, Method A

H_S (m)	T (s)										
	< 4	4 to 5	5 to 6	6 to 7	7 to 8	8 to 9	9 to 10	10 to 11	11 to 12	12 to 13	> 13
7 to 8				6E-06	3.5E-05	9.41E-05	0.00014	0.000137	9.71E-05	5.4E-05	2.5E-05
6 to 7			3E-06	4.4E-05	0.00022	0.000503	0.00066	0.000571	0.000363	0.000182	7.61E-05
5 to 6			2.9E-05	0.000342	0.001406	0.002723	0.003063	0.002309	0.001291	0.000576	0.000216
4 to 5		6E-06	0.00027	0.002484	0.008133	0.012862	0.012046	0.00769	0.003693	0.001433	0.000473
3 to 4		7.71E-05	0.00225	0.015006	0.037017	0.045451	0.033903	0.017607	0.007008	0.002291	0.000647
2 to 3	5E-06	0.000812	0.014324	0.062251	0.105412	0.092766	0.051397	0.020427	0.006386	0.001676	0.000387
1 to 2	8.91E-05	0.005701	0.047369	0.110025	0.109182	0.060523	0.022345	0.006195	0.0014	0.000273	4.8E-05
0 to 1	0.000475	0.00637	0.019102	0.018486	0.008173	0.002133	0.000391	5.7E-05	7.01E-06	1E-06	

Table 8. The range of safe and dangerous wave conditions for roll, $\beta = 90°$, stage 0, Method A

H_S (m)	T (s)										
	< 4	4 to 5	5 to 6	6 to 7	7 to 8	8 to 9	9 to 10	10 to 11	11 to 12	12 to 13	> 13
7 to 8				6E-06	3.5E-05	9.4E-05	0.00014	0.00014	9.7E-05	5.4E-05	2.5E-05
6 to 7			3E-06	4.4E-05	0.00022	0.0005	0.00066	0.00057	0.00036	0.00018	7.6E-05
5 to 6			2.9E-05	0.00034	0.00141	0.00272	0.00306	0.00231	0.00129	0.00058	0.00022
4 to 5		6E-06	0.00027	0.00248	0.00813	0.01286	0.01205	0.00769	0.00369	0.00143	0.00047
3 to 4		7.7E-05	0.00225	0.01501	0.03702	0.04545	0.0339	0.01761	0.00701	0.00229	0.00065
2 to 3	5E-06	0.00081	0.01432	0.06225	0.10541	0.09277	0.0514	0.02043	0.00639	0.00168	0.00039
1 to 2	8.9E-05	0.0057	0.04737	0.11003	0.10918	0.06052	0.02235	0.0062	0.0014	0.00027	4.8E-05
0 to 1	0.00048	0.00637	0.0191	0.01849	0.00817	0.00213	0.00039	5.7E-05	7E-06	1E-06	

Table 9. The range of safe and dangerous wave conditions for shear forces, $\beta = 60°$, stage 4, Section 7, Method B

H_S (m)	T (s)										
	< 4	4 to 5	5 to 6	6 to 7	7 to 8	8 to 9	9 to 10	10 to 11	11 to 12	12 to 13	> 13
7 to 8				6E-06	3.5E-05	9.41E-05	0.0001	0.00014	1E-04	5.4E-05	2.5E-05
6 to 7			3E-06	4E-05	0.00022	0.000503	0.0007	0.00057	0.0004	0.00018	7.6E-05
5 to 6			3E-05	0.0003	0.00141	0.002723	0.0031	0.00231	0.0013	0.00058	0.00022
4 to 5		6E-06	0.0003	0.0025	0.00813	0.012862	0.012	0.00769	0.0037	0.00143	0.00047
3 to 4		8E-05	0.0022	0.015	0.03702	0.045451	0.0339	0.01761	0.007	0.00229	0.00065
2 to 3	5E-06	0.0008	0.0143	0.0623	0.10541	0.092766	0.0514	0.02043	0.0064	0.00168	0.00039
1 to 2	9E-05	0.0057	0.0474	0.11	0.10918	0.060523	0.0223	0.0062	0.0014	0.00027	4.8E-05
0 to 1	0.0005	0.0064	0.0191	0.0185	0.00817	0.002133	0.0004	5.7E-05	7E-06	1E-06	

Table 10. The range of safe and dangerous wave conditions for bending moment, $\beta = 60°$, stage 2, Section 5, Method B

H_S (m)	T (s)										
	< 4	4 to 5	5 to 6	6 to 7	7 to 8	8 to 9	9 to 10	10 to 11	11 to 12	12 to 13	> 13
7 to 8				6E-06	3.5E-05	9.41E-05	0.00014	0.000137	9.71E-05	5.4E-05	2.5E-05
6 to 7			3E-06	4.4E-05	0.00022	0.000503	0.00066	0.000571	0.000363	0.000182	7.61E-05
5 to 6			2.9E-05	0.000342	0.001406	0.002723	0.003063	0.002309	0.001291	0.000576	0.000216
4 to 5		6E-06	0.00027	0.002484	0.008133	0.012862	0.012046	0.00769	0.003693	0.001433	0.000473
3 to 4		7.71E-05	0.00225	0.015006	0.037017	0.045451	0.033903	0.017607	0.007008	0.002291	0.000647
2 to 3	5E-06	0.000812	0.014324	0.062251	0.105412	0.092766	0.051397	0.020427	0.006386	0.001676	0.000387
1 to 2	8.91E-05	0.005701	0.047369	0.110025	0.109182	0.060523	0.022345	0.006195	0.0014	0.000273	4.8E-05
0 to 1	0.000475	0.00637	0.019102	0.018486	0.008173	0.002133	0.000391	5.7E-05	7.01E-06	1E-06	

Table 11. The range of safe and dangerous wave conditions for roll, $\beta = 90°$, stage 2, Method B

H_S (m)	T (s)										
	< 4	4 to 5	5 to 6	6 to 7	7 to 8	8 to 9	9 to 10	10 to 11	11 to 12	12 to 13	> 13
7 to 8				6E-06	3.5E-05	9.41E-05	0.00014	0.000137	9.71E-05	5.4E-05	2.5E-05
6 to 7			3E-06	4.4E-05	0.00022	0.000503	0.00066	0.000571	0.000363	0.000182	7.61E-05
5 to 6			2.9E-05	0.000342	0.001406	0.002723	0.003063	0.002309	0.001291	0.000576	0.000216
4 to 5		6E-06	0.00027	0.002484	0.008133	0.012862	0.012046	0.00769	0.003693	0.001433	0.000473
3 to 4		7.71E-05	0.00225	0.015006	0.037017	0.045451	0.033903	0.017607	0.007008	0.002291	0.000647
2 to 3	5E-06	0.000812	0.014324	0.062251	0.105412	0.092766	0.051397	0.020427	0.006386	0.001676	0.000387
1 to 2	8.91E-05	0.005701	0.047369	0.110025	0.109182	0.060523	0.022345	0.006195	0.0014	0.000273	4.8E-05
0 to 1	0.000475	0.00637	0.019102	0.018486	0.008173	0.002133	0.000391	5.7E-05	7.01E-06	1E-06	

The values of the E_T index were determined based on tables 6–11. These values were calculated as the sum of wave height and period occurrence probability, for which Γ function equals "1" (marked in green, in Tables 6–11). Table 12 shows E_T index values calculated by the use of Tables 6–11.

Table 12. E_T index values

Method	Effect of wave	E_T
Method A	Shear Force, $\beta = 180°$, stage 7, Section 3	0.79
	Bending moment, $\beta = 180°$, stage 0, Section 4	0.98
	Roll, $\beta = 90°$, stage 0	0.90
Method B	Shear Force, $\beta = 60°$, stage 4, Section 7	1
	Bending moment, $\beta = 60°$, stage 2, Section 5	0.78
	Roll, $\beta = 90°$, stage 2	0.90

Discussion

Tables 3 and 4 show that:

- The number of loading stages when using method B has fewer stages than method A, which offers a much shorter loading time;
- The differences in transverse metacentric height during loading are approximately the same.

Results of internal forces during loading operation in still water (Figures 3 and 4) show that:

- In both loading methods, shear forces are approximately the same (maximal shear force during loading sequence B is slightly higher);
- During loading via Method B, bending moments are much higher than method A.

Results for the vertical shear forces and bending moments during the loading operation on waves (Figures 5 and 6) show that:

- the most unfavorable wave period for shearing forces and bending moments is around 7–8 s;
- bending moments are almost similar when the ship is loaded by the use of both loading methods;
- shearing forces are also similar, except for the shear force during the B-type loading in the case of a wave direction of 60°. In this case, the shear force is almost twice as high as in the other directions.

The roll motion results during the loading operation, presented in Figure 7, shows that for both loading methods the roll motion is similar. During loading, the metacentric height had large value from 3.27 m to 2.62 m. Figure 7 confirmed that such a large metacentric height caused a high value of natural roll frequency and led to excessive stability. In such conditions, the ship could have a tendency to achieve sub-resonance roll motion. In this case, the maximum roll motion occurs at a small wave period from 6 to 8 seconds, as shown in Figure 8.

Tables 6–11 show the effects of waves around the Clarion–Clipperton Zone on shear forces, bending moments and roll motion at key loading stages. Table 12 presents an assessment of ship behavior on the Clarion-Clipperton Zone through the use of an operational effectiveness index. This table shows that during loading method A, the E_T efficiency index reaches values from 0.79 to 0.98. E_T efficiency is most limited by shearing forces at the 7th stage of loading operation, while the least by bending moments during loading method A. Table 6 presents detailed dangerous wave ranges, taking into account shear forces at this loading phase. This table shows that loading can be safely carried out at waves up to:

- 3 meters in height and for any wave period;
- 4 meters in height for a wave period greater than 11 s.

In the same way, during loading through the use of loading method B, the E_T index reaches values from 0.79 to 0.98. However, with this loading method, efficiency is limited by bending moments at the 2nd loading phase and shearing forces do not limit the E_T index at all. Table 10 presents detailed dangerous wave ranges, taking into account bending moments at this loading phase. This table shows that loading can be safely carried out in waves up to:

- 3 meters in height and for any wave period;
- 4 meters in height for a wave period up to 6 s, and greater than 12 s.

Tables 8, 11 and 12 show that the loading method does not affect roll motion. Using methods A or B, loading can be safely carried out in the waves up to:

- 3 meters in height and for any wave period;
- up to 4 meters in height, with the exception of a wave period from 6 to 8 s.

Tables 8 and 11 confirm that 6–8 second wave periods may cause excessive roll motion.

Conclusions

In this research, internal forces and roll motion during a nodule loading onto a ship at sea were analyzed. This study has shown that standard loading sequences available in the loading manual could not be used for loading polymetallic nodules at sea.

Therefore, new alternative sequences were developed, taking into account waving conditions at sea and their shear forces, bending moments and roll motion applied to the ship. The following two nodule loading methods were developed:

- Method A – where each cargo hold is loaded separately;
- Method B – where two cargo holds are loaded simultaneously.

In this research, these methods were compared by taking vertical shear forces, bending moments, ship motion and waving into account.

The number of allowed loading stages when using method B were fewer than method A, which offers a much shorter loading time. For both loading methods shear forces in still water were approximately the same, and the maximum shear force during loading sequence B was slightly higher. The differences in transverse metacentric height during loading were approximately the same. While loading using Method B, bending moments in still water were found to be much higher than in method A.

In this research it was verified whether waves could have an influence on the occurrence of excessive ship motion and vertical shear forces and bending moments. This research shows that:

- the most unfavorable wave period for shear forces, bending moments and roll motion is around 7–8 seconds;
- shear forces, bending moments and roll motion are almost identical when the ship is loaded by the use of both loading methods, except for shear forces during loading method B, in the case of a wave direction of 60°. In this case, the shear force is almost twice as high as in the other directions.

The study carried out a full assessment of the ship behavior, which took into account the wave conditions that occur around the Clarion–Clipperton Zone by the use of an operational efficiency index. This research has shown that this index can be successfully applied to this assessment. This part of the study clearly showed that:

- loading operations can be safely carried out under wave conditions with a height of up to 3 m, regardless of the wave period of both loading methods;
- the operational efficiency index was limited by excessive shear forces only during loading method A;
- the operational efficiency index was limited by excessive bending moments during loading method B;
- roll motion clearly influenced the operational efficiency index from using both loading methods.

This research clearly shows that nodule loading onto a 32,000 DWT bulk carrier may cause excessive internal forces and roll for wave heights above 3 m. For the safe loading of nodules on higher waves, a bulk carrier with other design characteristics would be more suitable.

References

1. Abramowski, T. & Cepowski, T. (2013) *Preliminary Design Considerations for a Ship to Mine Polymetallic Nodules in the Clarion-Clipperton Zone*. Tenth ISOPE Ocean Mining and Gas Hydrates Symposium, 22–26 September, Szczecin, Poland.
2. Abramowski, T. & Szelangiewicz, T. (2011) Eksploatacja złóż polimetalicznych konkrecji z dna oceanu. *Górnictwo i Geoinżynieria* 4/1, pp. 63–72.
3. Bortnowska, M. (2008) Research on preliminary concept of ship intended for mining poly-metallic concretions from sea bed. *Polish Maritime Research* 15(1), pp. 29–36; doi: 10.2478/v10012-007-0048-3.
4. Cepowski, T. (2007) Approximation of the index for assessing ship sea-keeping performance on the basis of ship design parameters. *Polish Maritime Research* 14(3), pp. 21–26; doi: 10.2478/v10012-007-0014-0.
5. Frank, W. (1967) *Oscillation of Cylinders in or below the Free Surface of a Fluid*. Report 2375. Naval Ship Research and Development Center, Washington, U.S.A.
6. Ikeda, Y., Himeno, Y. & Tanaka, N. (1978) *A Prediction Method for Ship Rolling*. Department of Naval Architecture, University of Osaka Prefecture, Japan, Report 00405.
7. Jensen, J.J. & Pedersen, P.T. (1981) Bending Moments and Shear Forces in Ships Sailing in Irregular Waves. *Journal of Ship Research* 25(4), pp. 243–251; doi: 10.5957/jsr.1981.25.4.243.
8. Journée, J.M.J. (2001) *Theoretical Manual of SEAWAY* (*Release 4.19*). Technical Report 1216a, Delft University of Technology, Ship hydromechanics Laboratory, Delft, The Netherlands.
9. Karppinen, T. (1987) *Criteria for Seakeeping Performance Predictions*. ESPOO.
10. Kukkanen, T. (2012) *Numerical and experimental studies of nonlinear wave loads of ships*. PhD thesis, VTT Technical Research Centre of Finland.
11. McTaggart, K., Datta, I., Stirling, A., Gibson, S. & Glen, I. (1997) Motions and Loads of a Hydroelastic Frigate Model in Severe Sea*s*. *Transactions SNAME* 105, pp. 427–454.
12. Nimmo, M. (2012) NI-43-101 *Technical Report Clarion-Clipperton Zone Project, Pacific Ocean*. Golder Associates Pty Ltd, Australia.
13. Nishi, Y. (2012) Static analysis of axially moving cables applied for mining nodules on the deep sea floor. *Applied Ocean Research* 34, pp. 45–51; doi: 10.1016/j.apor.2011.10.003.
14. Parunov, J. & Senjanović, I. (2004) Use of Vertical Wave Bending Moments from Hydrodynamic Analysis in Design of Oil Tankers. *International Journal of Maritime Engineering* 146(a4); doi: 10.3940/rina.ijme.2004.a4.5204.
15. Phelps, B.P. (1997) *Determination of Wave Loads for Ship Structural Analysis*. DSTO Aeronautical and Maritime Research Laboratory. Melbourne, Australia.
16. Sharma, R. (2011) Deep-sea mining: economic, technical, technological and environmental considerations for sustainable development. *Marine Technology Society Journal* 45(5), pp. 28–41; doi: 10.4031/MTSJ.45.5.2.
17. Soares, C.G., Fonseca, N. & Pascoal, R. (2004) Long term prediction of non-linear vertical bending moments on a fast monohull. *Applied Ocean Research* 26(6), pp. 288–297.
18. Szelangiewicz, T. (2000) Ship's operational effectiveness factor as criterion cargo ship design estimation. *Marine Technology Transaction. Technika Morska* 11, pp. 231–244.

Cite as: Kacprzak, P. (2021) An analysis of shear forces, bending moments and roll motion during a nodule loading simulation for a ship at sea in the Clarion–Clipperton Zone. *Scientific Journals of the Maritime University of Szczecin, Zeszyty Naukowe Akademii Morskiej w Szczecinie* 65 (137), 9–20.

Scientific Journals
of the Maritime University of Szczecin

Zeszyty Naukowe
Akademii Morskiej w Szczecinie

2021, 65 (137), 21–26
ISSN 1733-8670 (Printed)
ISSN 2392-0378 (Online)
DOI: 10.17402/457

Received: 26.10.2020
Accepted: 02.03.2021
Published: 31.03.2021

Selected operational limitations in the operation of passenger and cargo ships under SOLAS Convention (1974)

Julianna Stępień[1], Malwina Pilarska[2]

[2] https://orcid.org/0000-0002-11404161

[1] Maritime University of Szczecin, Department of Port Operation and Sea Fleet
11 Henryka Pobożnego St., 71-899 Szczecin, Poland
[2] West Pomeranian University of Technology
Department of Airconditioning and Refrigeration Transport
41 Piastów Ave., 71-065 Szczecin, Poland
e-mail: malwinapilarska@wp.pl
corresponding author

Keywords: SOLAS Convention, passenger ships, ferry safety, life-saving appliances, on board ships, maritime safety, mechanical propulsions

JEL Classification: Q25, Q48, R41, D81

Abstract

Presented are regulations concerning the operation of passenger ships (with particular emphasis on Polish ferries) designed to increase maritime safety the SOLAS Convention, established in 1974 and codified in 2002, codifies these regulations, and the International Maritime Organization mandates additional regulations, created in response to a rapidly increasing number of maritime disasters. The analyses described herein were based on restrictions established for the "Jan Śniadecki" and "Mikołaj Kopernik" ferries. Safety of ro-ro units, which also typically have a significant number of people on board, was also analyzed. Also included in the study were ship operational- limitation characteristics with respect to structure, unsinkability, and stability of machinery and electrical equipment, fire protection, operational requirements, and rescue measures and devices, along with their purpuroses. Safety management consists of taking appropriate actions to prevent or minimize the effects of an accident or a disaster and is assessed on the basis of calculations and experience gleaned from analogous cases. Safety management can proceed if a problem has been thoroughly assessed. The potential risk of negative consequences with respect to the safety of the transport process as a whole must be considered, and the safety of the whole must not be risked for that of a particular part of it. A safety management decision can be made when its necessity is not in doubt. A problem is assumed to have only one solution. The effectiveness of the previously used method should be carefully assessed before proceeding to the next method. Security management is not easy and requires much professional knowledge and experience.

Introduction

Safety constitutes an extremely important element of maritime shipping, and the International Convention for the Safety of Life at Sea (SOLAS, 1974) is the most well-known Convention on safety regulations involving ships in since May 25, 1980, and in Poland since June 15, 1984 (Jankowski, Purowski & Olszak, 1996), the SOLAS Convention was adopted on November 1, 1974, by the International Conference for the Safety of Life at Sea. It replaced and repealed the previous Convention, which was signed in London on June 17, 1960, and was to become effective either 12 months from the date on which at least 25 countries became signatories to the Convention or on May 25, 1980, whichever date occurred first.

Identification studies

The consolidated text of the 2002 SOLAS Convention consists of two parts, the first of which contains the 1974 SOLAS Convention and the 1988 protocols, requirements, and certificates. Its second part consists of Resolution A. 883 (21), entitled "Uniform Worldwide Implementation of the Harmonized System of Supervision and Certification (HSSC)", the list of certificates and documents that every ship should carry on board, and lists of resolutions adopted at four successive conferences of the contracting signatory governments. Issues and ship requirements addressed by the Convention's provisions are the following:

- Ship construction, unsinkability measures, and stability as well as machinery and electrical installation;
- Fire protection regulations;
- Life-saving appliances and devices;
- Radiocommunication arrangements;
- Conditions to maintain navigational safety;
- Cargo transportation specifications to avoid endangering ship and cargo safety;
- Provisions relating to the transport of potentially dangerous goods;
- Safety provisions for nuclear-powered ships;
- Principles of safe ship operation and management;
- Security measures for high-speed craft;
- Special measures intended to increase maritime safety; and
- Additional safety measures for bulk carriers.

To ensure the effectiveness of the Convention's provisions its signatory governments have issued appropriate decrees, laws, and regulations, in effect mandating adoption of all measures to ensure maritime safety. All other agreements, treaties, and conventions relating to life at sea and applying to ships when the SOLAS Convention is inapplicable or to matters it does not cover remain in over their respective defined periods. When agreements, treaties, and conventions conflict with SOLAS Convention provisions, the latter take precedence and prevail.

The IMO (International Maritime Organization) and Conferences consider proposed amendments to SOLAS Convention provisions. Any instrument of acceptance, approval, or accession to the Convention shall become effective three (3) months after its deposit date with the IMO's secretary general. A government may terminate the Convention only after five (5) years have elapsed since its entry into force for that government. Such a denunciation shall take effect one (1) year from the date the document of denunciation was received. The Convention has been deposited with the secretary general of the IMO, who is obliged to deliver copies to the governments which have signed or acceded to it (IMO, 1974).

SOLAS Convention Particulars

Regulations contained in the first chapter of the Convention apply only to ships engaged in international voyages. However, provisions of the SOLAS Convention do not apply to the following vessel types:

- Ships lacking mechanical propulsion;
- Ships not engaged in commercial navigation, e.g., yachts;
- Wooden ships of primitive construction;
- Fishing vessels;
- Ships for troop transportation and warships; and
- Vessels operating only in the Great Lakes of North America and on the River St. Lawrence.

A government official may perform ship inspections and reviews which the government may entrust to appointed inspectors. As Regulation 11 states, no changes may be made to a ship after a survey of it has been conducted. If a ship is involved in an accident or damage is detected following a survey, the ship's master or operator must report the incident or findings, respectively, to the authorities or to the inspector who issued the relevant certificate, who should then initiate an inspection to determine whether a survey is needed. A Passenger Ship Safety Certificate is valid for one year, whereas the comparable certificate for cargo ships is valid for a time period not exceeding five years. In addition, the government of a ship involved in an accident is to undertake an accident investigation subject to SOLAS, and, upon conclusion of the investigation, that government is required to provide IOM with information on its results (IMO, 1974).

With regard to their construction, unsinkability, and stability, machinery and electrical installations on ships should be designed, maintained, and constructed in accordance with the requirements of the classification society. For instance, oil tankers and bulk carriers must have an effective corrosion protection system, and a tanker's crew should have safe access to the bow even in difficult weather conditions. The floodable length of passenger ships refers to spaces below the line of the bulkhead (IMO, 1974; Plewiński, 1996). The Convention also stipulates location of the fore peak, or collision, bulkhead. In addition, the ship should have a stern peak

bulkhead and others located at the front and rear of the machinery space. Double bottom provisions apply to passenger and cargo ships other than tankers. On oil tankers, access to spaces in the cargo area is required. Regulation 14 deals with the construction and preliminary testing of watertight bulkheads and other structural elements of passenger and cargo ships. Each bulkhead should be constructed so as to withstand the pressure of a water column of the maximum height that could occur during the failure. Steps and recesses in bulkheads should be watertight and possess strength comparable to that of the rest of the bulkhead. The SOLAS Convention also specifies how side scuttles, watertight doors, watertight decks, tunnels, keels, and trunks are to be constructed. Distribution boxes and manually controlled valves in the gas piping system are to be located so as to be accessible. After completion of construction, a ship should be subjected to an inclining test, which should be repeated every five years the ship is in use (IMO, 1974; Jankowski, Purowski & Olszak, 1996).

The SOLAS Convention's section on ship construction, fire protection, and fire detection and extinguishing provides information for ships constructed on or after July 1, 2002. This section's content also applies to ships undergoing repair, dimensions or passenger accommodation spaces have been significantly and service life extended. Regulation 2 deals with fire safety tasks and "functional requirements", which concern division of a ship into primary horizontal and vertical zones and separation of rooms from the rest of the ship by means of structural and thermal partitions (IMO, 1974; Jankowski, Purowski & Olszak, 1996; Szyca, 1996). Also covered, inter alia, are limits on use of flammable materials; detection, limiting, and extinguishing of any fire its origin; constant readiness of fire-fighting equipment and devices and minimizing likelihood of igniting flammable cargo vapors. To prevent ignition of flammable materials or liquids (IMO, 1974), the following actions are specified:

- Control leakage of flammable liquids and minimize accumulation of flammable vapors;
- Reduce flammability of combustible materials and ignition sources;
- Maintain cargo-tank atmospheres out of explosive range;
- Use no liquid fuels having a flash point below 60°C; and
- Properly store, distribute, and use liquid fuel.

In addition, liquid fuel tanks must be located outside machinery spaces and must constitute a separate part of the hull structure. The Convention also stipulates protection of surfaces, i.e., installations, that are subject to high temperatures through use of lubricating oil, other flammable oils, liquid fuel in periodically unattended machinery spaces, gas fuel for commercial purposes, etc., and ballasting. Also discussed are inert gas installations on chemical and gas carriers, including their general requirements gas-measurement instruments, topics related to protection for cargo area and cargo pump rooms, fire potential and smoke, and toxicity.

Part C of Chapter II-2 is dedicated to fire suppression. In the event of a fire, patrols are to detect and locate and then alert the navigation bridge of the fire's occurrence and location. A permanent fire-detection and alarm system is to be installed in periodically unattended engine rooms and machinery spaces where automatic and remote control systems are installed. Smoke detectors must be deployed in living quarters, staircases, corridors, and ventilation ducts and along escape routes. On board passenger ships, cargo spaces must be equipped with detection and alarm systems. Regulation 8's purpose is to reduce the spread of smoke, and so. It specifies, inter alia protection of control posts located outside machinery spaces, smoke extraction from machinery spaces, and draft barriers. Regulation 10 governs isolation of fire to its point of origin, mandating use of technical and structural divisions to create compartments and divisions within a ship's structure. Moreover, adequate thermal insulation is to be installed within divisions commensurate with the fire risk these compartments and their adjacent spaces pose (IMO, 1974; Jankowski, Purowski & Olszak, 1996; Szyca, 1996).

Regulation 10 also describes the act of firefighting. For it to be effective, functional requirements must be met; that is, fixed fire extinguishing systems must be used, and fire extinguishing equipment must be easily accessible. Moreover, ships are to be equipped with fire pumps, hydrants, delivery hoses, and pipelines, and the regulation specifies the number and arrangement of and pressure within hydrants for both passenger and cargo ships. Specifically, the maximum water pressure in each hydrant should not exceed the pressure at which their associated delivery hoses were checked. Passenger ships should be equipped with at least three pumps gross tonnage of 4,000 and more, at least two pumps capacity of less than 4,000, at least two with less than 1,000, and one of the latter should be independently propelled (IMO, 1974; Oleszek, 1996; 1997).

Part E of Chapter II-2 deals with performance (i.e., operational) requirements. The objective of

Regulation 14 is to maintaining and monitoring the effectiveness of ship fire safety measures. Fire safety systems and extinguishing installations and equipment must always be ready for immediate use, and periodic tests and inspections must ensure their continued readiness. Fire protection systems, i.e., fire detection and alarm systems, escape route systems and equipment, bulkheads, and openings protections should be maintained to keep them in good condition. Maintenance and testing of these installations are to be performed according to guidelines developed by IOM, and all vessels should have maintenance plans available for inspection at any time. According to Regulation 14, these plans should include the following (IMO, 1974; Oleszek, 1996; 1997):

- Fire-fighting and water installations, fire pumps, and hydrants, including hoses, nozzles, and international connectors;
- Fire detection and fire alarm installations;
- Fixed fire extinguishing systems and other fire extinguishing equipment;
- Automatic sprinkler systems equipped with fire detection and alarm;
- Ventilation systems with fire and smoke dampers, fans, and associated controls;
- Emergency cut-off of the fuel supply;
- Fire doors, including surging;
- General alarm systems;
- Emergency escape breathing devices;
- Fire extinguishers, including spare charges; and
- Propelled fire-fighting equipment.

In addition, passenger ships carrying more than 36 passengers must have a maintenance plan for low-location lighting and notification systems. Regulation 15 mandates posting of general plans that show locations of control stations on each deck; details of the ship's detection, alarm, and sprinkler system; locations of fire-fighting equipment; and access routes to particular compartments. Part G of Chapter II-2 concerns special requirements for ships equipped with helipads, including helicopter equipment, landing pad construction, escape routes, fire-fighting equipment, drainage, helicopter refueling facilities, and landing pad operating manual and fire service. Regulation 19 concerns transport of dangerous goods, including water supply, ignition sources, detection installations, ventilation, portable fire extinguishers, water sprinklers, or documents of compliance propelled (IMO, 1974; Oleszek, 1996; 1997).

The five regulations contained in the Convention's Chapter 3 deal with life-saving appliances and devices and apply to ships constructed on or after July 1, 1998. Exempt from these provisions are ships that sail not more than 20 nautical miles from the nearest land mass and passenger ships used in special shipping for the transport of large numbers of special passengers (e.g., pilgrims). The chapter's Regulation 4 mandates testing of life-saving appliances to confirm that they meet IMO requirements, and Regulation 6. Its Paragraph 2 discusses radio-equipment for life-saving appliances and applies to all passenger and cargo ships of 300 gross tonnage and over. Table 1 shows the number of radar radios and transponders with which a ship should be equipped, depending on its capacity (IMO, 1974; Plewiński, 1995).

Table 1. Ship's required number of radar radios and transponders dependent on ship capacity

Ship's gross tonnage	For ships of 300–500 gross tonnage	For ships of 500 gross tonnage and more
VHF radio for two-way communication	At least 2 pieces	At least 3 pieces
Radar transponders	At least 1 shall be posted on each cargo ship	At least 1 on each side of each passenger ship

VHF radios for two-way communication and radar transponders must meet the technical and operational requirements adopted by the IMO. In ships equipped with two radar transponders and lifeboats, one transponder should be placed in the "free fall" boat and the other in the immediate vicinity of the navigation bridge. At least 12 rockets must be kept on board and located in or near the control room. In passenger ships, the general alarm must be audible on all open decks, and on-board notification systems' audibility above noise level must be assured in all spaces.

Regulation 10 deals with manning and supervision of survival craft passenger ships. Boarding ladders are to be provided along a passenger ship's sides at each survival craft launching site, whose purpose is to ensure the safe launch of survival craft, including ensuring their clean separation from propeller and hull overhangs. Survival craft launches are best performed along a ship's straight sides. Survival units should meet the following criteria:

- Positioned as closely as is safe and practical to the water's Surface;
- Positioned in a safe and sheltered place protected to the greatest extent possible from potential damage due to fire or explosion; and
- Always fully equipped and ready for use;

Table 2. Characteristics of personal life-saving appliances to be carried on passenger ships

Rescue measure	Characteristics and location on the ship
Lifebuoys	– Positioned so as to provide passengers and crew easy access. – At least one lifebuoy in the vicinity of the stern should be fitted with a 30-m floating lifeline. Half of lifebuoys on board should be fitted with self-igniting light buoys. – At least two (2) lifebuoys must have self-activating smoke buoys. – Each lifebuoy is to be marked with both the name of the ship to which it belongs and that ship's home port in capital Latin script.
Lifejackets	– One for every person on board the ship. – Number of lifejackets for children should equal at least 10% of the number of passengers on board. – Lifejackets for watchkeepers must be stowed in the wheelhouse. – Lifejackets for remainder of crew and for passengers should be stored in easily accessible and well-marked locations. – Lifejackets for free-fall boats should not obstruct access to boat.
Rescue and protective suits	– Number sufficient to be worn by all those assigned to rescue boat crew or marine evacuation system. – Not needed when ship operates solely in warm climate zones

- Lastly, lifeboats can be kept continually in position ready to be launched for a period not exceeding 5 minutes.

Regulation 15 describes regulations governing set up of marine evacuation systems. Ships' sides should include no openings, and each marine evacuation system must be arranged so that the parcel, platform, box with mechanism, and other positioning devices do not interfere with other life-saving appliances and their launch devices. Facilities for embarking on a lifeboat are also to be provided, and time to embarkation on a fully equipped rescue boat should not exceed 5 minutes in calm water. In addition, rescue-boat embarkation and recovery arrangements should ensure easy and safe use of stretchers for injured persons (IMO, 1974; Plewiński, 1995).

Regulation 19, on the other hand, deals with training and drills in leaving ship and includes safety measures and practical exercises including, inter alia, abandon ship and fire drills. In and fire drills. addition, each crew member must be briefed on the following, related topics:

- Mode of operation and use of pneumatic life rafts;
- Hypothermia issues;
- First aid;
- Use of emergency measures in difficult weather conditions; and
- Method of operation of fire extinguisher devices.

According to Regulation 20, rescue measures should undergo inspection, including verification of completeness and condition, once a month, and each pneumatic life raft and sea evacuation system is subject to technical inspection every 12 months. All emergency measures and devices are to comply with the requirements set forth by the International Code of Emergency Measures (LSP Code).

Table 2 presents characteristics of personal life-saving appliances and rescue equipment i.e., lifebuoys, lifejackets, rescue suits, and protective suits – to be carried on passenger ships.

Clear instructions for action in the event of an alarm should be prepared for and made available to each person on board, displayed in conspicuous places throughout the ship (i.e., control room, engine room, crew accommodation, and passenger cabins). A ship's crew should include persons trained to assist passengers and to operate survival craft and their launching devices, and each unit is to be commanded by a designated deck officer or chartered lifeguard. Life boats and rafts should be positioned as closely as possible to accommodation and service spaces, and muster stations are to be in close proximity to emergency unit embarkation areas. Passengers who will be on a ship for more than 24 hours must undergo training in use of seat belts and in what to do in the event of an emergency.

Passenger craft that undertake voyages other than short ones in general and short international ones in

Table 3. Based on SOLAS 1974, the minimum number of lifebuoys to be carried by a passenger ship depending on its length (IMO, 1974)

The length of the ship [m]	The minimum number of lifebuoys
Less than 60	8
60–120	12
120–180	18
180–240	24
240 and more	30

Table 4. Ferries "Mikołaj Kopernik" and "Jan Śniadecki" basic information

Ferry data	"Mikołaj Kopernik"	"Jan Śniadecki"
Gross tonnage	8734	14 417
Ship type	Railway and car ferry	Railway and car ferry
Number of passengers taken	36	57
Speed	14 knots	17 knots
Construction date	08–05–1974	15–04–1988
Number of IMO	7336721	8604711
Flag under which the unit is registered	Saint Vincent and the Grenadines (Central America)	Cyprus
Home port	Kingstown (The port and the capital on the Caribbean Sea)	Limassol
Call sign	J8SK6	P3TX6
Ship class	KM PASSENGER/FERRY I (Jankowski, Purowski & Olszak, 1996) L2	KM PASSENGER/FERRY I (Jankowski, Purowski & Olszak, 1996) L2
PRS number	110052	110068
Maximum draft	4.5 m	5.10 m
Unit load capacity	2079 tons	5544 tons

particular and that do not comply with subdivision requirements are to be equipped with partially or fully enclosed lifeboats capable of accommodating 50 percent of the total number of persons on board. Conversely, passenger ships engaged in short international voyages must be equipped with partially or fully covered lifeboats capable of accommodating 30 percent of their passengers. In both cases, life boats should be evenly distributed on each of a ship's sides. Moreover, this ship type is to be equipped with sufficient pneumatic or rigid life rafts to accommodate the total number of persons on board (IMO, 1974; Plewiński, 1995; Oleszek, 1996) and with lifebuoys in numbers dependent on the ship's length, as shown in Table 3.

Table 4 presents information on the ferries "Mikołaj Kopernik" and "Jan Śniadecki". For the "Mikołaj Kopernik", the Polish Register of Shipping (PRS) approved restrictions that were then issued on February 22, 2002, in Gdańsk under flag country authorization also approved and issued restrictions for the "Jan Śniadecki" under flag country authorization on July 30, 2002, in Gdańsk.

Conclusions

For years, the International Maritime Organization (IMO) has improvement in maritime safety regulations. Additionally, since its inception in 1974, the SOLAS Convention has been and continues to be subject to continual revision with the periodic introduction of new safety regulations. In Poland, the Polish Register of Shipping, whose purpose is to help ensure ships' technical safety, controls and implement safety regulations on the basis of the Convention and other, safety-oriented provisions. The Register mandates safety standards and then supervises their implementation during ship construction and operation. Due to the rapidly increasing number of accidents involving passenger craft, a list of operational limitations was drawn up in 1995 based on regulation V/30 of the 1974 SOLAS Convention, and since that time, each ship must have an up-to-date List of Operating Restrictions.

References

1. IMO (1974) International Convention for the Safety of Life at Sea, 1974, done at London on November 1, 1974 Journal of Laws of 1984, No. 61, item 318 (as ameanded).
2. Jankowski, J., Purowski, H. & Olszak, Z. (1996) New safety standards for damaged ferries. *PRS Information* 5.
3. Oleszek, G. (1996) Security of Passenger Ships. *PRS Information Bulletin* 5.
4. Oleszek, G. (1997) Ship Safety Under Convenient Flags. *The directions for the Sea and Trade* 3.
5. Plewiński, L. (1995) Selected passenger Safety Problems. *Maritime Law and Jurisprudence* 35.
6. Plewiński, L. (1996) Accidents, analyzes – and what next? *Shipbuilding and Maritime Economy* 3.
7. Szyca, G. (1996) Safer ferries. *The directions for the Sea and Trade*, No. 3–4.

Cite as: Stępień, J. & Pilarska, M. (2021) Selected operational limitations in the operation of passenger and cargo ships under SOLAS Convention (1974). *Scientific Journals of the Maritime University of Szczecin, Zeszyty Naukowe Akademii Morskiej w Szczecinie* 65 (137), 21–26.

Mechanical Engineering

Scientific Journals
of the Maritime University of Szczecin

Zeszyty Naukowe
Akademii Morskiej w Szczecinie

2021, 65 (137), 29–37
ISSN 1733-8670 (Printed)
ISSN 2392-0378 (Online)
DOI: 10.17402/458

Received: 22.10.2019
Accepted: 01.03.2021
Published: 31.03.2021

Finite element analysis of the dynamically created portal in the huge machine tool of "travelling column" type

Stanislau Dounar[1], Alexandre Iakimovitch[2], Andrzej Jakubowski[3*]

[1] https://orcid.org/0000-0002-6201-8340
[2] https://orcid.org/0000-0002-1138-1350
[3] https://orcid.org/0000-0002-0331-3147

[1,2] Belarusian National Technical University, Mechanical Engineering Faculty
Nezalezhnasci 65, 220127 Minsk, Belarus
[3] Maritime University of Szczecin, Faculty of Marine Engineering
Waly Chrobrego 1-2, 70-500 Szczecin, Poland
e-mail: a.jakubowski@am.szczecin.pl
* corresponding author

Keywords: FEA, portal, travelling column, rigidity, resonance, torsion, pecking
JEL Classification: C630, L600, L610

Abstract
In this paper, a special configuration for the huge multipurpose machine tool of "travelling column" type was investigated by the finite element analysis. Internal degrees of freedom of a bulky system consisting of the ram, stock, column, sledge and bed, were implemented by the hydrostatic guides. A simulation of coupling two assembled columns into the portal structure was completed. The results of this work showed that temporal joining raises the spindle static rigidity by 1.39–1.91 times depending on the direction (mostly longitudinal – along the X-axis). The simulation also revealed the robustness of a whole-machine resonance pattern (11.7–39.0 Hz) to "column–to–portal coupling". Eight types of eigenmodes were analyzed for frequency intervals from 0 to 80 Hz. A decrease by 2.9 times of the resonance peaks of a frequency response function was observed in the case of a portal structure creation. In case of columns-to-portal transition, stable cutting just at resonance frequencies (resonance overriding) becomes allowable. Overall, the "Portal" structure is recommended for intermittent cutting machining by raised high spindle unit at frequencies below 40 Hz.

Introduction

Multipurpose machine tools of the "travelling column" type are consigned to milling, drilling and boring large and tall workpieces. The workpiece is usually unmovable when machined. The column which is assembled with a stock, a ram, and a spindle unit carrying the tool, moves. The tool has three degrees of freedom besides its own rotation. The machine tool is bulky, precise, and high-priced; as a result, it works for many years and is renovated rather than replaced.

This work is related to a renovation project focusing on a group of unified "travelling column" machine tools of one branch. The large structural parts – columns and bed sections – were preserved with the refinishing of the hydrostatic guides. Naturally aged parts from cast iron are expected to be nearly free from residual stress, thus dimensionally stable which is a valuable feature for the precise machine tool. The stocks, rams, and spindle units were newly designed and produced. *Computerized numerical control* (CNC) system was provided for machine tool. Reconfiguration of the structural parts

(columns, sledges, bed sections) was also provided during renovation. Furthermore, a new "travelling column" configuration is presented in this work and its capabilities from the view of the rigidity of the configuration are investigated by *finite element analysis* (FEA) simulation (Zienkiewicz & Taylor, 2000).

Machine tool configuration and the aim of the work

This work is devoted to a software comparison between two configurations (structures) of the "travelling column" machine tool (Herrero & Bueno, 2001; Munoa et al., 2013) – the "Monocolumn" (Figure 1a) and the "Portal" (Figure 1b). The last configuration is temporary, just "on-demand emerging" one. It may be noted as *situate portal* and else *dynamically created portal* (DCP). DCP or briefly "Portal" is built by two coupled monocolumns moving close together. Other times, every column may move alone, according to its own CNC program.

A column with the ram Rm1 (assembled) is depicted in Figure 1a. This column touches its paired, symmetrical column, ram Rm2, in Figure 1b. Ram Rm1 is advanced at 1.6 m and the parallel ram Rm2 is nearly fully retracted.

A monocolumn assembly (Figure 1a) provides cutting using the double telescopic spindle unit (at the left end of ram Rm1). The precise boring spindle (Figure 1b), may advance axially (along Z) up to 2.6 m. This range is provided partly by the ram (0.59×0.59 m) axial advance. The Ram side surface 2 is slipping into the hydrostatic guides inside stock 3. Corner areas of stock 3 are marked 3a, 3b, 3c, 3d. The stock causes a vertical degree of freedom (along Y) due to hydrostatic guides (5a–5b) on column 5. The stock has a moving range of 4.25 m, and the column is of 6.7 m in height. The column is fixed to sledge 7, slipping longitudinally along X by hydrostatic guides 7a–7b on the underlying bed (not shown); the spindles are driven by motor 8.

The main problem of the monocolumn is a low dynamic rigidity at the spindle in the direction X. It is caused mainly by torsional resonance M3. The axis of torsion is vertical (parallel to Y) and it migrates inside triangle 3a–3b–5a. Even a small angle of torsion turns into big linear displacements at the ends of "1b–8" line (leverage effect).

The spindle flexibility is particularly high in the top stock position marked as "raised high spindle" (RHS – Figure 2, right). The adverse stock position near the bottom of the column is named the "low down spindle" (LDS – Figure 2, left). The spindle moving up from LDS to RHS causes vibration problems and cutting process instability. This limits precision and output if the tall workpiece is machined.

As seen in Figure 1, a stock is placed on the right from the column (right design). The renovated machine group possesses columns as of right design so of the left one. The modern tendency is to mount two or more travelling columns upon a bed, and to machine several workpieces in a parallel way.

During the renovation, it was proposed to install two monocolumns – L and R (Figure 2) – upon the bed with common guides; columns may provide machining independently under different CNC channels supervising. Two diverse workpieces, W1 and W2 (Figure 2), undergo separate boring and milling by tools T1 and T2. The stock at the right column R, is in the RHS position with the advanced ram.

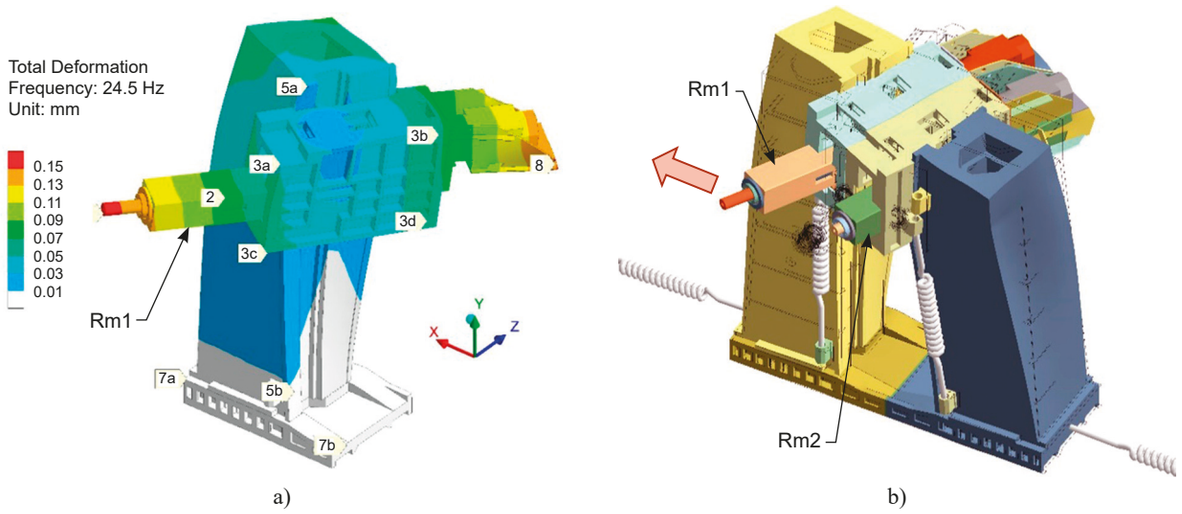

a) b)

Figure 1. Torsional resonance M3 of "Travelling column" machine tools for configurations: "Monocolumn" (a; 24.5 Hz) and "Portal" (b; 24.04 Hz). Arrow – exciting harmonic force F_x^d

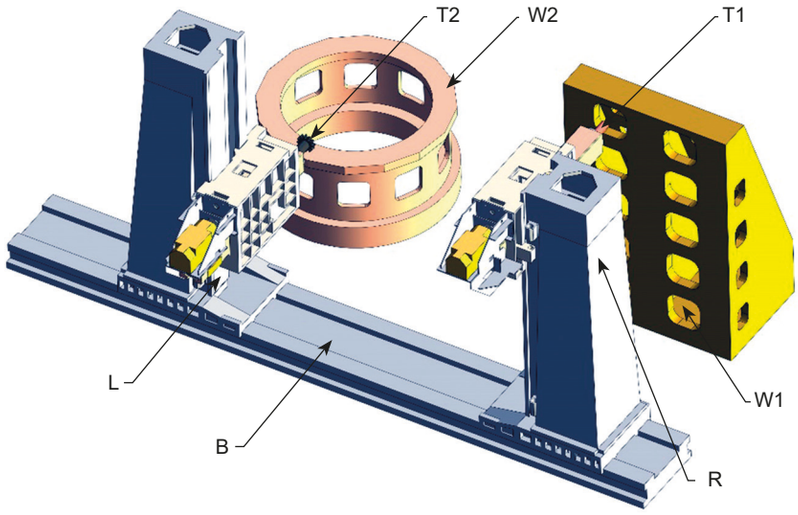

Figure 2. Parallel machining of workpieces W1, W2 by tools T1, T2, placed at the left and right monocolumns L, R (B – common bed). L relates to the low-down spindle (LDS) and R – to raised high spindle (RHS)

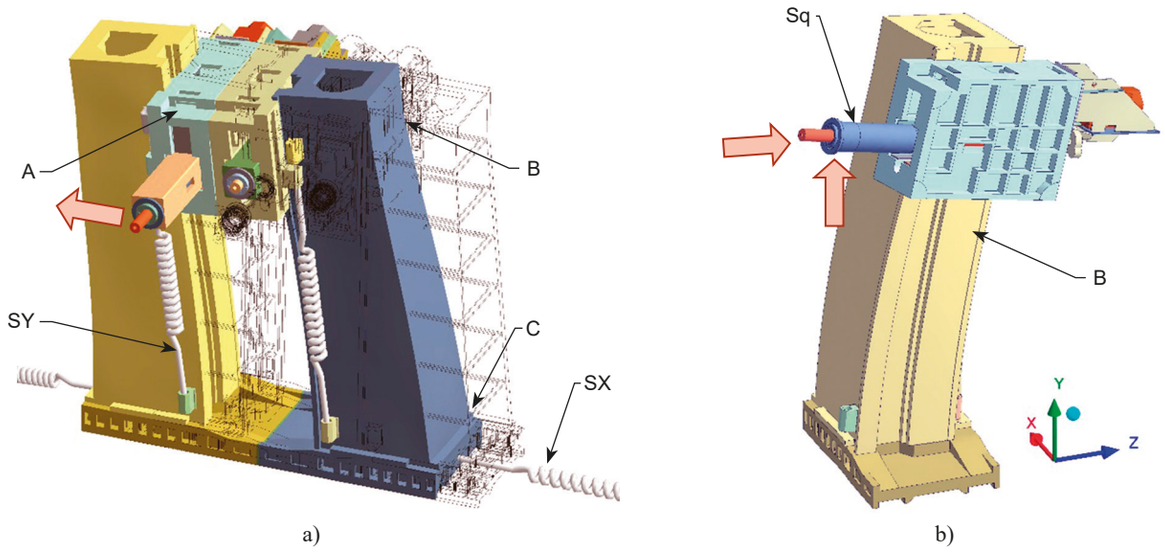

Figure 3. Structures “Portal” and “Monocolumn”, rocking at low frequencies during bending resonances excitement: a) eigenmode M1 (12.48 Hz); b) eigenmode M2 (12.72 Hz). Arrows – harmonic forces F_x^d, F_y^d, F_z^d, able to excite corresponding modes. Sq – spindle unit quill

The stock at the left column is moved down 3 m to the LDS position with the ram retracted; such a position brings sufficient spindle rigidity.

The machine tool with two independent columns on common guides is well known (Munoa et al., 2013). The feature of the presented configuration is that one column has a right-side design (R) and second column has a left-sided (L) one. The columns with stocks mirror each other; both stocks are facing each other. This configuration is convenient to provide collision-free, two-ram machining of the large workpiece. However, the main benefit of the mirroring columns lies in a critical case of raised high spindle (RHS) machining. Monocolumns of the left and right design may be joined in the new load-bearing system – “Portal” (Figures 1b, 3a and 4b). Columns are to touch each other by stock sides and lock up rigidity contour. The double structure (“Portal”) provides additional static and dynamic rigidity when RHS cutting is provided, demonstrating the need for FEA simulation as is the goal of the work presented.

The “Monocolumn” and “Portal” structures are depicted in Figure 3 and Figure 4. The arrows relate to cutting force components, applied from the workpiece to spindles while the springs simulate feed drives.

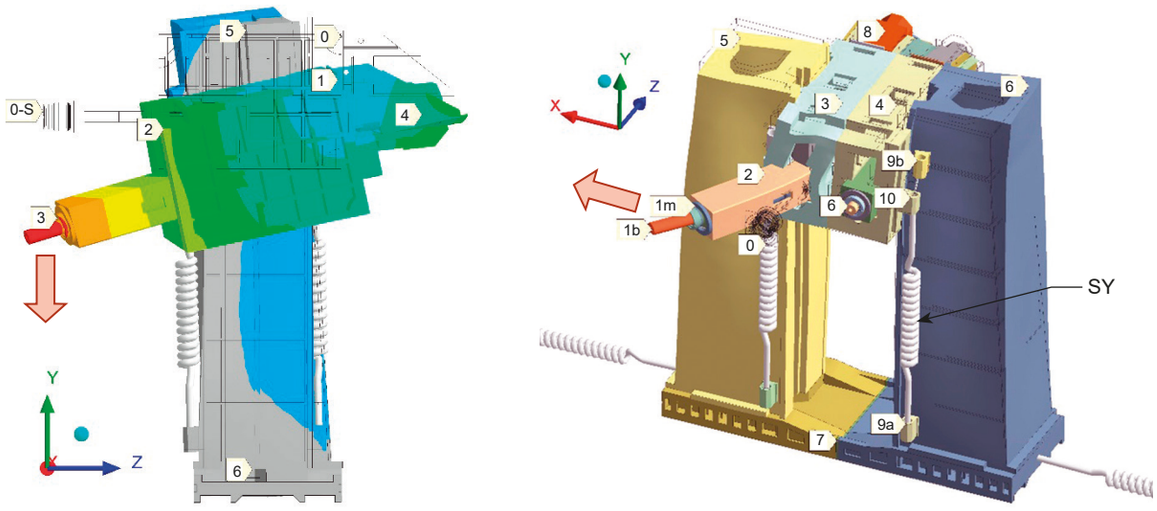

Figure. 4. "Monocolumn" (a – M4; 23.51 Hz; spindle force F_y) and "Portal" (b – M7; 70.82 Hz; spindle force F_x) exited according to eigenmodes

The marker systems on Figure 1 and Figure 4b are the same. Stocks 3, 4 are brought together by the CNC and are clamped to each other on corners 3a–3d (Figure 1). This is because preliminary FEA simulation has revealed the necessity to bond stocks without any slipping possibility. Otherwise, the effect of portal creation would be negligible. Monolithic system of stocks 3, 4 (Figure 4b) are named "stock-pack". Both columns and "stock-pack" create portal 5–3–4–6. Vertical opening between columns has a width of 2 m and a height of 7.1 m (counting from top to guides X). The portal rests on two sledges, contacting along line 7. The whole structure is driven in the X direction by the SX springs pair. Each spring behaves as a backlash-free, rack-pinion drive.

There are two parallel vertical drives (ball screws) for every stock – on the spindle side and on the motor side of column too. Every screw is simulated by a pair of SY springs. They abut on 9a, 9b column bracket and interact with nut 10 on the stock.

All hydrostatic guides are considered fully free from sliding with no friction and resonance according to eigenmode M1 may be freely excited by a horizontal force F_x^d (arrow on Figure 3a). The following movements for portal during M1 excitation include:

- each column bending (marks B, C),
- sledges reciprocating along X-guides (mark C),
- stock-pack oscillating vertically relatively to columns Y-guides (mark A).

It is clear that column bending is the main participant in spindle X-amplitude while sledge X-oscillation is on a second position and far away.

The DCP is represented as a no monolithic contour which causes inner slipping borders on the hydrostatic guides. The hydrostatic guides may be clamped and fixed, however, it leads to small inaccuracies caused by oil layer closing–opening. Therefore, all guides are assumed to be fulfilled with an ideal liquid.

It is assumed (in this paper) that after the portal structure creation, only one ram is used to machine at the same time (e.g., 2 on Figure 4b) and tt is driven by a spring SZ (hidden inside the stock). Ram 2 carrying the spindle unit consists of the milling spindle 1m and boring spindle 1b (going through milling one). Both spindles are designed for intermittent cutting, when cutting force may oscillate.

FEA-model and machine tool parameters

An FEA-model is built for static, modal, and harmonic analysis of "Monocolumn" and "Portal" structures. The experience (Vasilevich et al., 2015; Vasilevich et al., 2016) gained during the simulation of heavy "travelling column" machine tools, is used. Every cast iron structural part of the machine tool was presented by a separate finite element mesh. These meshes were joined together by a special surface finite element mesh set (contact pairs). Mostly contact pairs were assigned "bonded" status (no movements on contact surfaces) and hydrostatic guides were simulated as contact pairs with "no separation" status meaning free sliding without the possibility open contact or interference for neighboring bodies. Note that both stocks in the stock-pack interact only at corner areas (3a, 3b, 3c and

3d on Figure 1a), where contact pairs are tuned to "bonded" status.

The spindle unit bearings were secured against rotation and the damping ratio was taken as $\xi = 4\%$ during the harmonic simulation. Every spring SX has a rigidity of 600 N/μm, and each spring SZ has a rigidity of 400 N/μm. Every stock is supported in the vertical direction by a spring SY system with a total rigidity of 400 N/μm. The spindle unit radial rigidity is tuned in the FEA model as equal to 950 N/μm at the milling spindle (ϕ332 mm) end and 120 N/μm at the boring spindle (ϕ200 mm) end. The latter value relates to a boring spindle pushing forward 500 mm from the milling one. The spindle unit rigidity is much higher than the spindle rigidity of monocolumn $J^{st,d}_{\text{mono}}$ or portal $J^{st,d}_{\text{port}}$. The latter considers the flexibility of a whole load-bearing system of the machine tool.

Static comparison of "Column" and "Portal" structures

This paper focuses on the static rigidity of the spindle for monocolumn (J^{st}_{mono}) and of that for portal (J^{st}_{port}) as well as the same dynamic parameters J^{d}_{mono} and J^{d}_{port}. The spindle rigidity is almost the same as the tool rigidity for the investigated kind of machine tools. Rigidity is important both for machining precision and for cutting process stability (falling to auto-oscillations). The main threat is "regenerative chatter" (Jafarzadeh & Movahhedy, 2017; Lu et al., 2018). It is a currently accepted necessity (Olvera et al., 2012; Lopez de Lacalle & Lamikiz, 2008) to provide rigidity above the threshold $[J^{\text{thres}}_{x,y,z}] = 20$ N/μm in any direction. This applies to both static and dynamic rigidity at the end of the tool-bearing spindle. An excess of the threshold $[J^{\text{thres}}_{x,y,z}]$ guarantees cutting process stability. If spindle rigidity were lower ~10 N/μm, auto-oscillations become very likely.

A static testing force, $F^{st}_{x,y,z}$, of 1 kN was applied to the milling spindle end along coordinates X, Y, Z when the machine tool was in the RHS position. The value of the force is not the issue for FEA-model linearity and simulated spindle displacements allows for calculation of rigidity (Table 1). It is sufficient because is higher than the threshold level $[J^{\text{thres}}_{x,y,z}]$ at 20 N/μm for both the monocolumn and the portal structures.

The monocolumn spindle is the most flexible in the X direction (rigidity threshold is exceeded by three times only). This is due to a stock-ram torsional movement about axis Y. In static mode, the portal is a more rigid structure than the monocolumn with a maximal difference (1.91 times) in the longitudinal direction X. In other directions, the portal is one and half times stiffer than the monocolumn.

Table 1. Spindle static rigidity for configurations "Monocolumn" and "Portal" along coordinate axes

Milling spindle rigidity by axes, N/μm	Monocolumn (J^{st}_{mono})	Portal (J^{st}_{port})	Rigidities ratio $J^{st}_{\text{port}}/J^{st}_{\text{mono}}$
X	61.6	118.3	191%
Y	90.4	135.5	149%
Z	123.7	173.0	139%

The monocolumn has different rigidities in the X, Y, Z directions (e.g., rigidity along Z in double exceeds one along X (Table 1)). The portal demonstrates a more stable behavior when the cutting force vector rotates. Directional rigidities differ no more, than 1.46 times; this is a positive trait of the portal.

Modal analysis and important resonances

Modal analysis disclosed a similarity of eigenmodes patterns for "Monocolumn" and "Portal" configurations. As eigenmode frequencies, so eigenmode shapes are near the same (Table 2).

The main (first, lowest) resonance M1, and the second one M2 proved to be "one-fourth wave" column oscillations in the X and Z directions respectively (Figure 3). Eigenmode M1 includes sledge reciprocation along with the X guides. However, column bending is the dominant movement here.

Eigenmode M3 is described above. Mode M4 excitement leads to (Figure 4a) stock oscillations (0 to 1 transition – named *Y-oscillation*), but mainly to ram-stock pecking. Pecking consists of alternate rotary motion of the stock. Line 1–2 loses horizontal orientation, ram axis 3–4 becomes declined, and the spindle unit 3 displaces considerably from the initial position 0-S due to the "leverage effect".

Pecking is the main pattern for mode M5 and is presented in mode M6 as well. Stock pecking eigenmodes (M4–M6) harms diameter precision of the machining. These modes should be damped or omitted (Portentoso et al., 2017; Stepan et al., 2017). Ram pecking is caused by the stock and Y-guides collective skewing.

Eigenmodes M5–M6 have a complex movement template. Besides stock pecking, they include ram axial oscillation (*Z-oscillation*) and column *XY-swinging* (column top goes to the left when sledge goes to the right along X-guides). Eigenmodes M5–M6 are split. For example, modes M6a and M6b have only different phase angles between Z-oscillations and column XY-swinging.

Table 2. Frequency and shape of eigenmodes

No.	Eigen-mode	Frequency, Hz		Pattern of oscillation movement (1, 2, 3 – order of influence)
		Monocolumn	Portal	
1	M1	11.70	12.48	Rocking along X (along with bed guides)
2	M2	12.72	13.34	Rocking across X (across bed guides)
3	M3	24.29	24.04	Torsion about Y
4	M4	23.51	26.85	Y-oscillation of stock-pack (1) plus stock-pack pecking (2)
5	M5a	30.78	30.44	Stock-pack pecking (1) plus Z-oscillation of rams (2)
6	M5b	–	31.63	Z-oscillation of rams (1) plus stock-pack pecking (2)
7	M6a	38.68	38.29	Z-oscillation of rams (1), XY-plane column swinging (2), stock-pack pecking (3)
8	M6b	38.72	39.02	Z-oscillation of rams (1), XY-plane column swinging (2), stock-pack pecking (3)
9	M7	74.10	70.82	Ram bending in XZ-plane in phase to motor swinging
10	M8	77.98	73.52	Ram bending in XZ-plane in antiphase to motor swinging

Eigenmodes M1–M6 excitation embrace all machine tools so that the modes should be called *whole-machine* ones. Modes M1–M6 pertain to low-frequency interval and M5–M6 to middle-frequency one. Modes M7–M8 relate to local and high-frequency resonances. Here (Figure 4b), only ram bending is observed. The ram console (1.6 m long) resonates similar to the "one-fourth wave" scheme and the massive motor partially counterbalances ram bending. The spindle unit and the motor move in-phase for M7 mode and in an antiphase manner at the frequency of M8 mode.

Harmonic analysis

Excitation was provided by harmonic force with 1 kN amplitude, directed one by one along X, Y, Z. Force was applied at the boring and milling spindle ends (arrows on Figures 1, 3, 4). This is the *frequency response function* (FRF) entry parameter for every figure. Displacement amplitude, in the place of force application, serves as the FRF's exit parameter. The FEA tests were provided with the frequency step of 1 Hz in the interval 0–100 Hz for a damping ratio of 4%, uniformly distributed across structural parts.

The spindle unit did not reveal its own dynamics at such relatively low frequencies. The first resonance of the spindle unit – "spindle bends in bearings" – was observed at 211.8 Hz. At all FRFs shown below, special attention should be paid to resonance peaks higher than 50 µm. It means that dynamic rigidity decreases below threshold 20 N/µm.

A pair of milling spindle FRFs are represented in Figure 5 for the case of longitudinal (X) excitation.

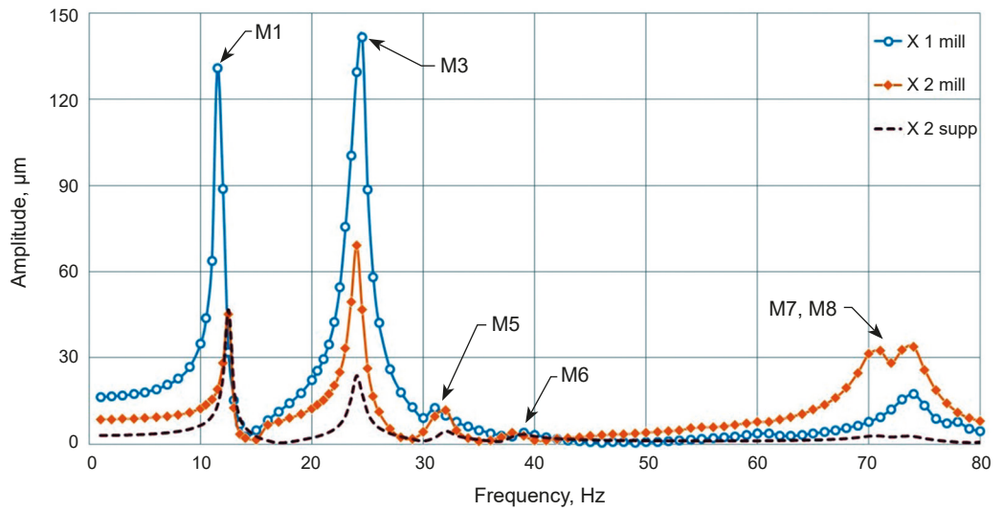

Figure 5. Milling spindle longitudinal FRF (spindle force F_x^d along X – spindle face displacement along X) for monocolumn (X 1 mill) and portal (X 2 mill)

Curve "X 1 mill" relates to the monocolumn structure and curve "X 2 mill" relates to the portal one. Curve "X 2 supp" presents a supporting face (at stock) amplitude. The leverage effect of long ram is absent here. So, curve "X 2 supp" describes column movements and is the lowest on the picture.

The FRF in Figure 5 demonstrates whole-machine resonance peaks (M1–M6). On the left from M1, pre-resonance (static) interval is placed (≤ 10 Hz). On the right from the weak peak M6, post-resonance interval is stretched. It is interrupted by local-character resonances M7–M8. The range from ~35 to ~65 Hz seems to be very calm and appropriate for intermittent cutting.

The main conclusion from the FRF in Figure 5 is that a monocolumn-to-portal transition effectively reduces resonance peaks, thus only for whole-machine resonances. The spindle amplitude is lowered by 2.9 times for bending eigenmode M1 and by 2.04 times for torsional mode M3.

Critically high amplitudes (≥ 50 μm) are observed for portal configuration only inside a narrow frequency slot (23.5–24.5 Hz) if mode M3 is excited. Other resonance frequencies permit intermittent cutting (a form of dynamic excitation). The possibility to machine near resonance will be named below *resonance overriding* (RovR).

Figure 6 presents the monocolumn and the portal FRFs in the Y direction (force F_y^d at the milling spindle end – displacement Y amplitude in the same position). Undoubtedly, the portal is a much more rigid structure in the low-frequency resonances vicinity. The peak of the strong M2 mode is 2.27 times lower for the portal than for the monocolumn.

The portal effectively counteracts to stock-pack pecking M4 (dynamic rigidity higher by 2.78 times) signifying that resonance M4 was dangerous for the monocolumn in case of vertical excitation. Here stock skewing is significantly amplified by the leverage effect at the long, advanced ram.

The level of modes M5, M6 excitation is similar for both configurations of the "travelling column". This is because of the local scale of ram axial oscillations along Z. Such resonance may be reduced by a *tuned-mass damper* (TMD) or more complicated solutions (Munoa et al., 2013).

Generally, the DCP is a positive design solution to withstand resonance excitation in the vertical direction. Machining with RovR is permissible for all whole-machine resonances.

Harmonic force F_z^d was applied in Z direction to the end of the boring spindle. A related pair of FRFs (Figure 7) pointed out to strong excitation in mode M2. Bending oscillations of a monocolumn are inappropriately high with the amplitude reaching 88 μm and the rigidity going down to 11.3 N/μm. The monocolumn-to-portal coupling increases rigidity by 1.69 times just to the threshold $[J_z^{\text{thres}}] = 20$ N/μm. The portal creation matches with other measures of auto-oscillation prevention (Muhammad et al., 2017).

The portal influences the dynamic rigidity near M4–M6 in an alternative manner. Column-to-portal coupling enhances rocking about M4–M5. On the other hand, it damps oscillation near the M6 peak. The monocolumn FRF in Figure 7 ("Z 1 bore") demonstrates peak M1 i.e., bending resonance in the X direction. Such resonance may be excited by

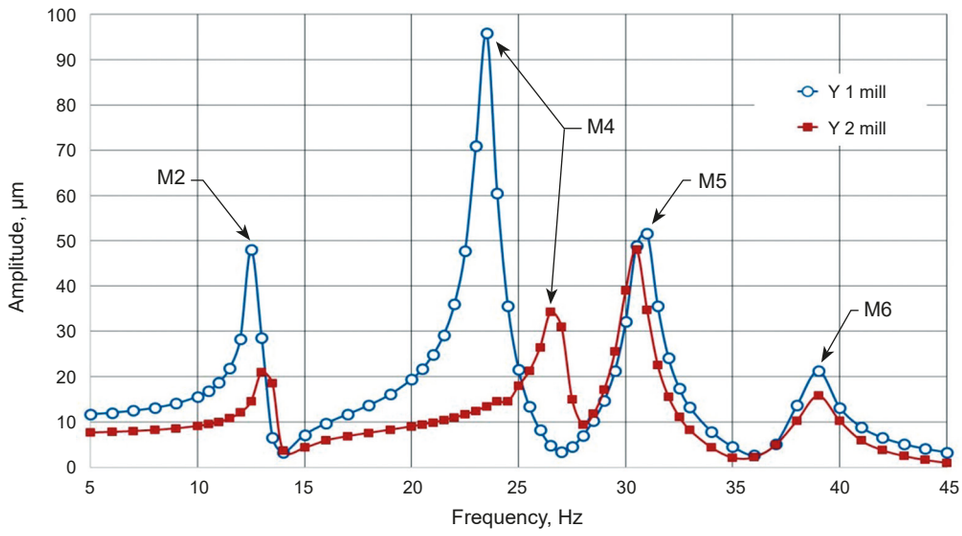

Figure 6. Vertical milling spindle FRF (spindle force F_y^d along Y – spindle displacement along Y) for structures: "Monocolumn" (Y 1 mill) and "Portal" (Y 1 mill)

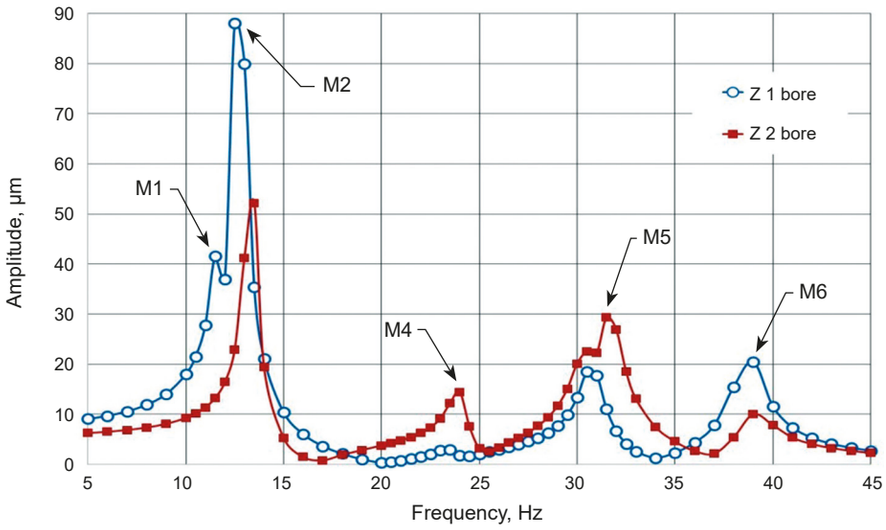

Figure 7. Axial boring spindle FRF (spindle force F_z^d along Z – spindle displacement along Z) for structures: "Monocolumn" (Z 1 bore) and "Portal" (Z 1 bore)

force F_z^d in Z direction only by the developed effect of oscillation crossing. The portal FRF ("Z 2 bore") has no definite M1 peak. Thus, portal configuration alleviates crossing effect. This is useful for cutting process precision and stability.

Discussion

Simulation has shown the portal structure ability to damp effectively low frequency, rough resonances M1–M4. It is not dependent on the cutting force current direction. Also, torsional resonance M3 alleviation is the most valuable feature of the "Portal" configuration. Resonant stock pecking is restrained differently by columns-to-portal coupling. No one peak is weakened for the set of "M5a, M5b, M6a, M6b" peaks The portal withstands effectively only if stock skewing is forced from X and Y directions. Axial (Z) ram oscillations (consisting of M5, M6 eigenmodes) are ambivalent to monocolumn and portal structures. As well, high-frequency ram bending (M7, M8) is not influenced by changes in machine tool configuration. The portal should be created if cutting is intermittent, with leading force harmonics at frequencies ≤ 40 Hz. Ram Z-oscillation may be counterbalanced by additional harmonic moment from the drive Z motor. Such intellectual functions are included in options for modern CNC systems.

Conclusions

Left to right monocolumns coupling into portal have enhanced spindle static rigidity by 1.91, 1.49, 1.39 times along X, Y, Z axes (for RHS case), respectively. A rigidity level of at least 118 N/µm is provided for most flexible direction X (with fully advanced ram).

Monocolumn-to-portal joining influences the eigenmode pattern which is a little concerning as frequencies shape the resonance. Whole-machine eigenmodes remain the same. The portal structure creation significantly damps resonance peaks M1, M2, M3, M4 (range 12–38 Hz) by 1.7–2.9 times. Dynamic rigidity doubles (204%) for the most dangerous, torsional resonance M3 (24.04 Hz). The portal structure may be ineffective for higher frequency resonances, tied with axial oscillation (M5, M6) and ram bending (M7, M8) inside the stock. Due to main FRFs peak lowering, the portal structure allows *resonance overriding* (*RovR*) for all whole-machine resonances. This means admissibility to machine workpieces just at resonance frequencies in all investigated range from 0 to 89 Hz. Intermittent cutting excitation on M1–M4 frequencies does not lead to the portal losing critical rigidity, as well as cutting auto-oscillation.

Monocolumn-to-portal transition reduces the crossing of oscillation between the X and Y direction. It is important to secure the diametrical accuracy of workpiece holes. Coupling monocolumns into the portal is recommended to decrease machine tool vibrations if technological force frequencies are below 40 Hz. If intermittent cutting is speedier, monocolumns with raised high stock become more stable itself for the effect of post-resonance damping. There is no need for additional reinforcement of such a column.

References

1. Herrero, A. & Bueno, R. (2001) *Development of the three axes travelling column ultraprecision milling machine*. 10th International Conference on precision engineering in Iokohama: Initiatives of precision engineering at the beginning of the millennium, pp. 529–533. Japan.
2. Jafarzadeh, E. & Movahhedy, M.R. (2017) Numerical simulation of interaction of mode coupling and regenerative chatter in machining. *Journal of Manufacturing Processes* 27, pp. 252–260.
3. López De Lacalle, L.N. & Lamikiz, A. (Eds.) (2008) *Machine Tools for High Performance Machining*. London: Springer-Verlag.
4. Lu, K., Lian, Z., Gu, F. & Liu, H. (2018) Model-based chatter stability prediction and detection for the turning of the flexible workpiece. *Mechanical Systems and Signal Processing* 100, pp. 814–826.
5. Muhammad, B.B., Wan, M., Feng, J. & Zhang, W.-H. (2017) Dynamic damping of machining vibration: a review. *International Journal of Advanced Manufacturing Technology* 89, pp. 2935–2952.
6. Munoa, J., Mancisidor, I., Loix, N., Uniarte, L.G., Barcena, R. & Zatarain M. (2013) Chatter suppression in the ram-type travelling column milling machines using biaxial inertial actuator. *CIRP Annals* 62 (1), pp. 407–410.
7. Olvera, D., López De Lacalle, L.N., Compean, F.I., Fz-Valdivielso, A., Lamikiz, A. & Campa, F.J. (2012) Analysis of tool tip radial stiffness of turn-milling centers. *International Journal of Advanced Manufacturing Technologies* 60, pp. 883–891.
8. Portentoso, M., Pennacchi, P. & Chatterton, S. (2017) Comparison of the dynamic response of two columns of milling machines made of standard carpentry and metal foam sandwiches. *Journal of Vibration and Control* 23 (17), pp. 2782–2794.
9. Stepan, G., Kiss, A.K., Ghalahamchi, B., Sopanen, J. & Bachrathy, D. (2017) Chatter avoidance in cutting highly flexible workpieces. *CIRP Annals* 66 (1), pp. 377–380.
10. Vasilevich, Y.V., Dounar, S.S. & Karabaniuk, I.A. (2016) Finite element analysis of concrete filler influence on dynamic rigidity of heavy machine tool portal. *Science & Technique* 15 (3), pp. 233–241.
11. Vasilevich, Y.V., Dovnar, S.S., Truskovsky, A.S. & Shumsky, I.I. (2015) Modelling and analysis of dynamics in bearing system of drilling, milling and boring machine with mono-column. *Science & Technique* 3, pp. 9–19.
12. Zienkiewicz, O.C. & Taylor, R.L. (2000) *The finite element method. Volume 1, Basis*. Oxford, Boston: Butterworth-Heinemann.

Cite as: Dounar, S., Iakimovitch, A. & Jakubowski, A. (2021) Finite element analysis of the dynamically created portal in the huge machine tool of “travelling column” type. *Scientific Journals of the Maritime University of Szczecin, Zeszyty Naukowe Akademii Morskiej w Szczecinie* 65 (137), 29–37.

Scientific Journals
of the Maritime University of Szczecin

Zeszyty Naukowe
Akademii Morskiej w Szczecinie

2021, 65 (137), 38–50
ISSN 1733-8670 (Printed)
ISSN 2392-0378 (Online)
DOI: 10.17402/459

Received: 13.10.2020
Accepted: 18.02.2021
Published: 31.03.2021

Numerical simulation of the seakeeping of a military trimaran hull by a novel overset mesh method in regular and irregular waves

Parviz Ghadimi[1], Saeid Karami[2], Amin Nazemian[3]

[1] https://orcid.org/0000-0002-9315-5428
[2] https://orcid.org/0000-0001-8959-3487
[3] https://orcid.org/0000-0001-6861-4488

[1,3] Amirkabir University of Technology, Department of Maritime Engineering
424 Hafez Ave, Tehran, Iran, e-mail: {pghadimi; anazemian}@aut.ac.ir
[2] Malek Ashtar University, Department of Maritime Engineering
Tehran, Iran, e-mail: s_karami_mut_ac@dr.com
corresponding author

Keywords: trimaran, hydrodynamic performance, seakeeping, overset mesh, numerical simulation, regular and irregular waves

JEL Classification: C61, C63, C65, L95

Abstract

The hydrodynamic performance of trimaran hulls has been previously investigated for optimum performance in calm water, but there is still a limited understanding of its motion response; therefore, a CFD-based numerical approach was developed and applied on a trimaran hull in the presence of regular and irregular waves. To validate the CFD method, a comparison was conducted using both experimental and 3D panel method data. In this study, two different turbulence models were surveyed, and the SST Menter k-Omega (k-ω) turbulence model was shown to be a more accurate model than the realizable k-Epsilon (k-ε) model. The different features of the proposed numerical model include the implementation of an overset mesh method, unique mesh plan refinement, and wave-damping region. The discrepancy between the experimental data and the results of other seakeeping calculation methods have always been problematic, especially for low-speed strip theory and 3D panel methods, but good consistency was observed between the proposed CFD model and experimental data. Unlike potential-based or conformal mapping seakeeping analysis methods, the effect of nonlinear waves, hull shape above the waterline, and other ship dynamic phenomena were considered in this CFD application. The proposed CFD method reduces the simulation time and computational efforts for ship motion calculations.

Nomenclature

A_w – wave amplitude (a.k.a. ξ_0 or ξ_3)
a_0 – vertical acceleration
B – overall ship breadth
C_T – total resistance coefficient
C_μ – realizable timescale coefficient (empirical)
Fn – Froude number = $\sqrt{\frac{U}{gL_{pp}}}$
g – gravitational acceleration
H_w – wave height
H_s – significant wave height
k_{xx} – radii of gyration for roll motion
k_{yy} – radii of gyration for pitch motion
k_{zz} – radii of gyration for yaw motion
k – turbulent kinetic energy
k_w – wave number
L_w – wavelength (a.k.a. λ)
L_{pp} – length between perpendicular

L_{wl} – length of waterline
P – pressure
q_ϕ – forcing source term for wave absorbing
r – refinement ratio
R_T – total resistance
T – viscous stress tensor
T_w – wave period
U – ship velocity
u_i – fluid velocity
$\overline{u}_i$ – mean velocity
u'_i – fluctuating velocity
V – volume of cell
V_i – volume of phase i
x^* – wave forcing zone
α_i – volume fraction of phase i
γ – forcing coefficient
μ_t – eddy viscosity
μ – kinematic viscosity
μ_s – vessel's moving direction
ρ – fluid density
η_3 – heave motion
η_4 – roll motion
η_5 – pitch motion
ε – turbulent dissipation rate
υ – kinematic viscosity
λ_s – scale factor
ω_w – wave frequency
ω_e – encounter wave frequency
Δ – ship displacement

Introduction

The hull form of a trimaran consists of a main hull and two side hulls, whose primary duty is to stabilize the ship. The unique features of this type of vessel are appropriate for general arrangements, especially their vast deck area, low resistance at high speed, and suitable resistance against damage. Despite extensive investigations into trimaran design concerning their resistance and components, limited research has been performed on seakeeping and real sea conditions. Most studies have concluded that the dynamic performance of these vessels is better than equivalent monohull vessels (Elcin, 2003; Ghadimi, Nazemian & Sheikholeslami, 2019; Gong et al., 2020). Most research has been conducted for resistance calculations and trimaran hull configurations that affect the flow characteristics around the hull (Xu & Zou, 2001; Sahoo & Lawrence, 2005; Slutski, 2008; Yanuar et al., 2013; Brizzolara et al., 2015; Akbari Vakilabadi et al., 2018; Nazemian & Ghadimi, 2020a). Hydrodynamic investigations in calm water are significantly different from wavy water surfaces. Few studies have been devoted to seakeeping analyses of trimarans (Pastoor, Van't Veer & Harmsen, 2004; Fang & Too, 2006; Chou et al., 2008; Deng et al., 2019). The non-compliance between numerical and experimental results are problematic, especially for low-speed strip theory and 3D panel methods (Kurultay, 2003; Grafton, 2007; Dobashi, 2014). Due to the use of potential theory, most previous numerical approaches are limited in terms of considering the effect of viscosity and turbulence. Furthermore, traditional seakeeping analyses are limited to some constraints like linear theory, zero-speed conditions, wall-sided hulls, etc. (Bertorello et al., 2001; Yang et al., 2002; Doctors, 2015; Wang, Ma & Duan, 2018; Du, Hefazi & Sahoo, 2019; Li & Li, 2019).

CFD simulations of ship motion have been conducted in the past decade due to improvements in computer systems and CFD solvers. Simonsen et al. (Simonsen et al., 2013) performed a comprehensive CFD and EFD study on a KCS ship hull based on ship motion under different maritime conditions. Their research served as a benchmark study and uncertainty analyses for similar attempts. Wu et al. (Wu et al., 2011) studied a high-speed trimaran in regular head waves by using a CFD solver and compared their results with experimental data. Wu et al. proved the appropriate performance of the CFD tool by RANS equation solutions for seakeeping analyses.

CFD-based advanced studies have been developed in the past decade by some researchers. Hebblewhite et al. (Hebblewhite, Sahoo & Doctors, 2007) performed numerical and experimental investigations to determine the effects of the longitudinal position of the side hulls on the motions in the heave and pitch of a trimaran hull. Jia et al. (Jia, Zong & Shi, 2009) studied the resistance and seakeeping characteristics of a transom stern trimaran for different Froude numbers and sidehull arrangements. Tezdogan, Demirel, and Turan (Tezdogan, Demirel & Turan, 2014) used the RANS equation solver to study the seakeeping and operability of a commercial marine vessel. Another research of Tezdogan et al. (Tezdogan et al., 2014) illustrated that the RANS solver considers the effects of breaking waves, turbulence, and viscosity, which are not considered in the numerical simulations based on potential flow theories. Ghadimi et al. (Ghadimi, Nazemian & Ghadimi, 2019) investigated the sidehull arrangement of a wave-piercing trimaran in the presence of regular waves with different characteristics. They concluded that a lower stagger distance and higher clearance of the sidehull improved the seakeeping of a trimaran hull. Nowruzi et al. (Nowruzi et al., 2020) simulated

a trimaran hull using the CFD tool in different turbulence models and gridding configurations.

The surveyed literature shows that CFD solvers can predict the calm water resistance more accurately than other analytical or potential-based resistance calculation methods. Nevertheless, seakeeping performance assessments by CFD solvers require long computing times and effort, which are not suitable for comprehensive industrial investigations; thus, there is a lack of accurate and fast CFD approaches for the dynamics of marine vehicles. This paper has two main purposes. First, a low-cost and efficient CFD tool is developed for seakeeping analyses of marine vessels. Second, the response motion of a military trimaran hullform is surveyed in regular and irregular waves. To accomplish these tasks, a wave-piercing bow trimaran hull was simulated in the presence headsea waves by using a RANS equation solver (Star CCM+). Computations were validated and verified by available experimental data and Ansys AQWA solver. The experimental results of Akbari Vakilabadi et al. (Akbari Vakilabadi, Khedmati & Seif, 2014) and the 3D panel method were implemented to compare CFD calculations, and the main differences are discussed. A seakeeping study of a wave-piercing bow trimaran was implemented at different Froude numbers of 0.37 and 0.51 at different wavelengths. Ship motion was simulated by an overset mesh zone, which led to high-quality gridding around the hull. In addition, a VOF wave forcing method was applied to the numerical CFD model to create a damping zone to avoid the blockage effect and was extended to virtual towing tank boundaries, which reduced the number of meshes. Finally, a comparison of the obtained results illustrated the capability and superiority of the applied seakeeping analyses method for regular and irregular wave conditions.

Problem definition

Due to the numerous maritime conditions for seagoing ships, the numerical analysis method should not be time-consuming in the design process. The selected methods must be both accurate and efficient. For example, simple seakeeping analyses for a ship consists of 240 runs (1).

Every run takes one day of CPU-time (see the presented example of relation (1)). Different maritime and sea environment conditions in seakeeping analyses lead to variations in ship operation modes. Two ship weight loading cases, two different ship speeds, two sea states and their corresponding wave

$$\frac{\text{ship weight}}{2}\cdot\frac{\text{speed (kn)}\,[16.30]}{2}\cdot \frac{\text{wave height (m)}\,[4.6]}{2}\cdot \frac{\text{heading (deg)}\,[180,135,90,45,0]}{5}\cdot \frac{\text{wave length}\,[0.5L,0.75L,1L,1.25L,1.5L,2L]}{6}=240 \quad (1)$$

heights, five heading angles, and six wavelengths are the seakeeping parameters used to construct a RAO plot; therefore, CFD analyses are not an efficient or acceptable method for seakeeping studies. In this regard, the present paper offers a numerical simulation that reduces the processing time without reducing accuracy. The present investigation includes a damping force method, gridding technique, and numerical parameters for the simulation, such as a turbulence model and time discretization methods. In this study, a model of wave-piercing bow trimaran ships is studied. The dimensional characteristics of this ship and model (λ_s = 80) are shown in Table 1. The ship has a wave-piercing bow, and the lateral bodies are made in the form of a Wigley hull that has been studied by Akbari Vakilabadi et al. (Akbari Vakilabadi, Khedmati & Seif, 2014). Figure 1 shows the 3D view of the trimaran model that was used in their tests. During rotation, radii of gyrations must be defined, which are presented in the last two rows of Table 1. k_{xx} is the radius of gyration of roll motion and is defined to be equal to 0.444 B; k_{yy} and k_{zz} are the radius of gyration for the pitch and yaw motions, respectively, which are equal to 0.246 L; L is the ship length; B is the overall trimaran beam.

Table 1. Specifications of the trimaran ship hull: the main vessel and the model type (Akbari Vakilabadi, Khedmati & Seif, 2014; Nazemian & Ghadimi, 2020b)

Specifications	Main vessel	Model
Overall length (m)	124	1.55
Draft length (m)	123.2	1.54
Total width (m)	22.2	0.2722
Main hull width (m)	5	2.5
Side hull length (m)	36	0.45
Draft (m)	4.384	0.0548
Clearance (side hull transverse distance)	9.7	0.1212
Stagger (side hull longitudinal distance)	0	0
Displacement	2248.8 (Ton)	4.39 (kg)
x-axis of the radii of gyration ratio (k_{xx}/B)	0.444	
y- and z-axis of the radii of gyration ratio (k_{yy}/L, k_{zz}/L)	0.246	

Figure 1. 3D view of the studied trimaran ship

Numerical scheme

Utilizing the Reynolds-Averaged Navier-Stokes (RANS) equation solver, seakeeping simulations were performed by StarCCM+ software. Furthermore, two different turbulent models are surveyed: the realizable k-ε and the SST Menter k-ω approach. The physical model was selected based on the StarCCM+ user guide (User Guide, 2020) and ITTC recommendations (ITTC Recommendations, 2011; 2014). The unsteady scheme with a physical time step of 0.01 s was used for temporal discretization, and the SIMPLE algorithm was applied for coupling the pressure and velocity equations. The governing equations of continuity in equation (2) and momentum conservation in equation (3) for the three-dimensional incompressible flow are expressed as follows:

$$\frac{\partial u_i}{\partial x_i} = 0 \tag{2}$$

$$\frac{\partial u_i}{\partial t} + \frac{\partial}{\partial x_i}\left(u_i u_j\right) = \\ = -\frac{1}{\rho}\frac{\partial p}{\partial x_i} + \mu\frac{\partial}{\partial x_j}\left(\frac{\partial u_i}{\partial x_j} + \frac{\partial u_j}{\partial x_i}\right) + \frac{\partial}{\partial x_j}\left(-\overline{u_i' u_j'}\right) \tag{3}$$

The mean pressure is represented by p, the fluid density ρ, and the kinematic viscosity of the fluid μ, where the velocity u_i can be decomposed into the mean velocity $\overline{u}_i$ and fluctuating velocity u'_i, which is expressed by equation (4):

$$u_i = \overline{u}_i + u_i' \tag{4}$$

The Reynolds stress tensor that appears in the momentum transport equation is calculated by:

$$\overline{u_i' u_j'} = -\mu_t\left(\frac{\partial u_i}{\partial x_j} + \frac{\partial u_j}{\partial x_i}\right) + \frac{2}{3}\delta_{ij}k \tag{5}$$

where μ_t is the eddy viscosity, which can be calculated by different methods. Two basic turbulence models, realizable k-ε and SST K-Omega approaches are applied herein. The turbulent viscosity (μ_t) for realizable k-ε and SST K-Omega turbulence models was calculated using equations (6) and (7), respectively:

$$\mu_t = C_\mu \frac{k^2}{\varepsilon} \tag{6}$$

$$\mu_t = kT \tag{7}$$

where C_μ is a realizable time scale coefficient; k is the turbulent kinetic energy; ε is the turbulent dissipation rate; T is the viscous stress tensor. The volume of fluid method was applied to capture the free surface of water. The fields of the phase volume fraction describe the distribution of phases and the interface position α_i. The volume fraction of phase i is defined as:

$$\alpha_i = \frac{V_i}{V} \tag{8}$$

where V is the volume of a cell, and V_i is the volume of phase i in the cell. The volume factions of all phases in this cell are satisfied with equation (9):

$$\sum_{i=1}^{N} \alpha_i = 1 \tag{9}$$

where N is the total number of phases. Since there are two phases (water and air), $N = 2$.

Two regular and irregular waves were applied in the seakeeping analyses by defining VOF waves. In the surrounding boundaries, a wave force function was added to the fluid transport (momentum) equations. The forcing source terms adapted the solution to the simplified solution that was imposed at the reduced domain boundary. This forcing term resolves wave reflection problems at the boundaries (Kim, O'Sullivan & Read, 2012; Kim et al., 2019; User Guide, 2020). This source term is defined by equation (10):

$$q_\phi = -\gamma\rho\left(\phi - \phi^*\right) \tag{10}$$

where γ is the forcing coefficient, which is expressed by equation (11); ρ is the fluid density; ϕ is the current solution of the momentum equation; ϕ^* the value regarding the forced solution. The defined forcing zone and its distance are displayed in Figure 2. The forcing source term was not applied within the inner zone (3D Navier-Stokes), but within the outer zone (Forcing zone), the forcing source term was activated along the solution domain boundaries. The forcing coefficient (γ) varied smoothly from zero at the inner edge of the forcing zone (x^*) to the maximum value at the boundary (the outer edge of the forcing zone) (Kim et al., 2019; User Guide, 2020).

$$\gamma = -\gamma_0 \cos^2\left(\frac{\pi x^*}{2}\right) \tag{11}$$

The inner and outer edges of the damping zone are respectively represented by x_{sd} and x_{ed}. Accordingly, $\cos^2$ is defined by:

$$\frac{\pi x^*}{2} = \frac{\pi}{2} + \frac{\pi}{2}\frac{x - x_{sd}}{x_{ed} - x_{sd}} \Rightarrow \text{herein}: x^* = \frac{x}{1.5} \quad (12)$$

The damping zone and forcing coefficient variation are depicted in Figure 2 by a contour and damping intensity plot.

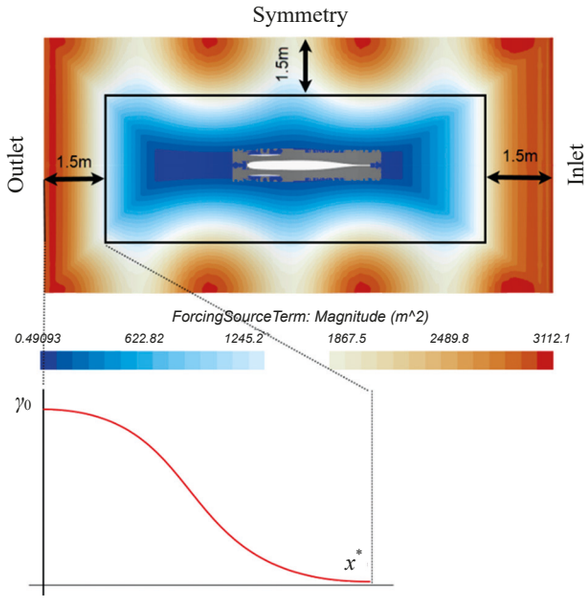

Figure 2. Wave forcing zone and boundary length distance (1.5 m) for the surrounding boundaries

Simulations were conducted by the dynamic fluid body interaction (DFBI) module in order to calculate the ship motions. The ship could freely move with 2 degrees of freedom of heave and pitch motions. The simulation domain and the name of its boundaries are shown in Figure 3. The inlet boundary defines the velocity inlet boundary condition and was located 1.5 *L* in front of the forward perpendicular. The top and bottom of the domain are defined as the inlet velocity and are located 1 *L* and 1.5 *L* from the trimaran's C.G., respectively. The pressure outlet boundary condition was applied at the outlet boundary, which extended 1.5 *L* from the aft perpendicular. The width of the virtual tank is 1 *L*, and the symmetry plane was defined for the side and symmetry boundaries of the computational domain. All of the defined distance and ship hull locations are displayed in Figure 4.

Mesh study

An unstructured trimmer mesh was adopted for mesh operations following the ITTC recommendations (ITTC Recommendations, 2011; 2014) and Star CCM+ user guide (User Guide, 2020). To capture waves acting on the free surfaces and sharp corners of the hull, surface and volumetric refinements were applied to the volume mesh. 25% of the base size mesh refinement was applied for the *x*-direction and 12.5% anisotropic mesh size was finer in the *z*-direction. *x*-direction and *z*-direction mesh refinement was performed to capture the wavelength and wave height around the free surfaces. Figure 5 illustrates the selected mesh characteristics. A mesh study was implemented to select the appropriate base size of the mesh cell. Mesh refining and grid convergence was continued until the solutions became independent of the mesh size.

The wave elevation on a free surface is a control variable for mesh convergence. The initial mesh

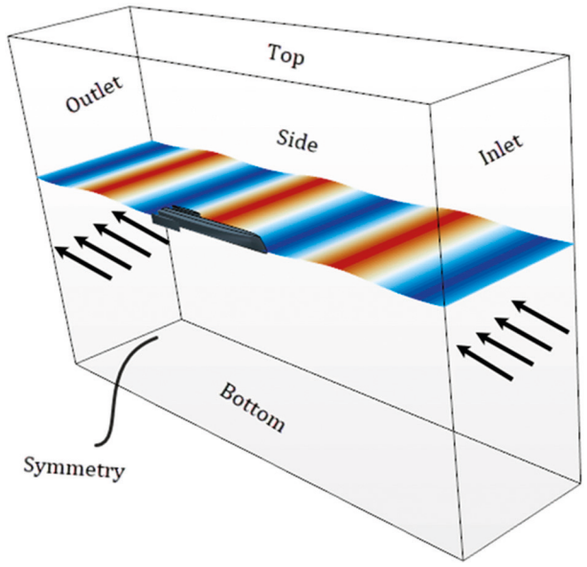

Figure 3. Computational domain and domain boundaries

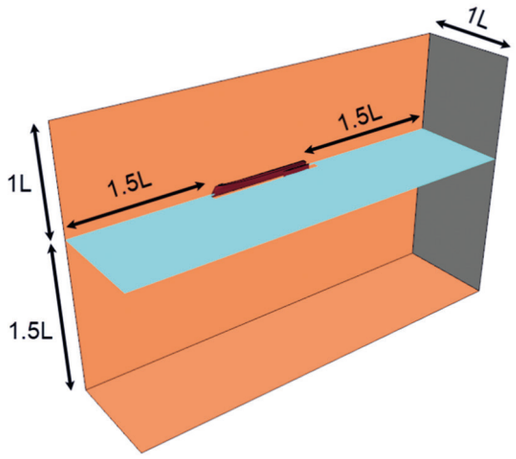

Figure 4. Trimaran ship location of the virtual tank and its boundaries

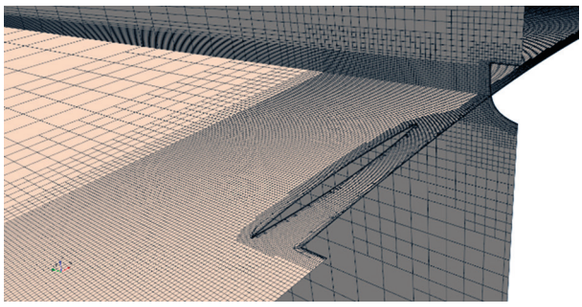

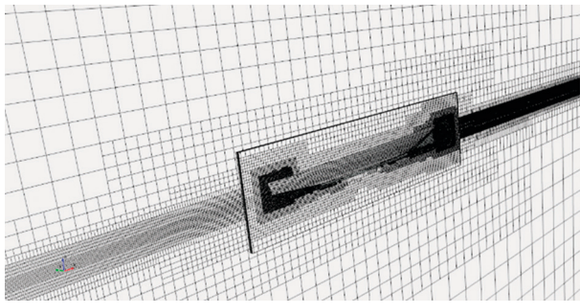

Figure 5. Domain and overset region gridding

size adopted in this investigation was $L_w/60$; four mesh plans were made according to the refinement ratio of $\sqrt[3]{2}$. A regular linear wave was adopted for mesh plan validation. The wave characteristics are described in Table 2, where T_w is the wave period, H_w is the wave height, L_w is the wavelength, k_w is the wave number, and A_w is the wave amplitude. In addition, the specific parameters of the mesh plans are shown in Table 3.

Table 2. Regular wave characteristics

T_w (s)	k_w	L_w (m)	H_w (m)	A_w (m)
1.07	3.5	1.8	0.05	0.025

Table 3. Mesh plan parameters and sizes

Mesh	Base size	Number of cells per wavelength	Number of cells per wave height	Total number
Grid1	0.125	60	12	725,340
Grid2	0.085	80	16	1,004,395
Grid3	0.06	105	20	1,358,273
Grid4	0.042	134	25	1,788,094

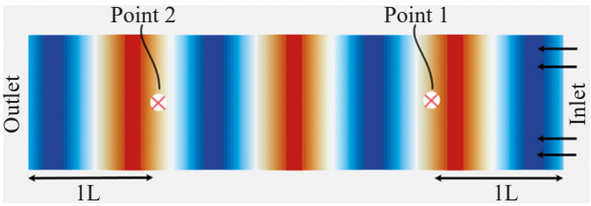

Figure 6. Two history probe points for surface elevation recording

Two history probe points were located 1 L from the inlet and outlet boundaries to record the wave elevation (Figure 6). The wave elevations at different grid plans for points 1 and 2 are shown in Figure 7a and Figure 7b, respectively. When the waves reached point 2, the wave amplitudes were reduced by about 4% compared to Point 1 due to physical and numerical dissipation. The differences in the wave elevation between the incident wave height and the measured wave height at point 2 calculated by these four types of meshes were 3.44%, 2.86%, 1.95%, and 1.52%, from grid 1 to grid 4. Considering the accuracy and computational costs, grid 3 was selected as the optimum mesh plan.

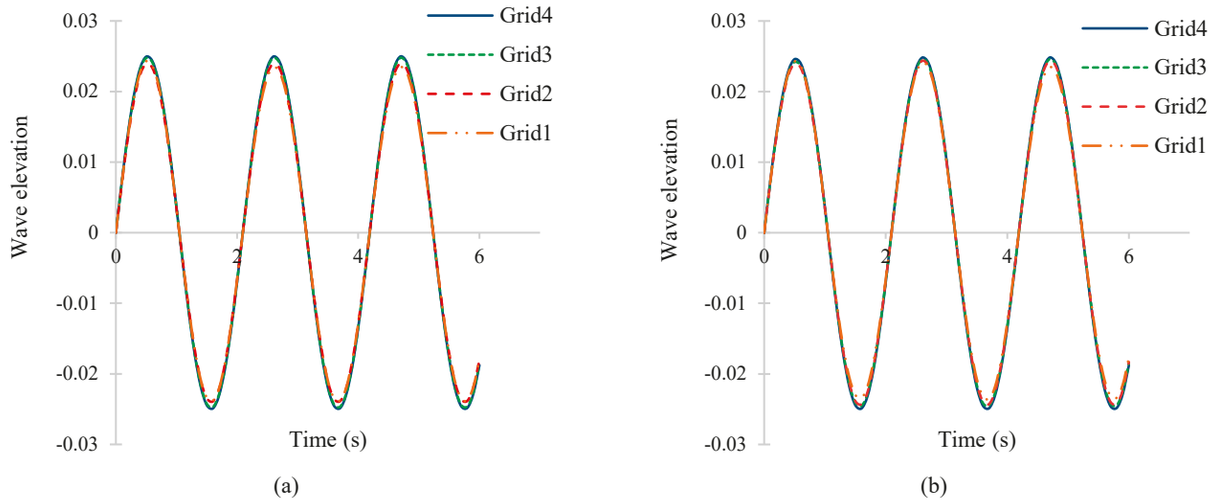

Figure 7. Wave elevation at (a) Point 1 near the inlet boundary and (b) Point 2 near the outlet boundary

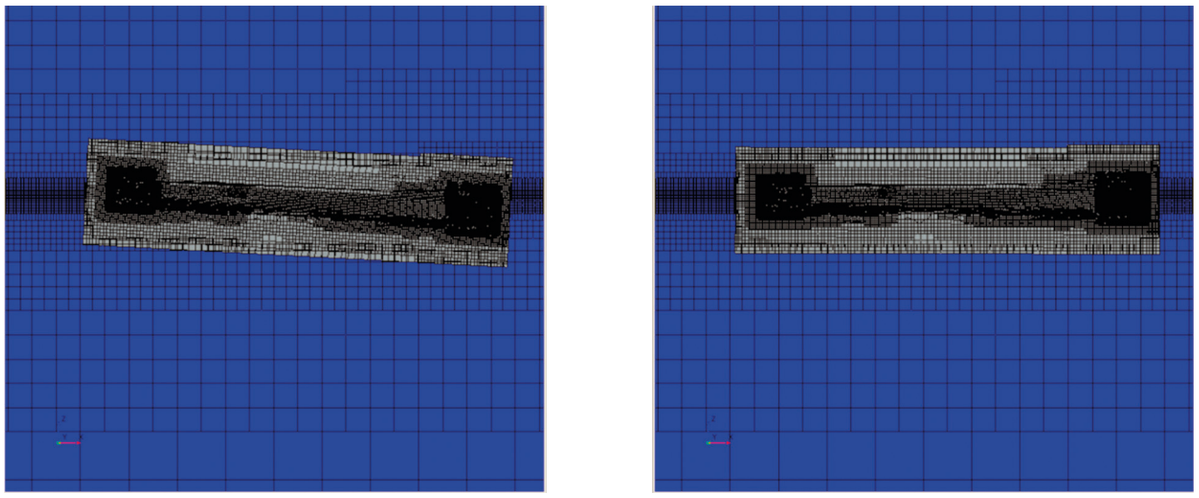

(a) Overset region movement

(b) Baseline overset region

Figure 8. The defined overset mesh regions

Overset mesh

An overset mesh region was developed in the computational domain. A high-resolution mesh configuration near the ship hull and free surface were adopted based on an overset mesh set-up (Simonsen et al., 2013; Nowruzi et al., 2020). The trimaran hull body includes an overset region. The overset mesh region moves with the hull (moving mesh) over a fixed background mesh of the domain. The overset mesh implementation reduces the computational time and generates a refined mesh system without compromising the accuracy. The overset mesh regions for the present numerical simulations are shown in Figure 8. In Figure 8a, the region translates and rotates at the end of the run. Accordingly, Figure 8b displays the initial position of the overset mesh region.

Validation and verification

A comparative study was implemented in two different turbulent models. The k-ω and k-ε models are similar to each other when solving two transport equations, but they are different in the choice of the second transported turbulence variable. The realizable k-ε model defines a new transport equation for the turbulent dissipation rate ε. The realizable two-layer k-ε model combines the model with a two-layer approach (Nowruzi et al., 2020; User Guide, 2020). The k-ω turbulence model is a two-equation model that solves transport equations for the turbulent kinetic energy k and the specific dissipation rate ω – the dissipation rate per unit turbulent kinetic energy ($\omega = \varepsilon/k$) – in order to determine the turbulent eddy viscosity. Menter's SST (shear-stress transport) k-ω model uses the insensitivity to free-stream conditions of the k-ε model in the far-field while retaining the advantages of the k-ω model near walls.

The two turbulence models mentioned above were utilized to examine their effectiveness in this study. In Figure 9, the motions are plotted against the physical time in headsea waves with a 0.025 m amplitude and wavelength of 1.8 m and a ship model speed of 1.44 m/s.

The comparison illustrates that both turbulent methods are suitable for seakeeping analyses, and the values of the SST k-ω turbulent method are closer than the k-ε method to experimental results. So, the SST k-ω turbulent method was selected for the following simulations.

Seakeeping analyses

A seakeeping study was carried out in regular and irregular waves under headsea conditions. The velocity of the ship model was U = 1.44 m/s, corresponding to a Froude number of 0.37. The coordinate system was located on the vessel's center of gravity, and it moves along the x-direction. Figure 10 illustrates the coordinate system and the defined directions of irregular waves. The outputs of the CFD simulations are represented by the response amplitude operator (RAO), and the 3D panel method results were acquired by Ansys AQWA software. To extract statistical parameter values, the moment of the spectrum was calculated. Thus, the wave spectrum was multiplied by the square of the RAOs to obtain the response spectrum. RAO is defined by (Bhattacharyya, 1978):

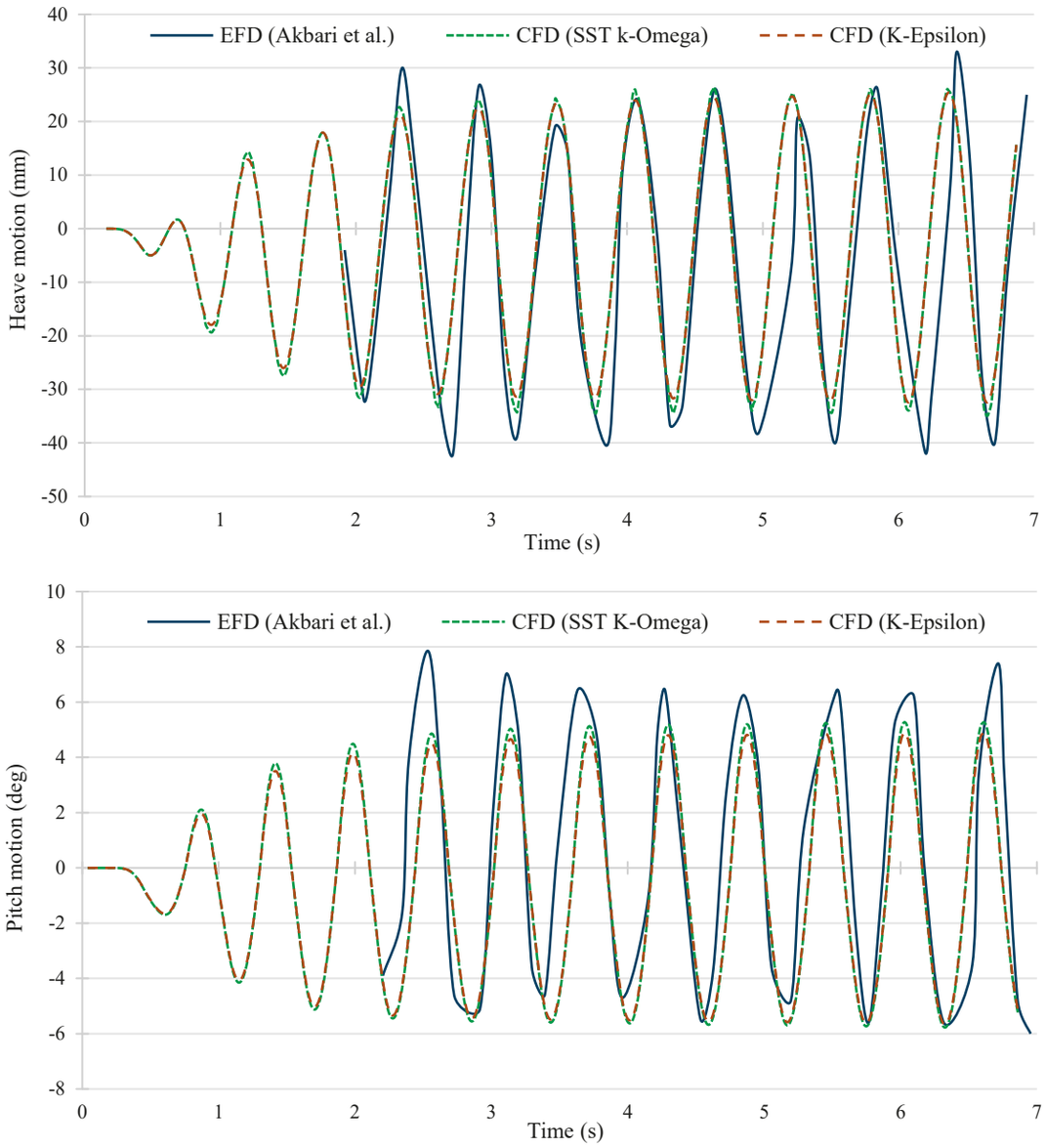

Figure 9. Two turbulence model results and experimental verification for heave and pitch motion in a ship model speed of 1.44 m/s, wave amplitude of 0.025 mm, and wavelength of 1.8 m

$$\text{Heave RAO} = \text{RAO}_3 = \frac{\eta_3}{\xi_0}$$

$$\text{Pitch RAO} = \text{RAO}_5 = \frac{\eta_5}{k\xi_0}$$

$$\text{Vertical acceleration} = \text{RAO}_a = \frac{a_0}{\omega_e^2 \xi_0} \quad (13)$$

$$S_x(\omega_e) = (\text{RAO}_x(\omega_e))^2 S_{\xi_0}(\omega_e), \quad x = 3.5 \quad (14)$$

The parameters η_3 and η_5 represent the heave and pitch motion values, respectively; a_0 is vertical acceleration; ξ_0 represents the wave amplitude (also shown as ξ_3); k is the wave number, which is used to non-dimensionalize the motions. In order to obtain the encounter spectrum $S_{\xi_0}(\omega_e)$ of the vessel from the sea spectrum $S_{\xi_0}(\omega_w)$ and change the wave frequency (ω_w) to the encounter frequency (ω_e), the following equations are used:

$$\omega_e = \omega_w - \frac{\omega_w^2}{g} U \cos\mu_s \quad (15)$$

$$S_{\xi_0}(\omega_e) = S_{\xi_0}(\omega_w) \frac{1}{1 - \frac{2\omega_w U}{g}\cos\mu_s} \quad (16)$$

The vessel's moving direction (μ_s) is 180°. Finally, the significant amplitude of motion and acceleration was calculated by the zeroth moment of the response spectrum.

$$\text{Significant value} = 2\sqrt{m_0} \tag{17}$$

$$m_n = \int_0^\infty \omega_e^n S_x(\omega_e) d\omega_e \Rightarrow m_0 = \int_0^\infty S_x(\omega_e) d\omega_e \tag{18}$$

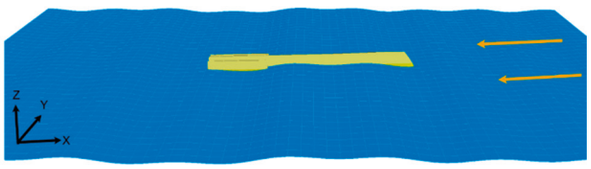

Figure 10. Irregular wave and coordinate system of seakeeping analyses

The experimental results of Akbari Vakilabadi et al. (Akbari Vakilabadi, Khedmati & Seif, 2014) were taken into consideration as an EFD comparison. They tested different wavelength-to-ship length ratios (λ/L) for an under-studied trimaran hull.

Results and discussion

Regular wave computations

The obtained results of the proposed numerical model are compared against experimental data and 3D panel method responses. All results pertain to the seakeeping behavior under headsea conditions and regular waves with an amplitude of 0.025 m. Figures 11 and 12 illustrate the comparison of the obtained RAO values for the vessel's heave motions at two different Froude numbers of 0.37 and 0.51, respectively. Figures 13 and 14 display the RAO values of the pitch motions for the mentioned ship speeds. Parameters η_3, η_4, and η_5 represent the heave, roll, and pitch motion values, respectively. ξ_3 represents the wave amplitude, and k is the wave number that is used to non-dimensionalize the motions. All of the obtained results are expressed for 6 different wavelengths, which include the horizontal axis of the graphs with a dimensionless ratio (λ/L). The CFD results are more consistent with the experimental results; however, the pitch motion results show a slight difference between the CFD and experimental results at Fn = 0.51. Based on the presented

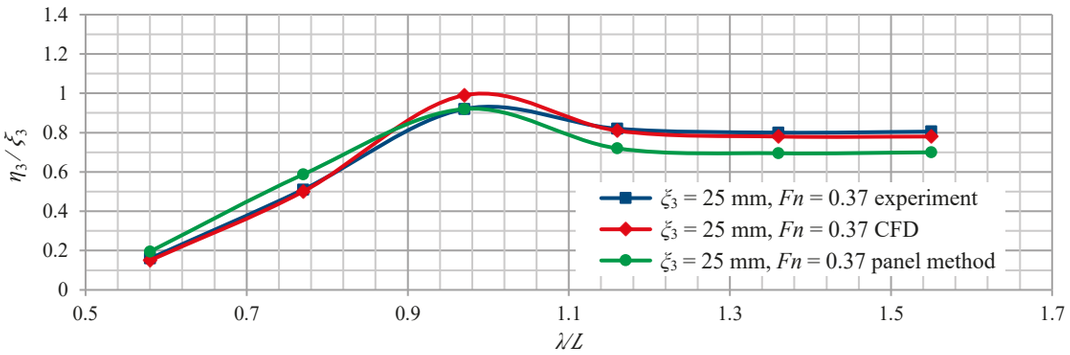

Figure 11. Heave RAO as a function of non-dimensional encountering wavelengths for the trimaran at a Froude number of 0.37 and a wave amplitude of 25 mm

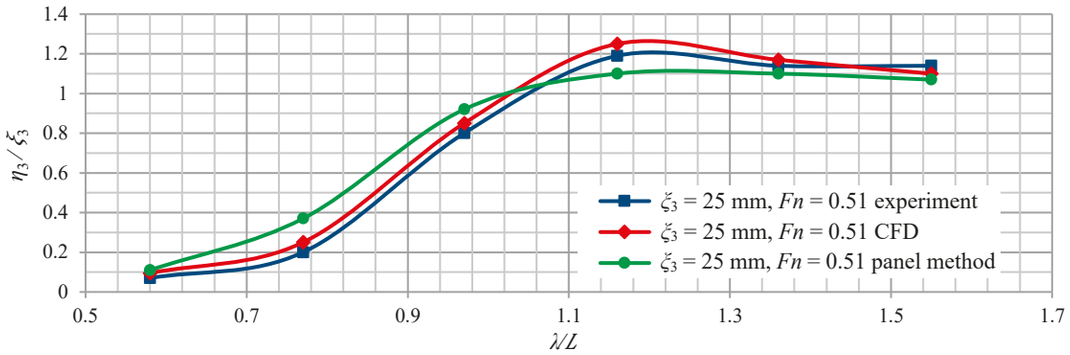

Figure 12. Heave RAO as a function of non-dimensional encountering wavelength for the trimaran at a Froude number of 0.51 and a wave amplitude of 25 mm

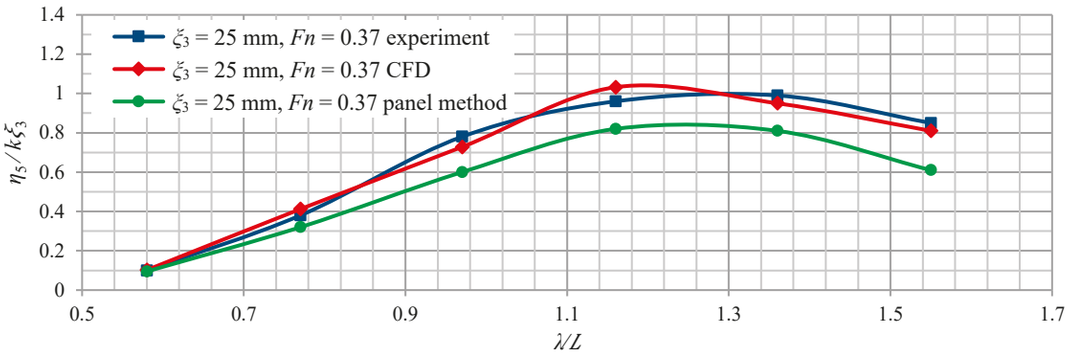

Figure 13. Pitch RAO as a function of non-dimensional encountering wavelength for the trimaran at a Froude number of 0.37 and wave amplitude of 25 mm

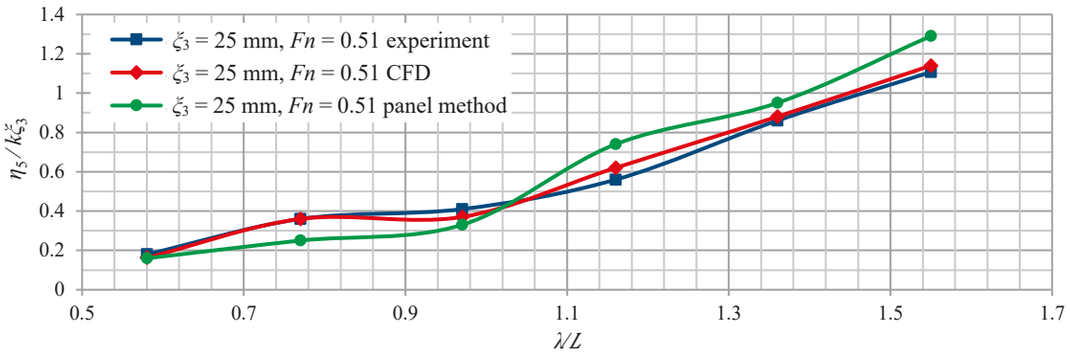

Figure 14. Heave RAO as a function of non-dimensional encountering wavelength for the trimaran at a Froude number of 0.37 and wave amplitude of 25 mm

comparisons, one may conclude that the proposed numerical model can accurately model motion characteristics. There is a significant difference between the 3D panel method results and the CFD and EFD data, especially the pitch motion at both speeds. This inconsistency was due to linearity assumptions and neglecting the effect of variations in the hullform above and below the waterline.

As observed in Figures 11 and 12, the heave motion of the trimaran does not change at high wavelength values. The RAO of the heave motion illustrates that the magnitude of the heave amplitudes was equal to the wave amplitudes at a higher λ/L. In heave motions at different Froude numbers and different pitch motions at $Fn = 0.37$, a resonance peak was observed. Besides, the pitch motion at higher speeds and higher wavelengths yielded rough motion conditions, which caused offensive dynamic phenomena to occur. CFD simulation results were similar to the experiment data at most wavelengths; however, in some cases, the calculated motion response was slightly higher than the measured

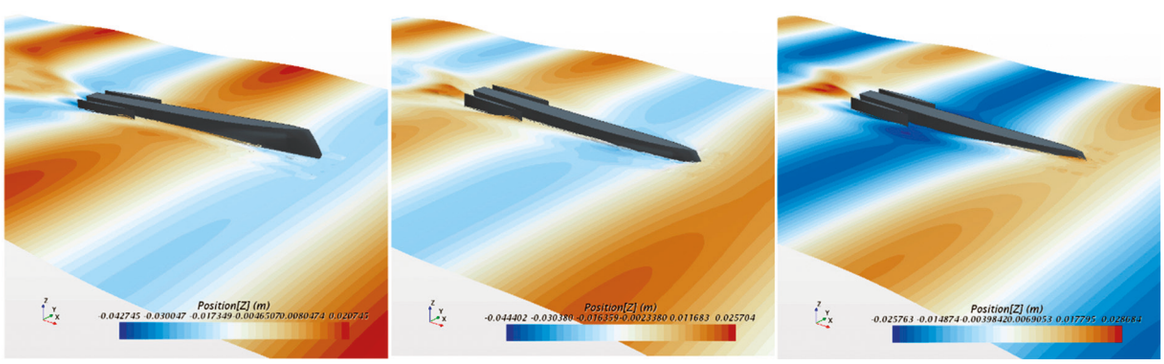

Figure 15. Ship motion at different time steps (i.e., slamming phenomena)

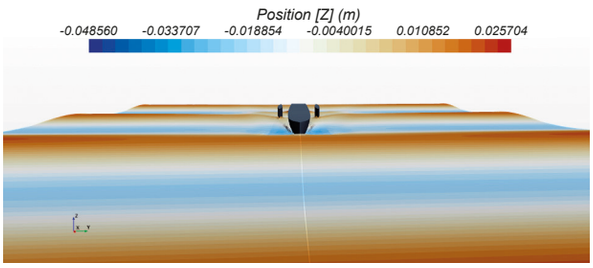

Figure 16. Front view of the ship motion in the presence of a regular wave

experimental value. This seemed to primarily happen at the resonance condition. A possible source of discrepancy may be the wave dissipation among the virtual tank.

Figure 15 shows the ship's motion at different time steps, which shows that regular headsea waves caused slamming phenomena. The forefoot region of the trimaran emerged from the water and then returned to the sea at a high vertical speed. The front view of the ship motion is depicted in Figure 16.

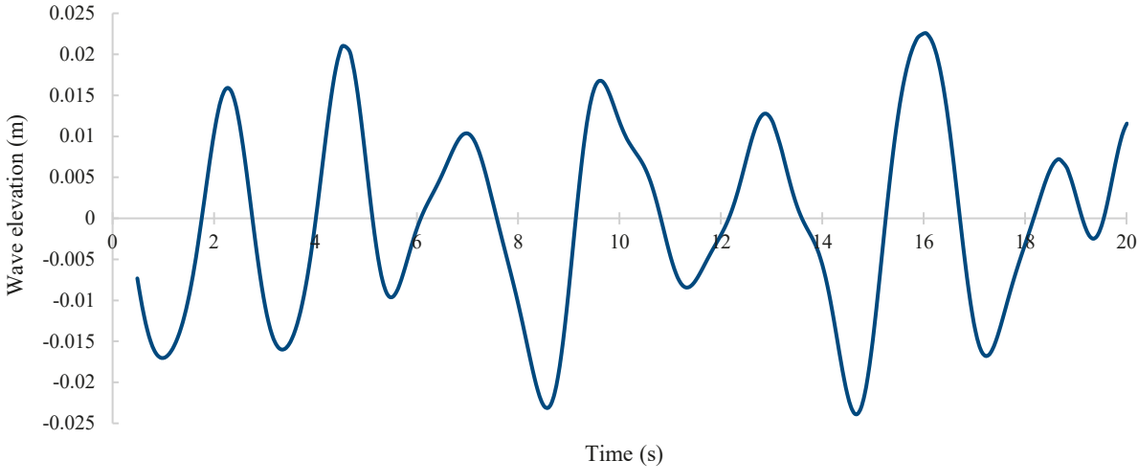

Figure 17. Time history of recorded irregular waves Pierson-Moscowitz spectrum under the headsea condition of *Hs*=0.05 m

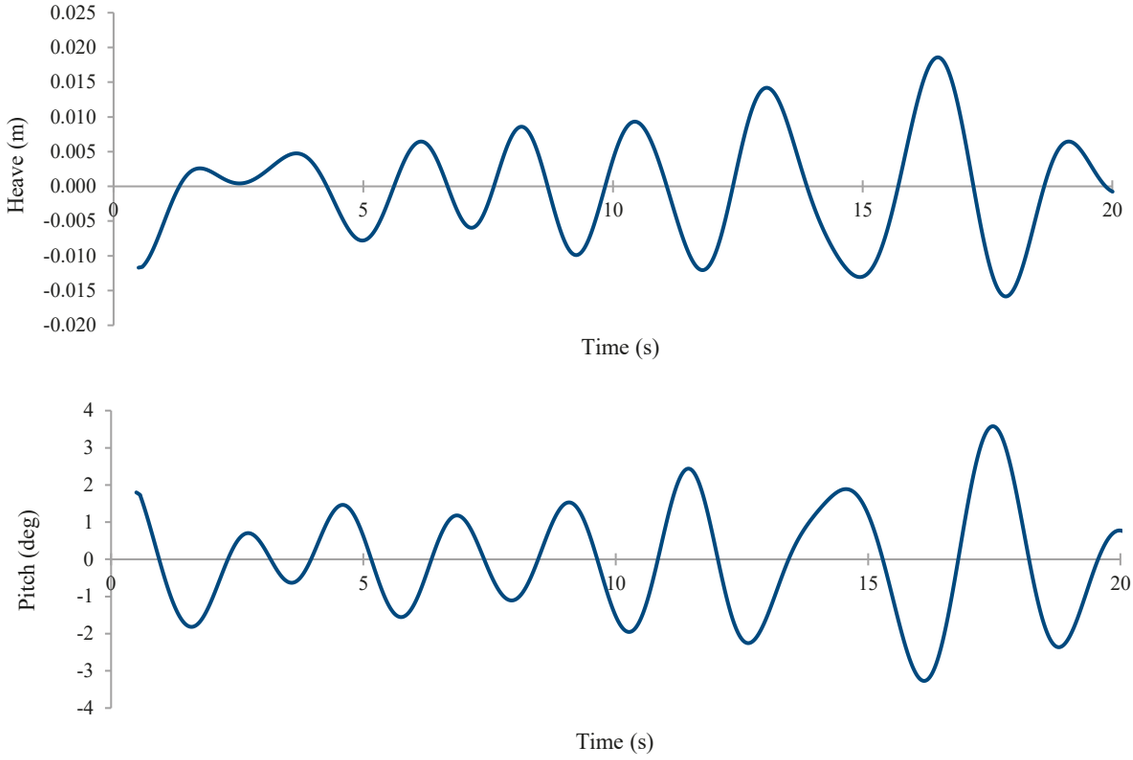

Figure 18. Heave and pitch motion waves encountered at 180° at a Froude number of 0.37

Irregular wave computations

In this section, a seakeeping simulation was carried out in the presence of irregular Pierson-Moscowitz spectrum waves. The significant wave height was considered to be 0.05 m and the modal period was 1.07 s. The ship velocity was 1.44 m/s (for the model) with a headsea. Figure 17 displays the time history of the recorded irregular waves over 20 s, and Figure 18 shows the heave and pitch motions of the hull in irregular time-domain waves.

The performance of the CFD model can be observed in the results. The viscosity effects, nonlinear phenomena, and complex hull bodies are challenges in seakeeping studies that can be analyzed by CFD simulations. Besides, the complicated ship motion in irregular waves can be simulated by considering real sea conditions. The present seakeeping study can be developed for other maritime projects.

Conclusions

Developing a more accurate and efficient numerical tool for seakeeping analyses of marine vessels was the basic aim of this paper. Accordingly, a CFD model for calculating the ship response in regular and irregular head sea waves was established. Two important techniques were used to accomplish this task. An overset mesh technique was implemented to simulate the vessel motion, and a wave forcing equation was applied to create a damping zone around the domain. The wave forcing term was executed in the damping region far from the hull, which reduced the domain size and number of meshes. The CFD results were consistent with the experimental data, as shown by the comparison of the time history for two different turbulent models and RAO plots for heave and pitch motions. Furthermore, two different turbulence models were investigated, and the SST Menter k-ω turbulence model was more accurate than the realizable k-ε model. A comparison of the proposed CFD model and 3D panel method with experimental results illustrated the accuracy and superiority of the present model for different maritime conditions. These comparisons were carried out at two different Froude numbers. The calculated pitch motion data in the 3D panel method was less consistent with the experimental results; however, in both heave and pitch motions, the CFD results showed compliance with the experiment data. In some cases, the CFD calculated motion response was slightly higher than the measured experimental values. A possible source of discrepancy may be the wave dissipation among the virtual tank, especially under resonance. Unlike traditional seakeeping analysis methods, the effect of nonlinear waves, hull shape above the waterline, and other ship dynamic phenomena were considered in the CFD applications. The presented CFD method reduces the simulation time and computational efforts for ship motion analyses. The proposed CFD tool may be useful for marine and maritime industrial applications for seakeeping studies.

Acknowledgment

This research received no specific grant from any funding agency in the public, commercial, or not-for-profit sectors, and there is no conflict of interest.

References

1. Akbari Vikilabadi, K., Khedmati, M.R., Hasanabadi, A. & Mohammadi, A. (2018) Resistance Prediction for a Novel Trimaran with Wave Piercing Bow. *International Journal of Maritime Technology* 9, pp. 33–40.
2. Akbari Vikilabadi, K., Khedmati, M.R. & Seif, M.S. (2014) Experimental study on heave and pitch motion characteristics of a wave-piercing trimaran. *Transactions of Famena* 38(3), pp. 13–26.
3. Bertorello, C., Bruzzone, D., Cassella, P. & Zotti, I. (2001) Trimaran Model Test Results and Comparison with Different High-Speed Craft. In: *Practical Design of Ships and Other Floating Structures* 1, pp. 143–149.
4. Bhattacharyya, R. (1978) *Dynamics of marine vehicles*. U.S. Naval Academy.
5. Brizzolara, S., Vernengo, G., Pasquinucci, C. & Harries, S. (2015) *Significance of parametric hull form definition on hydrodynamic performance optimization*. In: 6th International Conference on Computation Methods in Marine Engineering (Marine 2015), pp. 254–265.
6. Chou, SK., Wu, H.T., Wu, C.H. & Hwang, J.L. (2008) *Investigation on seakeeping performance of the high-speed trimaran*. Proceedings of the 8th National Congress on Hydrodynamics, Ji-nan, China.
7. Deng, R., Luo, F., Wu, T., Chen, S. & Li, Y. (2019) Time-domain numerical research of the hydrodynamic characteristics of a trimaran in calm water and regular waves. *Ocean Engineering* 194, 106669.
8. Dobashi, J. (2014) On the prediction method for ship motions of trimaran in oblique waves. *Journal of the Japan Society of Naval Architects and Ocean Engineers* 20, pp. 77–84.
9. Doctors, L.J. (2015) *Hydrodynamics of high-performance marine vessels*. Charleston, SC: CreateSpace Independent Publishing Platform.
10. Du, L., Hefazi, H. & Sahoo, P. (2019) Rapid resistance estimation method of non-Wigley trimarans. *Ships and Offshore Structures* 14(2), pp. 1–11.
11. Elcin, Z. (2003) *Wave making resistance characteristics of trimaran hulls*. Master's Thesis, Naval Postgraduate School, Monterey, California. Available from: https://apps.dtic.mil/sti/pdfs/ADA420575.pdf [Accessed: October 10, 2020].

12. Fang, M.C. & Too, G.Y. (2006) The Effect of Side Hull Arrangements on the Motions of the Trimaran Ship in Waves. *Naval Engineering Journal* 118(1), pp. 27–37.
13. Ghadimi, P., Nazemian, A. & Ghadimi, A. (2019) Numerical scrutiny of the influence of side hulls arrangement on the motion of a Trimaran vessel in regular waves through CFD analysis. *Journal of the Brazilian Society of Mechanical Science and Engineering* 41, 1.
14. Ghadimi, P., Nazemian, A. & Sheikholeslami, M. (2019) *Numerical simulation of the slamming phenomenon of a wave-piercing trimaran in the presence of irregular waves under various seagoing modes*. Proceedings of the Institution of Mechanical Engineers, Part M: Journal of Engineering for the Maritime Environment 233(4), pp. 1198–1211.
15. Gong, J., Yan, S., Ma, Q. & Li Y. (2020) Added resistance and seakeeping performance of trimarans in oblique waves. *Ocean Engineering* 216, 107721.
16. Grafton, T.J. (2007) *The roll motion of trimaran ships*. Doctor's of Philosophy Thesis, University College London. Available from: https://discovery.ucl.ac.uk/id/eprint/1445979/2/Grafton_vol2edit.pdf. [Accessed: October 10, 2020].
17. Hebblewhite, K., Sahoo, P.K. & Doctors, L. (2007) A case study: theoretical and experimental analysis of motion characteristics of a trimaran hull form. *Ships and Offshore Structures* 2, pp. 149–156.
18. ITTC Recommendations (2011) ITTC-Recommended Procedures and Guidelines, Practical Guidelines for Ship CFD Applications, 7.5-03-02-03.
19. ITTC Recommendations (2014) ITTC-Recommended Procedures and Guidelines, Practical Guidelines for Ship Resistance CFD, 7.5-03-02-04.
20. Jia, JB., Zong, Z. & Shi, H.Q. (2009) Model experiments of a trimaran with transom stern. *International Shipbuilding Progress* 56(3), pp. 119–133.
21. Kim, J.W., O'Sullivan, J. & Read, A. (2012) *Ringing Analysis on a Vertical Cylinder by Euler Overlay Method*. 31st International Conference on Ocean, Offshore and Arctic Engineering, paper No. OMAE2012-84091, pp. 855–866, Rio de Janeiro, Brasil.
22. Kim, Y., Park, C., Kim, J., Lee, H. & Jin, I. (2019) Numerical simulations of added resistance in regular head waves on a container ship. *Brodogradnja* 70(2), pp. 61–86.
23. Kurultay, A.A. (2003) *Sensitivity analysis of the seakeeping behaviour of trimaran ships*. Master's Thesis, Naval Postgraduate School, Monterey, California (USA).
24. Li, A. & Li, Y. (2019) Numerical and experimental study of seakeeping performance of a high-speed trimaran with T-foil. *Polish Maritime Research* 26(3), pp. 65–77.
25. Nazemian, A. & Ghadimi, P. (2020a) Shape optimisation of trimaran ship hull using CFD-based simulation and adjoint solver. *Ships and Offshore Structures* October 2020, pp. 1–15.
26. Nazemian, A. & Ghadimi, P. (2020b) *Multi-objective optimization of trimaran sidehull arrangement via surrogate-based approach for reducing resistance and improving the seakeeping performance*. Proceedings of the Institution of Mechanical Engineers, Part M: Journal of Engineering for the Maritime Environment. December 2020:1475090220980275.
27. Nowruzi, L., Enshaei, H., Lavroff, J., Kianejad, S.S. & Davis M.R. (2020) CFD Simulation of Motion Response of a Trimaran in Regular Head Waves. *International Journal of Maritime Engineering* 162(A1), pp. 91–106.
28. Pastoor, W., Van't Veer, R. & Harmsen E. (2004) *Seakeeping behaviour of a frigate-type trimaran*. Proceedings of the International Conference on the Design and Operation of Trimaran Ships, Royal Institute of Naval Architects (RINA), 29–30 April, London (U.K.).
29. Sahoo, P.K. & Lawrence, J. (2005) *The waves generated by a trimaran*. Proceedings of the 8th International Conference on the Fast Sea Transportatioin, Saint Petersburg, Russia.
30. Simonsen, C.D., Otzen, J.F., Joncquez, S. & Stern, F. (2013) EFD and CFD for KCS heaving and pitching in regular head waves. *Journal of Marine Science and Technology* 18, pp. 435–459.
31. Slutski, J. (2008) Resistance and component hull interactions of a high-speed trimaran sealift ship. NSWCCD, 50-TR-2008/093.
32. Tezdogan, T., Demirel, Y. K., Incecik, A. & Turan, O. (2014) *Hydrodynamics of heaving twin cylinders in a free surface using an unsteady-RANS method*. The 2nd International Conference on Maritime Technology (ICMT2014).
33. Tezdogan, T., Demirel, Y.K. & Turan, O. (2014) Operability assessment of high-speed passenger ships based on human comfort criteria. *Ocean Engineering* 89, pp. 32–52.
34. User Guide (2020) StarCCM+ version 2020.1. SIEMENS Simcenter.
35. Wang, S., Ma, S. & Duan, W. (2018) Seakeeping optimization of trimaran outrigger layout based on NSGA-II. *Applied Ocean Research* 78, pp. 110–122.
36. Wu, C., Zhou, D., Gao, L. & Miao, Q. (2011) CFD computation of ship motions and added resistance for a high-speed trimaran in regular head waves. *International Journal of Naval Architecture and Ocean Engineering* 3(1), pp. 105–110.
37. Xu, H. & Zou, Z. (2001) *Numerical prediction of wave-making resistance of a trimaran*. Proceedings of 2nd International Workshop on Ship Hydrodynamics (IWSH'01), Wuhan, China, pp. 105–109.
38. Yang, C., Soto, O., Löhner, R. & Noblesse, F. (2002) Hydrodynamic optimization of a trimaran. *Ship Technology Research* 49(2), pp. 70–92.
39. Yanuar, Y., Gunawan, G., Talahatu, M.A., Indrawati, RT. & Jamaluddin, A. (2013) Resistance analysis of unsymmetrical trimaran model with outboard sidehulls configuration. *Journal of Marine Science and Application* 12 (3), pp. 293–297.

Cite as: Ghadimi, P., Karami, S. & Nazemian, A. (2021) Numerical simulation of the seakeeping of a military trimaran hull by a novel overset mesh method in regular and irregular waves. *Scientific Journals of the Maritime University of Szczecin, Zeszyty Naukowe Akademii Morskiej w Szczecinie* 65 (137), 38–50.

Scientific Journals
of the Maritime University of Szczecin

Zeszyty Naukowe
Akademii Morskiej w Szczecinie

2021, 65 (137), 51–57
ISSN 1733-8670 (Printed)
ISSN 2392-0378 (Online)
DOI: 10.17402/460

Received: 10.12.2020
Accepted: 29.03.2021
Published: 31.03.2021

The development of long-range heat transfer surfaces for marine diesel engine charge air coolers

Valerii Kuznetsov[1], Oleksiy Gogorenko[2], Svetlana Kuznetsova[3]

[1] https://orcid.org/0000-0002-3678-595X
[2] https://orcid.org/0000-0002-9157-6659
[3] https://orcid.org/0000-0003-0823-0583

Admiral Makarov National University of Shipbuilding
9 Heroiv Ukraine Ave., 54025, Mykolayiv, Ukraine
[1] Department of Marine Infrastructure Systems Engineering and Energy Management
e-mail: valeriy.kuznetsov@nuos.edu.ua
[2] Department of Internal Combustion Engines, Plants and Technical Exploitation
e-mail: oleksiy.gogorenko@gmail.com
[3] Operation of Ship's Power Plants and Heat Power Department
e-mail: svitlana.kuznetsova@nuos.edu.ua
corresponding author

Keywords: marine diesel engines, charge air cooler, heat transfer surface, efficiency, finns, dimples, non-round cross section tube

JEL Classification: L62, L91, R41

Abstract

Charge air cooling is essential for the efficient operation of marine diesel engines. This work presents the results of research on the characteristics of long-range heat transfer surfaces for marine diesel engines. Elliptical and flat-oval tubes were considered. This study was carried out using mathematical models that consisted of the equations for energy conservation, motion, continuity, and state. The RSM turbulence model was used to close the system of equations. To solve the resulting system of equations, the RANS approach was used, which was implemented in the software package Code Saturne with a free license and the SimScale cloud service. The mathematical model was verified by comparing the model results with the experimental results obtained using a prototype heat-exchange surface of a charge air cooler at a test bench. The discrepancy between the theoretical and experimental heat transfer coefficient α was $\leq 8.3\%$. An estimate of the compactness of smooth elliptical and flat-oval tube banks compared with round ones was carried out. A 19.6% increase in compactness was obtained for elliptical tubes and 17.5% for flat-oval tubes. Based on the profiled finning surfaces, it is possible to improve their thermohydraulic characteristics by up to 40% when using them together with elliptical tubes compared with round ones and up to 26% when using them with flat-oval tubes.

Introduction

Modern marine power engineering is based on diesel engines, which are used both as the main engines and drive motors for diesel-driven alternators (Significant Ships, 1991–2017). Modern marine diesel engines are combined and cannot operate without gas turbine charging. Increasing the density of the air charge in the compressor, followed by its effective cooling in the charge air cooler, helps increase the effective engine power, reduce specific fuel consumption, and also reduce harmful emissions in the exhaust gases.

The pressure ratio of the charge air in the modern turbochargers of marine diesel engines reaches 4–5, which increases the charge air temperature to

220–260°C. Since the temperature of the charge air entering the engine cylinders should be in the range of 30–40°C, it is necessary to cool it, which is carried out using charge air coolers. The heat transfer surfaces of such coolers are formed mainly from finned circular tubes, which makes it difficult to create compact heat exchangers (Bazhan, 1981). The advantage of tubular heat exchangers is their simple design and reliability; however, an increase in engine power increases the weight and size of coolers, which makes it difficult to create compact power plants.

It has been experimentally shown (Bazhan, 1981) that a 10°C decrease in temperature in the charge air cooler helps reduce the specific fuel consumption of the engine by 2 g/(kW·h). Pre-estimate calculations carried out by the authors of the operating cycle of a MAN B&W S60ME engine showed that by increasing the thermal efficiency of the cooler, the fuel consumption can be decreased by 1.4–1.6 g/(kW·h), and an additional decrease in consumption by 0.3–0.4 g/(kW·h) can be achieved by reducing the resistance of the heat exchanger; thus, it is necessary to consider the heat transfer methods and their intensification, in which an increase in heat transfer exceeds the increase in hydrodynamic resistance required to achieve it.

The formation of heat transfer surfaces based on circular tubes with discrete roughness (Gaus & Savicheva, 2020), which is performed by rolling various configurations, has been proposed. The proposed heat transfer surfaces require additional research to determine how their heat transfer characteristics depend on the rolling geometry.

For additional cooling, evaporative cooling was proposed (Somwanshi & Sarkar, 2020), but this method is difficult to use in transport power plants. The results of mathematical and physical modeling of a hybrid air cooler were presented.

For use in charge air coolers, smooth-tube and finned heat exchangers made of a material with a high thermal conductivity coefficient have been investigated (ACT, 2020; Kelvion, 2020). In such heat exchangers, an increase in resistance exceeds the increased heat transfer during heat transfer intensification, which makes it difficult to create compact heat exchangers.

Packets of flat-oval pipes with dimples have been proposed for use as heat transfer surfaces made of non-circular pipes (Kondratyuk, Pis'mennyi & Terekh, 2015; Khalatov, Kovalenko & Meyris, 2017); however, in these investigations, there was no comparison of the compactness characteristics with other types of pipes with non-circular cross-sections.

As a profiled finned surface (Kuntysh et al., 2012), it was proposed to use a tube with a circular cross-section with *L*-shaped fins with dimples; however, the proposed system of dimples, applied along the entire fin, is extremely low-tech, which will complicate the production of such fins. In addition, there are no recommendations for selecting dimple parameters depending on the conditions of use.

Dolphin Company (Dolphin Manufacturing LLC, 2020) offers heat exchangers with pipes with round and flat-plane cross-sections, which are finned with solid ribs for use as charge air coolers; however, the reduction of edge resistance as the main source of hydrodynamic resistance was not considered.

To estimate the compactness of the heat transfer surface (Wong, 1977), the coefficient of geometric compactness is used:

$$K_{\text{geom}} = \frac{F}{V} \tag{1}$$

where F and V are the area and volume of the heat transfer surface (m^2 and m^3), respectively.

In the open literature, many parameters have been proposed for estimating the heat transfer efficiency. For the flow conditions in tube banks, the Reynolds analogy factor is (Khalatov, 2005):

$$\text{FAR}_{\alpha} = \frac{\frac{Nu}{Nu_0}}{\frac{f}{f_0}} \tag{2}$$

where Nu is the Nusselt number, f is the drag coefficient, the index 0 corresponds to a cylindrical channel on both sides (as the most thermohydraulically investigated). A modified Reynolds analogy factor (Kuznetsov, 2020) can also be used

$$\text{FAR}_{k} = \frac{\frac{k}{k_0}}{\sum \frac{Eu}{Eu_0}} \tag{3}$$

where k is the overall heat transfer coefficient ($W/(m^2 \cdot K)$), Eu is the Euler number, index 0 corresponds to a cylindrical channel on both sides (as the most thermohydraulically investigated).

The analysis showed that, for use as heat transfer surfaces in recuperative charge air coolers, banks of smooth and profiled pipes with round sections and finned pipes are recommended, in which the increase

in resistance exceeds the increase in heat transfer. The main source of resistance of the heat transfer surface is the ribs, which makes it difficult to create compact heat exchangers. The use of finned pipes with a flat-plane cross-section is recommended, but methods for reducing the resistance of the ribs are not considered.

Methodology

The aim of this work was to estimate the thermal and hydraulic efficiency of using finned-profiled heat transfer surfaces with non-circular cross-section tubes for designing compact charge air coolers for marine diesel engines.

For this purpose, it is necessary to solve the following problems:

- To justify and verify the mathematical model for researching long-range heat transfer surfaces of charge air coolers.
- To make a comparative estimation of the compactness of profiled smooth elliptical and flat-oval banks of tubes compared with round-section tubes.
- To conduct a comparative estimation of the thermohydraulic efficiency of profiled elliptical and flat-oval tube banks compared with round-section tubes.

The *object of the research* is the processes of heat exchange in surface charge air coolers.

The *subject of the research* is the geometric parameters of surface compactness and their relation to heat exchange and the hydrodynamic parameters of the heat conversion processes occurring in charge air coolers.

The research method is the geometric modeling of the elements' location of the heat-transfer surface in the tube bank, and mathematical and physical modeling of heat transfer processes on heat transfer surfaces.

Simulation model

Mathematical modeling of the processes was carried out based on the numerical solution of the equations of conservation of energy, motion, continuity, and state. To close the system of equations based on the recommendations of (Bystrov et al., 2005), the RSM turbulence model was used. To solve the resulting system, the RANS approach was used, which was implemented in a software package with a free license, Code Saturne (Code_Saturne, 2020), and the SimScale cloud service (SimScale, 2020).

The mathematical model was verified by comparing the results of test modeling with the results of testing a prototype of the heat exchange surface of the charge air cooler (CAC) at the specialized test bench of the Department of Internal Combustion Engines, Plants and Technical Exploitation of the Admiral Makarov National University of Shipbuilding.

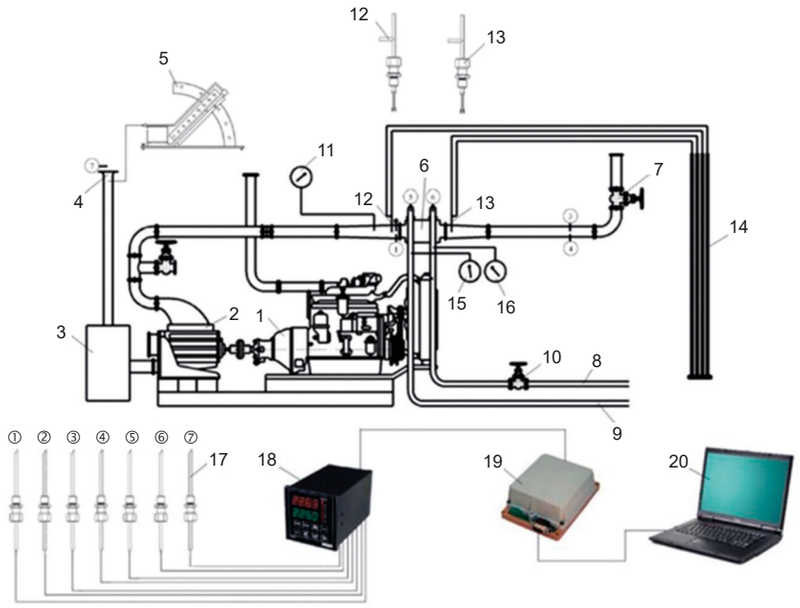

Figure 1. A schematic of the test bench: 1 – diesel engine; 2 – rotary-vane compressor; 3 – cistern; 4 – flow restrictor; 5 – micromanometer MMH-240; 6 – experimental CAC; 7 - orifice valve; 8 – inlet pipe of the water to CAC; 9 – outlet pipe of the water from CAC; 10 – slide-valve for the flow control through CAC; 11, 15, 16 – model manometers; 12, 13 – static-pressure tubes; 14 – block water piezometer tubes; 17 – Chromel-Copel thermocouples; 18 – eight-channel temperature monitoring device "OVEN"; 19 – interface adapter RS232 "OVEN" AC-2; 20 – PC

The test bench scheme is shown in Figure 1. The source of compressed air at the test bench was a rotary vane compressor (2), which was driven by a direct drive from a diesel engine (1) SMD-19. The capabilities of the stand made it possible to obtain air with an absolute pressure of 20–160 kPa and a flow rate of 0.1 to 0.5 kg/s, while the maximum air temperature ahead of the front of the experimental CAC was 110–130°C.

The scheme of the heat transfer surface is shown in Figure 2. The heat-transfer surface was an aligned bank of flat-oval tubes with continuous finning by flat transverse plates. The fins had a transverse pimple in the form of a triangular protrusion (Figure 2).

The heat transfer surface had the following geometric parameters: height of the tube cross-section d_w = 3.8 mm; distance between the tubes in the cross-row S_1 = 10 mm; step between the cross-rows of tubes S_2 = 23 mm; the largest dimension of the tube cross-section S_3 = 17 mm; step between the ribs S_4 = 2.05 mm; thickness of the fin plate δ_{pl} = 0.1 mm; beam height H_P = 110 mm; beam length L_P = 184 mm; beam width B_P = 100 mm.

Based on the test results, the criterion equation was obtained:

$$Nu = 0.4613 \cdot \mathrm{Re}^{0.4727} \qquad (4)$$

The geometric dimensions of the calculated geometric model used to verify the mathematical model were the same as those of the prototype. The mathematical model verification results are presented in Figure 3.

The discrepancy between the theoretical and experimental heat transfer coefficients α did not exceed 8.3%, which makes it possible to use the obtained mathematical model to further investigate the heat-hydraulic characteristics of heat exchange surfaces.

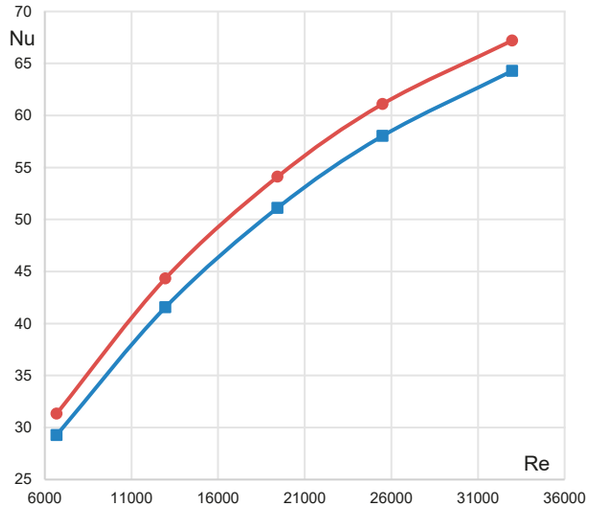

Figure 3. The results of mathematical model verification: ■ – values obtained from the equation (4); ● – simulation results

Results

To form heat transfer surfaces, the concept of "good" and "bad" streamlined surfaces obtained from classical hydromechanics was used. Tubes with flat-oval and elliptical cross-sections were considered as "well"-streamlined surfaces, which were compared with a "poorly"-streamlined surface – tubes with a circular cross-section.

The heat transfer surface area of the cooler can be represented as the sum of the surfaces of the non-finned and finned parts. Since smooth tubes are the actual basis for the formation of a heat-transfer surface, the compactness of surfaces consisting of smooth tubes is considered. In this consideration, the same surface area and the minimum possible flow area between the tubes were accepted (Figure 4).

Under the accepted conditions, the modified Reynolds analogy factor (2) – the parameter describing the efficiency of the overall heat transfer – FAR_k

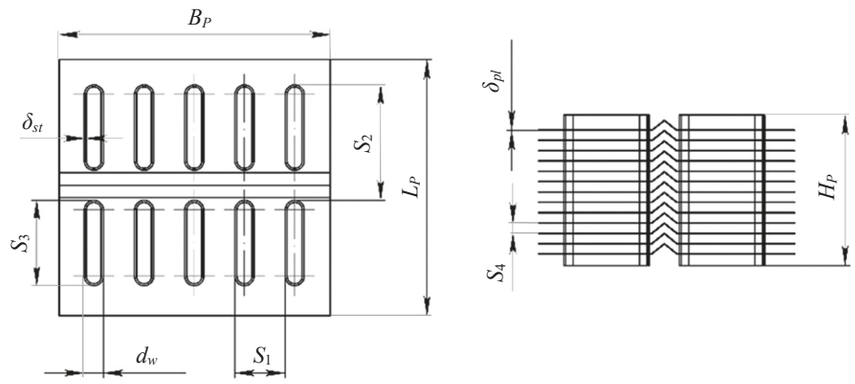

Figure 2. The scheme of the experimental heat transfer surface element

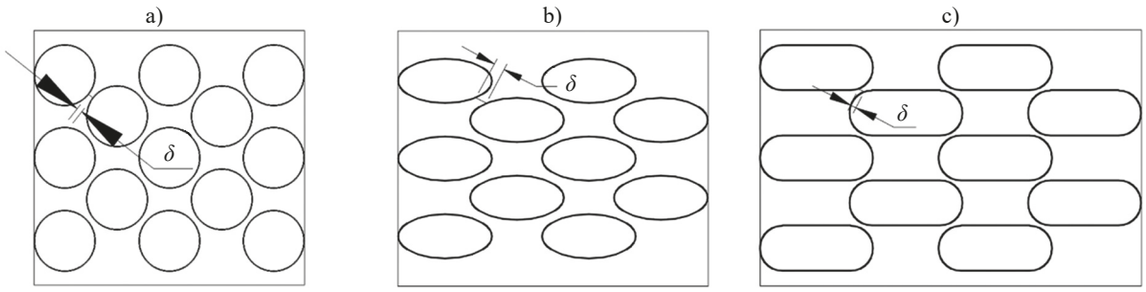

Figure 4. The smallest possible flow area between tubes in bundles: a) round tubes; b) elliptical tubes; c) flat-oval tubes

– will be equal to: for round tubes = 1; elliptical tubes = 1.67; flat-oval tubes = 1.35. The geometric compactness parameter will be: for round tubes = 0.094; elliptical tubes = 0.117; flat-oval tubes = 0.114.

The improvement of the finned portion of the heat transfer surface was carried out in the direction of the outstripping growth of heat transfer over the resistance growth. The use of dimple systems provides an effective way to improve this direction (Khalatov, 2005). When the flow passes along an edge with a dimple, a vortex-like structure, such as a natural vortex "tornado", is formed in it. This structure, leaving the dimple, carries the energy of the vortex into the external flow, which prevents flow separation while reducing the hydrodynamic resistance of the fins and the entire surface. According to data (Khalatov, 2005), depending on the size of the dimples, the negative (compared with the atmospheric) static pressure zone ranges from 30 to 80% of the dimple length. The maximum positive static pressure value is located near the trailing edge of the recess, after which it drops sharply due to flow separation, before becoming negative again. This allows for an increase in heat transfer over an increase in resistance.

The location of the dimples is determined as follows. We represent the fin in the form of a plate and determine the change along the length of the plate in the thickness of the laminar and turbulent boundary layers and the heat transfer coefficient. The following equations were used to calculate:

- The thickness of the laminar boundary layer

$$\delta_l(x) = \frac{4.64 \cdot x}{\sqrt{\mathrm{Re}_x}}$$

- The thickness of the turbulent boundary layer

$$\delta_t(x) = \frac{0.37 \cdot x}{\sqrt[5]{\mathrm{Re}_x}}$$

- The heat transfer coefficient

$$Nu_x = 0.0255 \cdot \mathrm{Re}_x^{0.8}$$

These equations were based on recommendations by (Wong, 1977).

The flow parameters – the air temperature t_f =150°C and speed w_f = 15 m/s – were taken from (Bazhan, 1981). The calculation results are shown in Figure 5.

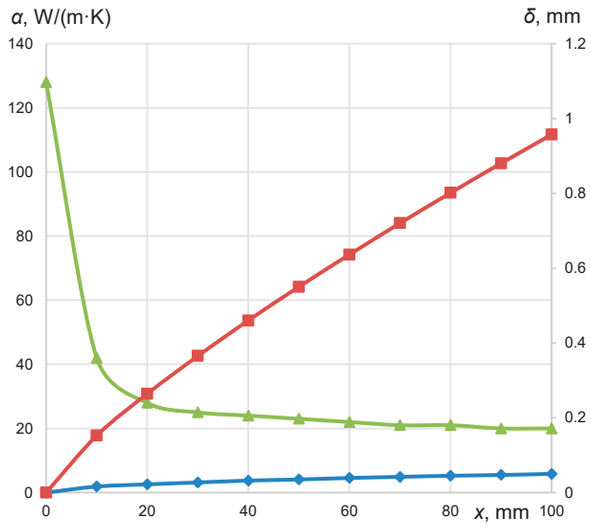

Figure 5. Changes in the characteristics of the boundary layer when flowing around the plate: ▲ – heat transfer coefficient; ♦ and ■ – the thicknesses of the laminar and turbulent boundary layers respectively

Analysis of the diagrams shows that the most significant change in the heat transfer coefficient and thickness of the laminar boundary layer occurs in the section from the beginning of the plate to x = 10 mm. At a distance of x = 10–20 mm, the decrease in the heat transfer coefficient stabilized and remained practically constant starting from the middle of the plate; therefore, the dimple layouts in Figure 6 were used.

Figure 6a shows a variant of the location of the dimple systems on a bank of flat-oval ribbed tubes, similar to that used in the mathematical model verification. The dimples are spaced 10 mm apart. Based on the geometrical dimensions of the model, the parameters of the dimples were taken according to

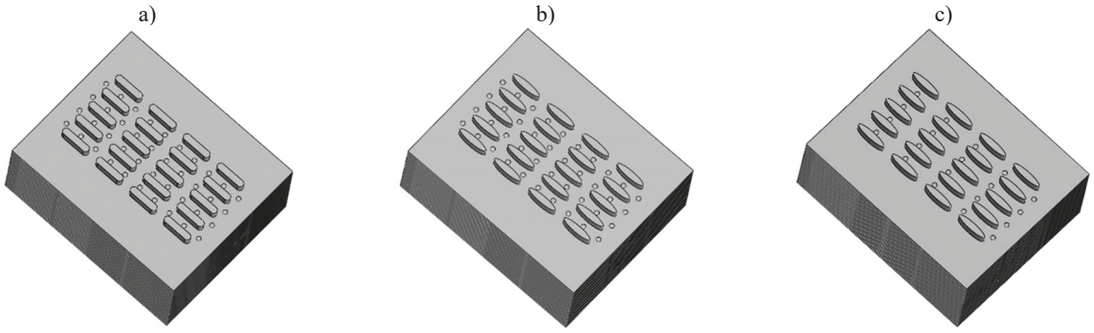

Figure 6. Layout schemes for dimples on the fins of profiled surfaces

the recommendations of (Khalatov, 2005). Figure 6b and 6c show the considered options with elliptical tubes. The hydraulic diameter and layout of the elliptical tubes were similar to that of the flat-oval layout. The differences lie in the step of the dimples – in Figure 6b – 10 mm, and 6c – 20 mm.

The calculation results are presented in Figure 7 as the dependence of the Reynolds analogy factor FAR_{α} on Re.

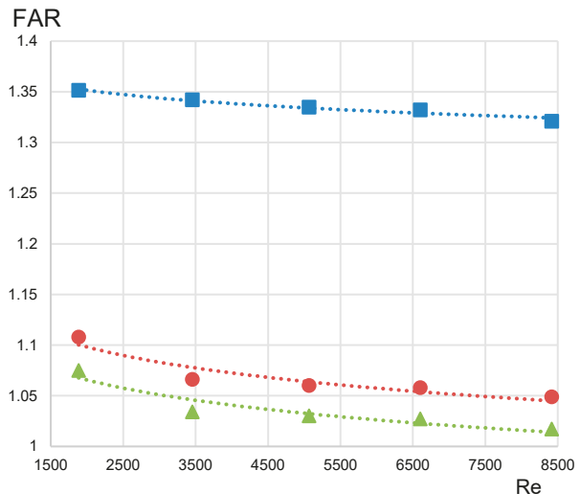

Figure 7. The efficiency of using the profiled heat exchange surfaces: ■ – $FAR_{\alpha 1}$; ● – $FAR_{\alpha 2}$; ▲ – $FAR_{\alpha 3}$

The results were calculated according to dependence (2) and are presented as follows: $FAR_{\alpha 1}$ – the efficiency of using smooth elliptical pipes compared with flat-oval pipes; $FAR_{\alpha 2}$ – the efficiency of using flat-oval tubes with dimples on the fins (Figure 6a) compared with tubes with a smooth fin; $FAR_{\alpha 3}$ – the efficiency of using elliptical tubes with dimples on the fins (Figure 6b) compared with tubes with smooth fins. The efficiency of variant 6c was ±3.2%, similar to variant 6b; therefore, it is not shown on the diagram.

A feature of the obtained results is the use of tubes with non-circular cross-sections to form a heat transfer plate-finned surface for charge air coolers. At the same time, due to the better hydrodynamic flow around the surface, the bank efficiency with smooth elliptical tubes was 31–35% higher than those with flat-oval ones; however, the use of dimple systems showed better efficiency on a flat-oval bank; thus, the final choice of the surface and layout of the dimple systems should be based on the desired design and technological production capabilities.

Further results will be aimed at investigating the effectiveness of various shapes and geometrical sizes of dimples in the conditions under consideration.

The obtained results can be used not only to create a heat exchange surface for charge air coolers for marine diesel engines, but also for other transport engines – locomotives, automobiles, as well as stationary diesel power stations – since they can reduce the weight and size of the coolers. In addition, the heat exchange surface investigated by the authors can also be used to create radiators operating in the cooling systems of internal combustion engines in various marine infrastructure power plants.

Conclusions

The mathematical model used to investigate the thermohydraulic characteristics of charge air coolers for marine diesel engines has been determined. It was verified using the experimental data obtained at a test bench, which confirmed the possibility of its further use.

A comparative estimate of the compactness of smooth elliptical and flat-oval tube bundles compared with round ones was carried out. The increase in compactness was 19.6% for elliptical tubes and 17.5% for flat oval tubes.

It has been established that based on the profiled finning surfaces, it is possible to improve the

thermohydraulic characteristics by up to 40% when used together with elliptical tubes instead of round ones and by up to 26% when using flat-oval tubes.

References

1. ACT (2020) *Charge Air Coolers*. [Online] Available from: http://appliedcool.com/products/charge-air-coolers/ [Accessed: November 18, 2020].
2. Bazhan, P.I. (1981) *Calculation and design of diesel coolers*. M.: Mashinostroyeniye.
3. Bystrov, Y., Isaev, S., Kudryavtsev, N. & Leontiev, A.I. (2005) *Numerical simulation of vortex intensification of heat transfer in pipe banks*. St. Petersburg: Sudostroyeniye.
4. Code_Saturne (2020) *Introducing Code_Saturne*. [Online] Available from: https://www.code-saturne.org/cms/ [Accessed: November 17, 2020].
5. Dolphin Manufacturing LLC (2020) [Online] Available from: http://www.dolphinml.com/downloads/ [Accessed: November 04, 2020].
6. Gaus, D. & Savicheva, Y.N. (2020) *Discrete-rough Heat Exchange Surfaces*. IOP Conference Series: Materials Science and Engineering 753, 042037, doi: 10.1088/1757-899X/753/4/042037.
7. Kelvion (2020) *New challanges sustainably mastered. Charge air coolers*. [Online] Available from// https://www.kelvion.com/products/product/charge-air-coolers// [Accessed: November 20, 2020].
8. Khalatov, A. (2005) *Heat transfer and fluid mechanics over surface indentations* (*dimples*). Kyiv: National Academy of Sciences of Ukraine, Institute of Engineering Thermophysics.
9. Khalatov, A., Kovalenko, G.V. & Meyris, A. (2017) Using of tubular heat exchange surfaces with dimples in the gas turbine regenerators. *Thermophysics and Thermal Power Engineering* 39(5), pp. 70–77.
10. Kondratyuk, V., Pis'mennyi, E. & Terekh, A. (2015) Heat transfer and aerodynamics of flat-oval tube bundles with dimples. *ScienceRise* 11(2 (16)), pp. 10–14; doi: 10.15587/2313-8416.2015.53141.
11. Kuntysh, V., Sankovich, E., Mulin, V., Piir, A. & Minnigaleev, A. (2012) Heat exchange tube. Description of the utility model to the patent BY 8250.
12. Kuznetsov, V. (2020) Multi-Level Estimation of the Heat Transfer Efficiency in the Power Plants Elements. *Problemele Energeticii Regionale* 3(47), pp. 29–38 (in Russian).
13. Significant Ships (1991–2017). The Royal Institution of Naval Architects.
14. SimScale (2020) *Computational Fluid Dynamics Software*. [Online] Available from: https://www.simscale.com/product/cfd/ [Accessed: 17th November 2020].
15. Somwanshi, A. & Sarkar, N. (2020) Design and analysis of a hybrid air and water cooler. *Engineering Science and Technology, an International Journal* 23(1), pp. 101–113.
16. Wong, H.Y. (1977) *Handbook of Essential Formulae and Data on Heat Transfer for Engineers*. London, New York: Longman.

Cite as: Kuznetsov, V., Gogorenko, O. & Kuznetsova, S. (2021) The development of long-range heat transfer surfaces for marine diesel engine charge air coolers. *Scientific Journals of the Maritime University of Szczecin, Zeszyty Naukowe Akademii Morskiej w Szczecinie* 65 (137), 51–57.

Economics, Management and Quality Science

Scientific Journals
of the Maritime University of Szczecin

Zeszyty Naukowe
Akademii Morskiej w Szczecinie

2021, 65 (137), 61–71
ISSN 1733-8670 (Printed)
ISSN 2392-0378 (Online)
DOI: 10.17402/461

Received: 13.05.2020
Accepted: 02.03.2021
Published: 31.03.2021

Identification of errors committed by Vessel Traffic Service operators

Diana Kotkowska[1], Krzysztof Marcjan[2]

[1] https://orcid.org/0000-0001-8233-2356
[2] https://orcid.org/0000-0002-9455-0403

Maritime University of Szczecin
1-2 Wały Chrobrego St., 70-500 Szczecin, Poland
e-mail: {d.kotkowska; k.marcjan}@am.szczecin.pl
corresponding author

Keywords: VTS system, VTS operator, human factor, human error identification, operator reliability, VTS simulation

JEL Classification: R4, C6, C9

Abstract
This paper examines the factors affecting the performance of VTS operators. A general review of the human factor as a determinant of navigational safety is presented. The elementary nature of the system and its structure are defined, and the ability of a VTS operator to perform planned tasks within a specified timeframe and in a specific manner is analyzed. A reliability assessment scheme is proposed, which is based on the interpretation of factors affecting the VTS operator's efficiency. The effective performance of VTS operators, along with the specific nature of the maritime environment and reliability of the vessel traffic management support, are key determinants in the process of ensuring the reliability and security of the entire system.

Introduction

Although many studies and literature reviews are available in the literature on the subject, there is no comprehensive analysis of the effectiveness of VTS (Vessel Traffic Service) systems. An assessment of the effectiveness of a VTS system plays a major role in ensuring efficient management of vessel traffic. Such an assessment requires a comprehensive analysis of the human factor (Uzarski & Abramowicz-Gerigk, 2014). Effectiveness is a key element integrating vessel traffic management at the operational and strategic levels. The lack of consolidated VTS system components may compromise the decision-making process and, thus, affect a VTS operator's performance.

Improving a VTS operator's performance requires a review of the entire system's operational efficiency. Since a system's security relies largely on relations between the human operator and their work environment (man-machine relation), its effectiveness must be analyzed in two aspects: effectiveness of the VTS operator and effectiveness of the system as a whole (including its internal processes). In order to determine the effectiveness of coherent goals in these two aspects, the authors of this paper have estimated the impact of negative factors.

A system consisting of a human and a technical object is dynamic in nature: it changes over time and affects its operating environment. Through interactions with other systems operating in the same environment, it can modify a predetermined action plan.

VTS operators play important roles in regulating maritime traffic systems. The correct operation of the entire system requires expert knowledge about how and when to react. The IALA V-103

recommendations require personnel to be adequately qualified and trained to perform their duties as VTS operators in accordance with IMO guidelines. The quality of the VTS system operation depends on the efficiency and effectiveness of all system components. In order to ensure the effective operation of the system, appropriate working conditions must be provided to allow the operator to fulfill their obligations and detect incidents. The VTS operator is responsible for the continuous and simultaneous observation of several screens while sitting in the same position; therefore, the workplace should be designed to enable appropriate monitoring of the VTS area. Assessment of human performance is based on the analysis of human behavior and a human's influence on certain environmental conditions (normal and emergency conditions). The HRA (Human Reliability Analysis) method is used to assess the human impact on an environment in terms of system performance. The method is based on analyzing the influence of human activity on a system. Mistakes made by an operator, even those that seem insignificant at first glance, can affect the efficiency and/or security of the system. Increasing the intensity of vessel traffic should not adversely affect the navigational safety and reliability of the VTS system. A ship's crew is responsible for its safe navigation (van Westrenen & Praetorius, 2014), while the VTS is supposed to help seafarers use waterways safely and efficiently (IALA, 2016).

VTS systems are complex social engineering systems, and people are important regulators that maintain the stability of the system (Rellinga et al., 2019). Hollnagel and Woods (Hollnagel & Woods, 2005) argued that human performance is limited by the conditions under which it occurs. In order to organize and analyze collected data, the most commonly used method for assessing human performance, i.e. cognitive task analysis (CTA), aims at understanding activities that require significant cognitive activities from the user. These include decision-making, problem-solving, memory, attention, and judgment. CTA is used to understand the tasks and outcomes that people are trying to achieve. This method examines how people think, what they know, what they are trying to understand, and how information is organized and structured (Crandall, Klein & Hoffman, 2006).

May and Barnard (May & Barnard, 2004) define cognitive task analysis (CTA) "as techniques for modeling the mental activity of a task operator". Crandall, Klein, and Hoffman (Crandall, Klein & Hoffman, 2006) argued that using more than one method or tool in a CTA provided a greater effect and clearer result. For this reason, this study uses applied cognitive task analysis (ACTA) and the critical decision method (CDM). ACTA is typically used to analyze cognitive needs as part of a task, while CDM focuses on non-routine incidents (Stanton et al., 2013).

This study was conducted on a group of ten operators to understand how VTS operators respond to various factors in everyday activities and unusual events. The research undertaken in the article was also aimed at developing a model of human behavior in the field of VTS reliability and safety assessment. The main goal was to assess the reliability of a VTS operator. In order to perform a comprehensive analysis, it was necessary to use many complementary measurement methods. In order to fully analyze the risks related to the work of VTS operators in this study, it was decided that a group of operators would perform exercises of various difficulty levels on a simulator. These methods allow us to identify factors that influence operator performance. The research made it possible to assess the sources of threats resulting from human activity as a part of the VTS system and to analyze human errors in the field of system reliability and safety.

The structure of work performed by a VTS operator

In the management of vessel traffic, VTS operators use the support of navigation systems. Land-based VTS operators coordinate the interchange of complex data in easily-understood formats.

A VTS system is a service center designed to ensure safe and effective navigation. The system's infrastructure relies on delivering authorized data, ship-to-shore and shore-to-ship, which enables the system to operate securely and reliably.

For this study, the VTS system will be presented in the form of two components: one representing a human-operator and one representing the work environment. We understand that a work environment is a tool necessary for the proper functioning of the system – the entire system of devices. The main observation tool is the radar, from which images are automatically applied to the electronic map. On the electronic map, data from the automatic identification system (AIS) transmission can be displayed, and data can also be entered manually.

VTS is also equipped with a system of TV cameras that allow for visual observations, and they are very useful in places such as locks and port areas. Communication between the VTS station and ships

is accomplished using VHF radiotelephony where each VTS station uses its own channel to communicate with ships. VTS provides weather information and warnings via indirect-wave radiotelephony and Navtex. In the recommendations of the IALA V128 (IALA Recommendation V-128 Operational and Technical Performance Requirements for VTS Equipment), the basic operational requirements of the VTS system are discussed, which relate to:

- VTS – Radar System,
- Automatic Identification System (AIS),
- Communication,
- Closed-circuit TV (CCTV) cameras,
- Hydro-meteorological devices,
- VTS Databases – Data System.

For this study, the VTS operator was defined as a person working at vessel traffic control – a unit that regulates vessel traffic in the area of VTS responsibility. The operator's tasks include supervising vessel traffic in the VTS area (12/24 hours shift system), running a nautical and hydrological-meteorological information service for the areas covered by the monitoring system, collecting and storing information in the system, and maintaining a database of monitored vessels. Their duties include running a sea assistance service for ships in the area of VTS responsibility, as well as cooperation with others, such as port authority traffic services or SAR. All of these tasks are achieved by providing three kinds of services: information on the movement of maritime units, organizational traffic, and navigational aids – assistants (IALA, 2008).

When a vessel is approaching the VTS area, the officer of the watch (OOW) reports to the VTS on the VHF (e.g., reports the planned route while the ship sails within the VTS area). Information is then exchanged (ship and cargo details, current position). The VTSO on watch responds by repeating the information provided by the vessel's OOW, based on which the OOW can either confirm or correct it. This process is called a closed-loop, and it is used to ensure that both parties correctly understand a given situation. VTSO provides OOW with up-to-date information on the VTS area, including the intensity of vessel traffic, possible disruptions to a ship's deviation from the planned course (e.g., possible interactions with another vessel), ongoing works in the water area, etc. (Śniegocki, 2002). The information may concern the current hydrographic or meteorological situation in relation to factors such as currents, tides, and fog.

Recently, there has been a growing interest in the analysis of of human reliability in technical facilities and systems technical systems in which a human being supervises the course industrial process (Kosmowski, 2008).

Between two elements – the VTS operator and the work environment – certain processes occur constantly due to their interactions (Figure 1).

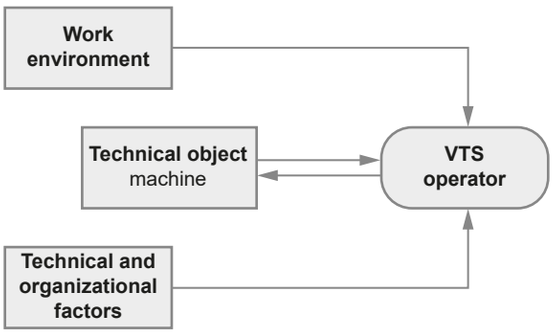

Figure 1. Model of the human–technical system (based on (Sienkiewicz, 1983))

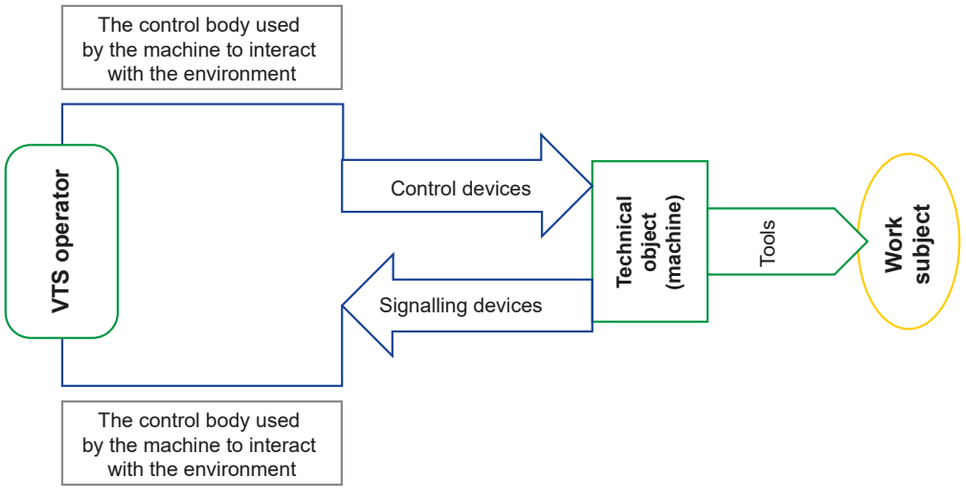

Figure 2. Diagram of interactions between the VTS operator and the technical facility (based on (Sienkiewicz, 1983))

Both of these elements work under specific conditions of the external environment, which affects each of these elements. These system elements also impact the environment; therefore, a more accurate concept is the human-device-environment system shown in Figure 2.

The human-machine/technical object system is characterized by the following features (Sienkiewicz, 1983):

- it can take purposeful actions;
- it can cooperate with other systems;
- it consists of other systems;
- it prevents interference;
- it creates conditions for itself and other systems to take action;
- it undergoes development and can change and improve itself.

For this study, an elementary human-machine system consists of a human and a predefined number of specific types of technical measures taken by the human to perform certain tasks at a certain time and in a certain manner. The system is elementary (one of its structural features), which means that, if deprived of any one of its components, it would be incapable of performing tasks as planned (Sienkiewicz, 1983).

Reliability of a VTS operator

As a human being, a VTS operator is prone to committing errors, as making mistakes is inherent to human nature. Thus, the "**human factor**" plays a vital part in ensuring the safety of maritime navigation. It comprises eight key areas:

- Interpreting situations (different people tend to interpret a given situation differently):

  The uncertainty, ambiguity, and complexity of an event affect the proper understanding of the situation. Excess information received by a VTS operator at a given moment is also of great importance. A person unknowingly makes an initial interpretation of the situation by taking into account their own past experience and substantive knowledge. The experience of similar situations includes dangerous situations, incidents, or serious accidents in the past. Based on this, the operator makes a preliminary interpretation at a given moment, which allows them to make a decision more quickly.
- Risk-taking:

  In human consciousness, risk decreases with increasing control of a situation. The perception by the VTS operator of the risk of an accident on board a sea-going vessel is twice as high as in the opinion of the crew. The risk assessment is primarily influenced by excessive self-confidence, lack of experience, ignorance, or the accompanying stress and fatigue at work.
- Decision-making:

  An important element that influences the human factor is the decision-making process. Decision-making is a compromise between the information available at a given moment and the time to act. Experience has a great influence on decision-making because an experienced operator in a similar situation intuitively makes a quicker decision. The reduction of time increases the productivity of work, which gives an operator more time to act, i.e. complete a task. Unfortunately, a "quick decision" sometimes affects the reliability of a task.
- Committing errors:

  Not every threat leads to an error, and not every error leads to an undesirable condition – it depends on the type of error and many accompanying factors. Errors are the decisions and actions that lead to a dangerous situation or accident. A mistake can also be defined as situations in which no appropriate decisions and actions were taken to prevent their occurrence. A person who has extensive experience and knowledge will perceive dangerous conditions differently than a less-experienced person.
- Getting tired/stressed:

  Psychophysical conditions are one of the most important human factors. Fatigue and stress affect factors such as workload, sleep quality, job satisfaction, environment, work atmosphere, and above all, optimal workplace ergonomics. In an operator's job, each day is different, e.g., the number of controlled vessels. Every day, the VTS operator learns to react to new situations. The ship traffic controller works in a 12/24 hour shift mode, which also has a significant impact on their fatigue.
- Communicating:

  Proper communication between a traffic controller and ship is influenced by the correct interpretation of a situation, as well as the practical use of the equipment and the correct use of available information. The number of controlled vessels is also of great importance for the continuous flow of information.

All the constituents of human nature mentioned above affect the reliability of any system that operates in collaboration with a human being. This study

focuses on decision-making because decisions made by VTS operators are crucial for the security and reliability of VTS systems (Kum et al., 2007).

For this study, **decision-making** shall be defined as the process to decide on taking the right action. Its objective is to evaluate the prevailing situation and choose the most favorable option (Klincewicz, 2016). Any situation in which a VTS operator, looking for the best solution among many available options, is required to make a choice, is inextricably linked with the decision-making process.

However, what happens when a human being – the VTS operator – falls into a routine and starts to make decisions automatically? Relying on experience, he/she chooses solutions that worked in the past and did not cause unwanted consequences, while at the same time being convinced of compliance with applicable regulations and correctness of their actions. This study, conducted on the Navi-Harbour 5000 simulator from Transas, has helped identify the reasons for errors made by VTS operators.

Vessel traffic management relies largely on the reliability of traffic control systems. The ever-growing density of traffic in VTS areas has necessitated the implementation of new technologies to ensure safe navigation.

Many companies (such as Kongsberg Gruppen, Transas (part of Wärtsilä), Rolta India, L3 Technologies, Saab, Kelvin Hughes, Indra, Atlas Elektronik, Vissim AS, and TERMA A/S) have developed state-of-the-art technologies to support secure and efficient vessel traffic management. They offer a variety of vessel traffic control solutions for a fully-functional VTS system.

Konsgsberg Gruppen (based in Norway), one of the leaders on the market, operates in Europe, North, and Latin America, as well as Africa. The vessel traffic management system Indra from Konsgsberg Gruppen is deployed, among others, on Poland's coastal waters and in Southampton (UK).

MaritimeControl™, another popular system released by Saab, offers proven solutions for vessel traffic management in VTS areas. Saab is an active member of the International Association of Lighthouse Authorities (IALA). Saab systems are used by vessel traffic services in Rotterdam, Hong Kong, and Ningbo.

Vessel traffic management systems from Transas, enjoying a great reputation all over the world, are used, inter alia, in Morocco and Mombasa. They have an open configuration, which means they can be easily extended with add-on applications.

Scope of the study

Navi-Harbour 5000 VTS simulator from Transas

This study aimed to identify errors committed by VTS operators and was conducted on the Navi-Harbour 5000 simulator from Transas. Fully compliant with the requirements defined in the IMO Guidelines for VTS (Resolution A.857(20)), the simulator offers a fully-functional VTS system equipped with such features as:

- receiving information about navigational situations,
- delivering data on tracked objects (in tabular and graphical formats),
- monitoring and planning vessel traffic in an area,
- generating alarms according to user-predefined criteria,
- storing digital data and vessel traffic images for further review and analysis (especially useful in the event of a system failure or a breach of applicable legal regulations by vessels in the VTS area) (NH UserManual, 2012).

All the simulator workstations have the same functionality and are operated in the same manner. The image of the VTS area is fully integrated with an electronic chart. By selecting a section of the chart, the traffic image can be focused on a specific area and the chart scaled appropriately. A wide selection of tools available in the main menu supports the easy operation of the system. The home window includes the following items:

- an electronic chart,
- the menu,
- information in a tabular format.

The main menu of the program contains a full list of functions that enable the user to fully control the system and properly perform the tasks of the VTS operator. It includes many additional functions that allow the operator's working environment to be adjusted to suit their needs (Figure 3).

The toolbar consists of buttons for quickly displaying information related to commands or selecting a specific tool. It is designed in a very practical and understandable way. A particular tool/function is launched after selecting the button assigned to it, which is on the main toolbar (this is an option for the most frequently-used tools). Of course, it is possible to start a specific function from the main menu or by using the function keys.

The use of the Navi-HarborTransas 5000 simulator permits the design of an exercise on studied areas with various conditions, e.g., changing traffic

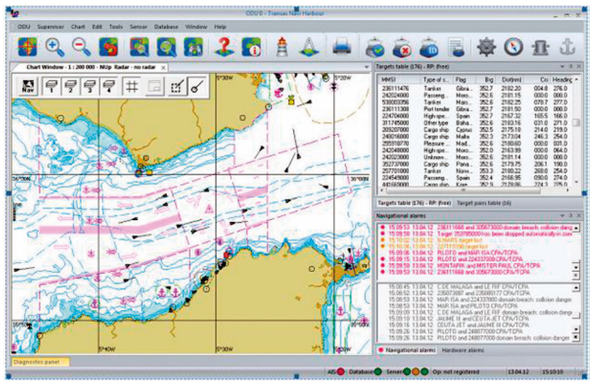

Figure 3. Home window of Navi-Harbour 5000 VTS simulator from Transas

volumes, emergencies, etc. It includes many additional functions that allow an operator to adapt the working environment to a given test scenario.

This research aimed to identify the sources of threats resulting from human activity as part of the VTS system and the analysis of human errors in the field of system reliability and safety. The concept of operator reliability is introduced as a tool to describe and evaluate the work of VTS operators (Kotkowska, Gucma & Marcjan, 2016). A scoring system for the performance of tasks by a VTS operator was introduced, which was based on the specific features of their work, such as the accuracy and processing of information obtained through the system. The research scheme has been divided into stages that are presented in Figure 4.

VTS operators – study participants

The study was conducted on a sample of ten specialized persons, including VTS operators. Each participant performed the same tasks with varying degrees of difficulty. The participants were divided into groups. Ten participants with different experiences and qualifications were used to diversify the obtained results. These people are very familiar with the area where the study was conducted and have been trained in the use of the Transas system. Currently, in the area that is the subject of research (the area of responsibility of VTS Szczecin and VTS Świnoujście), there are a total of 24 VTS operators (with similar qualifications as the operators who participated in the study) active in the profession. Ten participants thus constitutes almost half of the total population that meet similar requirements. A representative sample (ten operators), which, apart from the size, is very similar in terms of the distribution of certain features to the real population.

Simulation venue

During the simulation, the VTS operator and simulation coordinator were seated in separate rooms. All simulator workstations have the same functionality and are operated in the same manner. The image of the VTS area is fully integrated with an electronic chart.

One of the advanced functions of Navi-Harbour is the 3D VTS, which offers a three-dimensional image of traffic in the VTS area. This enhanced tool, which relies on VTMS data, enables viewing traffic from several perspectives.

The VTS system operated by the study participants offered the following functions, which included:

- Radar, AIS, CCTV, RDF, and Meteo-Hydro sensors;

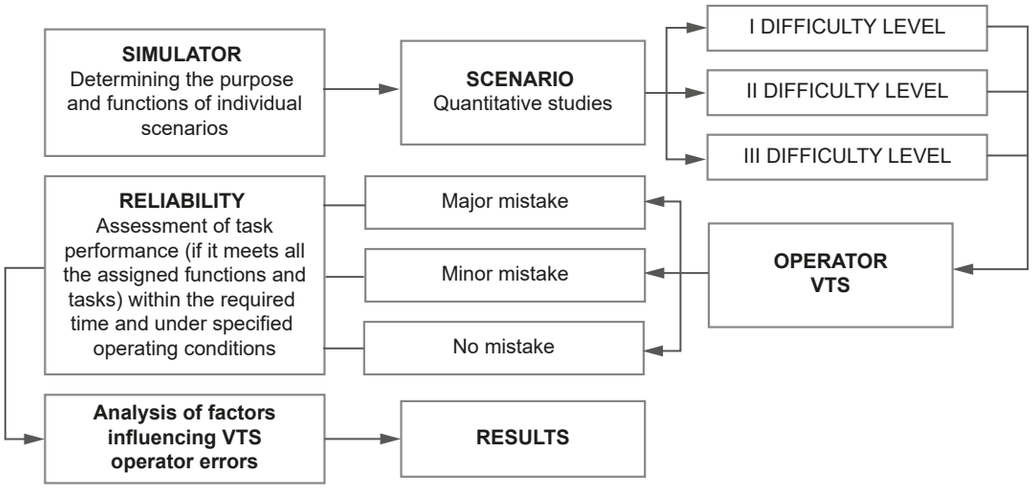

Figure 4. The research scheme

- manual and/or automatic adding and deleting of objects;
- manual and/or automatic identification of objects;
- video radar image;
- AIS data display;
- transmission and reception of AIS text telegrams;
- object echo simulation (creation, modification, and tracking);
- management of recommended routes;
- forecasting objects' maneuvers;
- managing alarms, including navigational alarms;
- recording and replaying;
- highly-functional charts, including the ability to edit and support the S-57 format.

The study participants were trained in the operation of all tools available at their workstations in order to familiarize them with the functionalities of the simulator.

The simulation schedule

The entire duration of the simulation was split into 6-hour watches. Each type of simulation was performed during a single watch. The scenario with the lowest degree of difficulty was scheduled for three watches; i.e., 18 hours. The scenarios with medium and high degrees of difficulty were scheduled for 12 hours each; i.e., the operator performed each scenario over two watches. In total, each VTS operator spent 42 hours participating in the study; i.e., stood seven watches.

Simulation scenarios

All simulation scenarios were developed in consultation with and on the basis of surveys conducted among current or former VTS employees.

Scenarios with a low degree of difficulty included situations that commonly occur during the watch of a VTS operator (Figure 5). They were applied in thirty simulations.

In each simulation, there was a moderate number of vessels within the VTS area. The maximum number of vessels underway (entering/leaving the Port of Szczecin/Świnoujście) was five, and the number of vessels anchored or moored ranged from ten to twenty. None of the vessels were hampered or carried dangerous goods.

The operator was supposed to have become familiar with the situation in the VTS area and, having identified the entering vessels, organize the traffic based on the applicable port regulations, including the positions in which the vessels were permitted to pass each other.

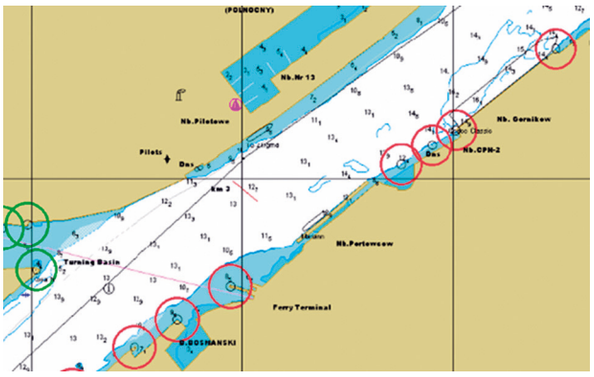

Figure 5. Example simulation with a low degree of difficulty

The VTS operator was also required to provide information to vessels entering the VTS area or getting underway and provide navigational assistance on-demand.

Conclusion scenarios with a medium degree of difficulty

Scenarios with a medium degree of difficulty included situations that frequently occur during the watch of a VTS operator, with a special focus on ships carrying dangerous cargo (Figure 6). The twenty simulations performed were varied but had some common characteristics. The traffic density was higher than normal. The number of vessels underway (entering/leaving the Port of Szczecin/Świnoujście) was more than six, and the number of vessels anchored or moored was more than twenty. The simulations included hampered vessels and/or vessels carrying dangerous cargo.

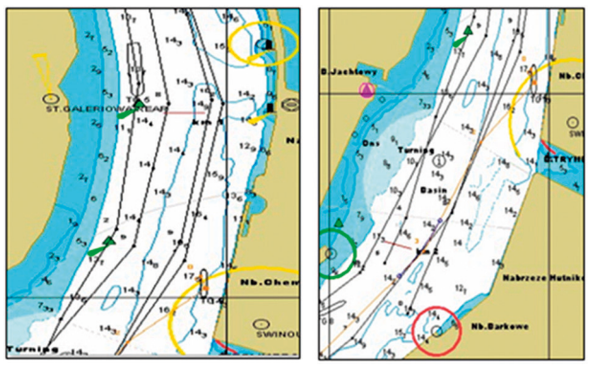

Figure 6. Example simulation with a medium degree of difficulty

Scenarios with a high degree of difficulty

Scenarios with a high degree of difficulty included situations that do not commonly occur during a VTS operator's watch (Figure 7). Each of

the twenty simulations was different and required a different solution. Some of them presented an additional difficulty caused by the high traffic density. At least two vessels in the VTS area carried dangerous goods. Moreover, some ships were hampered vessels or push tows. Some simulations involved emergencies and accidents (e.g., collision, grounding, or fire onboard). They were designed to induce the launch of appropriate emergency procedures (e.g., grounding). Additionally, certain restrictions to navigation were introduced; e.g., on the Świnoujście–Szczecin fairway (on the section from II BT to IV BT), navigation of vessels with a draft of more than 8.5 m was restricted to one-way traffic, and vessels were expected to keep to the middle part of the fairway.

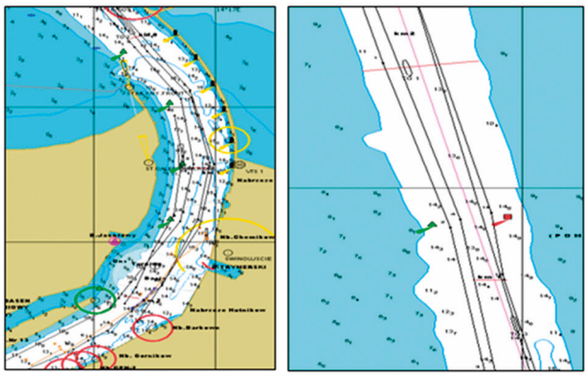

Figure 7. Example simulation with a high degree of difficulty

Results of the study

The example measurement table below shows the results of the simulations carried out in the study (Table 1). Fields marked with "X" indicate an error committed by the VTS operator. Empty fields indicate simulations carried out without errors or oversights. Remarks noted by the study coordinator during the performance of tasks by the VTS operators are marked with "R".

Figure 8 below shows the number of errors committed by the VTS operators in a simulated scenario with a low degree of difficulty.

Analysis of the results led to the conclusion that the VTS operators with the most work experience committed the most errors of all the study participants. The most common error was the **automatic granting of clearance** for entry. Some mistakes were also made when estimating the time when vessels passed each other.

Figure 9 shows the number of oversights committed during simulations. Oversights are irregularities

Table 1. Example measurement table

Simulation with a low degree of difficulty	VTS operator									
	Operator 1	Operator 2	Operator 3	Operator 4	Operator 5	Operator 6	Operator 7	Operator 8	Operator 9	Operator 10
Simulation 1	R									
Simulation 2										R
Simulation 3								R	R	
Simulation 4		R					R			R
Simulation 5	R			X					X	
Simulation 6	X						R			X
Simulation 7		R	R		R				R	
Simulation 8				R						R
Simulation 9					X			R	X	
Simulation 10			X		R					
Simulation 11		R		R			R	R		
Simulation 12										
Simulation 13									R	
Simulation 14	X	X					R	X		
Simulation 15					R					
Simulation 16						X			R	
Simulation 17										
Simulation 18	R	R		R			R			X
Simulation 19					R	R				
Simulation 20		R		R			R	X		R
Simulation 21					R					
Simulation 22	R			X	X			R		R
Simulation 23							R		X	
Simulation 24				X	R	R		R		R
Simulation 25	R		R				X			
Simulation 26								R		R
Simulation 27					R	R	R	X	R	
Simulation 28		R				R				X
Simulation 29	R		R					X		R
Simulation 30		R				R	X		R	R

X – an error by the VTS operator,
R – an oversight by the VTS operator

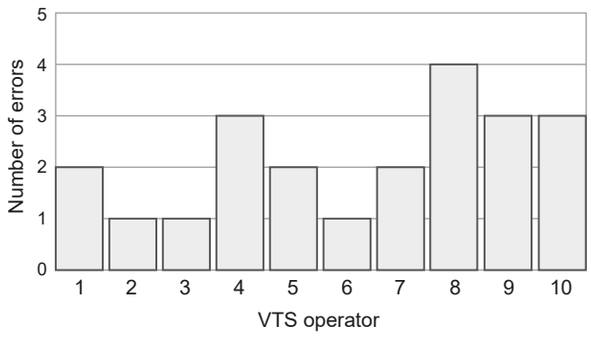

Figure 8. Scenario with a low degree of difficulty

that can cause danger to navigation, such as poor ship-VTS operator radio communications, misinterpretation of documents or other correspondence from other collaborating units, etc.

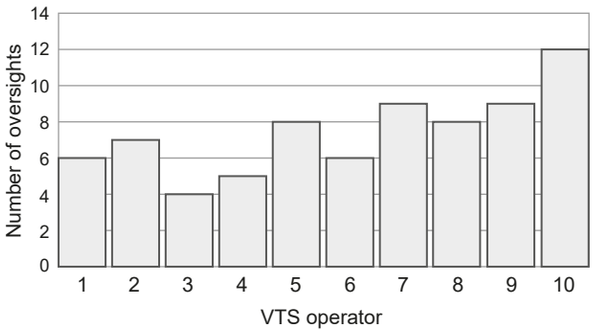

Figure 9. Scenario with a low degree of difficulty

Figure 10 presents a summary of the results obtained by each of the VTS operators in simulations with a low degree of difficulty.

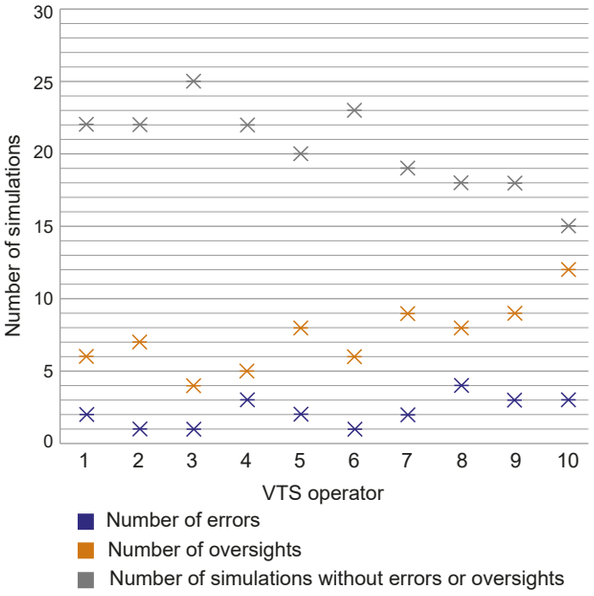

Figure 10. Scenario with a low degree of difficulty

Figures 11–13 present a summary of the results obtained by each of the VTS operators in simulations with a medium degree of difficulty.

Figures 14–16 present a summary of the results obtained by each of the VTS operators in simulations with a high degree of difficulty.

To summarize all the simulations carried out on Navi-Harbour 5000 from Transas, five types of errors committed by the VTS operators can be distinguished.

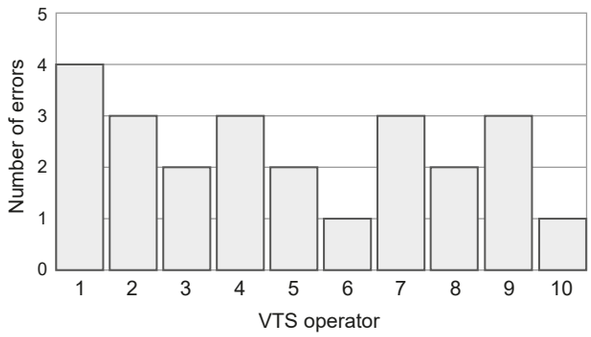

Figure 11. Scenario with a medium degree of difficulty

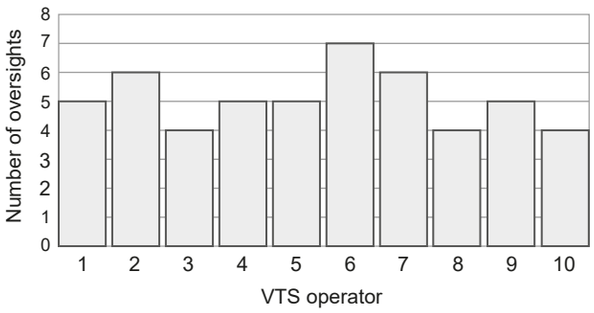

Figure 12. Scenario with a medium degree of difficulty

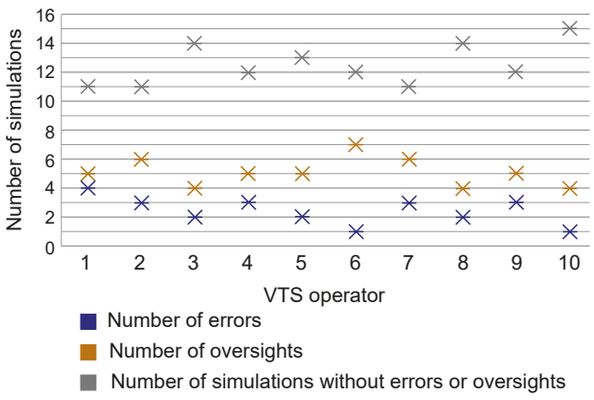

Figure 13. Scenario with a medium degree of difficulty

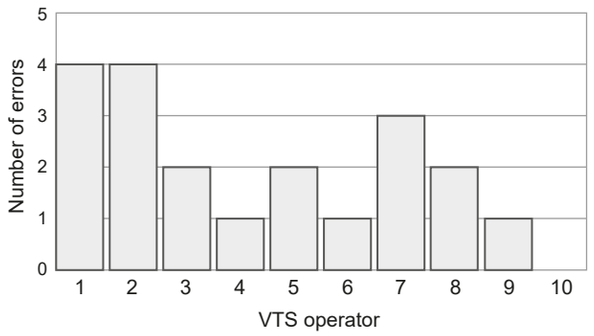

Figure 14. Scenario with a high degree of difficulty

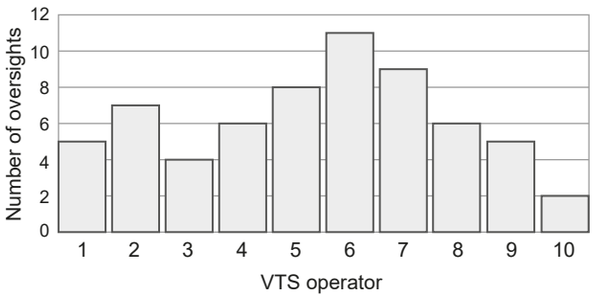

Figure 15. Scenario with a high degree of difficulty

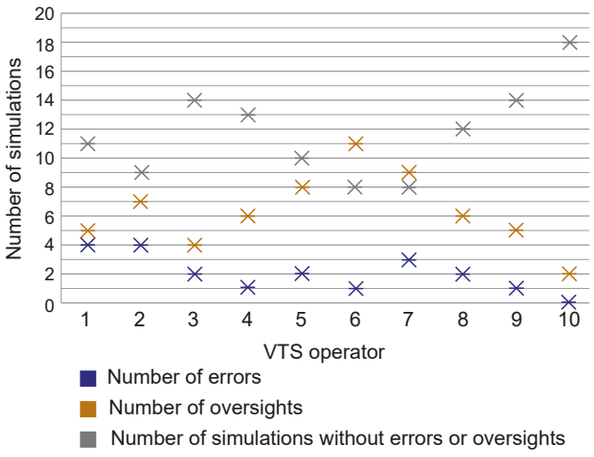

Figure 16. Scenario with a high degree of difficulty

One of them involved the VTS operators "acting on autopilot" when granting clearance for entry in which vessels entering the port on repeated occasions were not verified for any special conditions, etc. For example, a vessel reported with a request for permission to pass from Szczecin to Stepnica. Having obtained standard information on the number of passengers, the number of crewmembers, the person having the conn, etc., the VTS operator granted permission. However, just as the vessel was about to enter the Port of Stepnica, it turned out that the skipper did not hold a license to enter that port. As a result, the vessel was turned back.

Another common mistake was a failure to verify whether there was a berth available for the entering vessel.

The duty service is required to verify whether the vessel requesting permission to enter has all the necessary documents, whether there is berth clearance for it, as well as sufficiently deep water.

For example, a vessel was granted permission to enter by the duty service (during the simulation, the function was performed by the coordinator) provided that there was a berth clear to it. However, the VTS operator let the vessel enter, even though the berth was still not clear (another vessel moored at that berth was not ready to get underway due to precipitation and the nature of its cargo).

Other errors committed by the operators included a failure to monitor the under-keel clearance or miscalculations.

For example, all draft calculations were made for a water level of 512 cm for the Port of Szczecin and 507 cm for Police. When the water level in the harbor decreases, the VTS operator is required to continuously monitor the drafts of ingoing and outgoing vessels, as well as changes in the water level. Many participants in the study committed the same error – having received information "entry at the water level of 487", they let vessels enter even though the actual water level was lower.

Poor organization of traffic, resulting in vessels passing each other in places where passing was prohibited, was another error identified during the simulation. According to the Port Regulations, some vessels can move only in one direction, depending on their cargo or ship parameters. Some VTS operators miscalculated the standard duration of a passage or failed to consider a vessels' parameters, such as its length, breadth, and draft, resulting in vessels passing each other in positions where passing was prohibited.

Misinterpretation of official letters issued by the Port Authority was another common mistake committed by the VTS operators. In special circumstances, acting in accordance with the Port Regulations, the Port Authority may impose certain restrictions on ingoing or outgoing vessels, which do not normally result from the applicable vessel traffic regulations. Some scenarios involved such restrictions. For example, a tug towing a pontoon was granted permission to enter provided specific conditions were met (including, among other things, only at daytime and only if the wind force did not exceed 5 Beaufort scale). One of the VTS operators applied the conditions to the entry of the tug only, which was only 30 m long.

Conclusions

The scenarios carried out on the VTS simulator have provided insight into the most common mistakes committed by VTS operators, namely:

- VTS operators grant standard permission for entry without taking into consideration the prevailing circumstances.
- They fail to verify whether an entering vessel has a clear berth to proceed to and let it enter, even though entry is prohibited until the berth is clear.

- They tend to miscalculate, for instance, drafts of vessels, or fail to verify parameters that affect the safety of navigation.
- They plan traffic improperly.
- They tend to misinterpret documents and other official letters issued by units cooperating with the VTS.

All of the mistakes listed above were committed due to misinterpretation of the prevailing situation. The duties of a VTS operator were performed automatically. When a person repeats the same daily task in a standard manner, sooner or later they fall into a routine. This is especially evident in the group of VTS operators with more 20 years of work experience who, acting "on autopilot", committed more mistakes than others. A conclusion can be drawn that when organizing traffic, the VTS operator tends to make mistakes when relying on a routine. It should be noted here that the VTS operators with longer work experience tended to use the tools offered by the system – for example, to precisely calculate the time for two vessels to pass each other – less frequently than others. Their overconfidence often led to dangerous situations. Additionally, they would ignore warnings displayed on the screen (e.g., system or navigational alarms).

Fewer mistakes were made during simulations with a high degree of difficulty, as the operators took more time to handle the challenges. Before the final decision was made, they made sure that any danger to navigation was avoided.

To sum up, mistakes are caused by several factors resulting from taking the wrong actions. This paper looked at factors related to human nature, including a lack of experience or qualifications, poor communication, fatigue, and routine.

References

1. Crandall, B., Klein, G.A. & Hoffman, R.R. (2006) *Working Minds: A Practitioner's Guide to Cognitive Task Analysis*. Cambridge, MA: The MIT Press.
2. Hollnagel, E. & Woods, D.D. (2005) *Joint Cognitive Systems – Foundations of Cognitive Systems Engineering*. Boca Raton: Taylor & Francis, CRC Press Book.
3. IALA (2008) *IALA Vessel Traffic Services Manual. Edition 4*. International Association of Lighthouses Authorities IALA-AISM, Saint-Germain-enLaye, France.
4. IALA (2016) *IALA Annual Report 2016*. International Association of Lighthouses Authorities IALA-AISM, Saint-Germain-enLaye, France.
5. Klincewicz, K. (Ed.) (2016) *Zarządzanie, organizacje i organizowanie – przegląd perspektyw teoretycznych*. Warszawa, Wydział Zarządzania Uniwersytetu Warzawskiego.
6. Kosmowski, K.T. (2008) Human reliability analysis in the context of accident scenarios. *Journal of KONBiN* 3 (6), pp. 295–314; doi: 10.2478/v10040-008-0074-y.
7. Kotkowska, D., Gucma, L. & Marcjan, K. (2016) Methodological analysis of reliability assessments for vessel traffic service operators. *Scientific Journals of the Maritime University of Szczecin, Zeszyty Naukowe Akademii Morskiej w Szczecinie* 45 (117), pp. 168–173.
8. Kum, S., Furusho, M., Duru, O. & Satir T. (2007) Mental Workload of the VTS Operators by Utilising Heart Rate. *International Journal on Marine Navigation and Safety of Sea Transportation* 1(2), pp. 145–151.
9. May, J. & Barnard, P. (2004) Cognitive Task Analysis in Interacting Cognitive Subsystems. In: D. Diaper & N.A. Stanton (Eds.) *The handbook of task analysis for human-computer interaction*, pp. 291–325. Lawrence Erlbaum Associates Publishers.
10. NH UserManual (2012) Version: 4.40, Transas.
11. Rellinga, T., Lützhöft, M., Hildrea, H.P. & Ostnesa, R. (2019) How Vessel Traffic Service operators cope with complexity – only human performance absorbs human performance. *Theoretical Issues in Ergonomics Science* 21(20), pp. 1–24.
12. Sieńkiewicz, P. (1983) *Inżynieria systemów*. Warszawa, Wydawnictwo MON.
13. Stanton, N.A., Salmon, P.M., Rafferty, L.A., Walker, G.H., Baber, C. & Jenkins, D.P. (2013) *Human Factors Methods – A Practical Guide for Engineering and Design. 2nd Ed.* Vol. 53. Ashgate Publishing Limited.
14. Śniegocki, H. (2002) Errors in the presentation of the vessels course and speed for the VTS operator. *Annual of Navigation*, p. 81. Publisher: Polish Academy of Sciences.
15. Uzarski, M. & Abramowicz-Gerigk, T. (2014) Human factor in air and sea traffic management. *Prace Naukowe Politechniki Warszawskiej. Transport* 102, pp. 159–169.
16. van Westrenen, F. & Praetorius, G. (2014) Maritime traffic management: A need for central coordination? *Cognition, Technology & Work* 16, pp. 59–70.

Cite as: Kotkowska, D. & Marcjan, K. (2021) Identification of errors committed by Vessel Traffic Service operators. *Scientific Journals of the Maritime University of Szczecin, Zeszyty Naukowe Akademii Morskiej w Szczecinie* 65 (137), 61–71.

Scientific Journals
of the Maritime University of Szczecin

Zeszyty Naukowe
Akademii Morskiej w Szczecinie

2021, 65 (137), 72–83
ISSN 1733-8670 (Printed)
ISSN 2392-0378 (Online)
DOI: 10.17402/462

Received: 10.12.2020
Accepted: 12.03.2021
Published: 31.03.2021

Application of multi-criteria analysis for the introduction of green port management practices: an evaluation of energy efficient mobility in nautical ports

Helena Ukić Boljat[1], Siniša Vilke[2], Neven Grubišić[3], Livia Maglić[4]

[1] https://orcid.org/0000-0003-2109-9516
[2] https://orcid.org/0000-0001-9905-505X
[3] https://orcid.org/0000-0001-6322-849X
[4] https://orcid.org/0000-0002-0885-9026

[1] University of Split, Faculty of Maritime Studies
e-mail: hukic@pfst.hr
[2,3,4] University of Rijeka, Faculty of Maritime Studies
e-mail: [2]vilke@pfri.hr, [3]neven.grubisic@uniri.hr, [4]livia@pfri.hr
corresponding author

Keywords: nautical ports, sustainability challenges, green ports, Multi-Criteria Analysis (MCA), multi-criteria model, energy efficient mobility

JEL Classification: Q51, Q56, R40, D71

Abstract

In Europe, at the end of the 20th century, the growth of marinas followed the rapid development of recreational marine activities. This trend has now slowed and today the creation of new marinas or the extension of existing marinas is less common, mainly due to the enforcement of protective environmental regulations. As the port sector is facing some major sustainability challenges, like tackling the pollution generated from port activities, the "green port", or "green marina", concept has now become a requirement. Both types of nautical ports, public ports and private marinas, share the same responsibility to achieve management standards. The term "green port" in practice describes the responsible behavior of all stakeholders in the port's business, with a focus on the long-term vision towards the sustainable and climate-friendly development of the port's infrastructure. This paper aims to confirm the adequacy of multi-criteria analysis (MCA) for the evaluation and introduction of energy efficient mobility options in nautical ports. Within the paper, a multi-criteria based model for energy-efficient mobility selection is presented. This model is tested on two Croatian private marinas and obtained results indicating the most suitable action for both. The output of the model showed that by far the best energy-efficient solution was the installation of electric charging stations (ECS) for cars. The presented model can assist decision-makers in port authorities and marina administrations in planning and finding the best scenario for the development of energy efficient systems and services.

Introduction

In the past decade, within the port industry, an increasing commitment for the implementation of environmentally friendly solutions and the achievement of the "green port" status has been found. Numerous emerging "green" initiatives, that consider both environmental and economic aspects, have been developed. Sustainably managing port operations implies the intersection of the three main sustainability pillars, namely, environmental (to reduce the impact on the environment), social (community management), and economic (to help the organization benefit and enhance its economic performance) (UNCTAD, 2018). To improve their environmental profiles, port authorities often choose

green solutions and approaches for the sustainable management of port operations and energy management (Lam & Notteboom, 2014). Achievement of the green port status represents one of the key objectives of many ports worldwide. This "Green Port" status can be achieved through various approaches, such as improving energy efficiency, collecting and recycling rainwater and waste on board, and "zero-emission" policies (Longo et al., 2015). Ports and terminals especially focus on energy efficiency and management issues, which is in the line with top 10 environmental priorities of European ports. Hence, in the past four years (2016–2019) European port authorities marked energy efficiency as the second most important environmental priority (ESPO, 2019). Integration of innovative technologies, renewable energy utilization, and new operational processes have become the main tools for the reduction of energy consumption (Acciaro, Ghiara & Cusano, 2014). Furthermore, goals for the reduction of energy consumption are in the line with key strategic priorities of the European Union. In November 2018, the European Commission presented its long term strategy with seven strategic priorities towards a climate-neutral Europe by 2050, from which the benefits from energy efficiency represents a key part (Sdoukopoulos et al., 2019). On top of the stated goals and priorities within this Strategy, there are also other relevant European documents dealing with environmental problems in seaports (EU, 2002; 2005; 2009; 2014; 2015; 2016; 2019). Within this context, for the achievement of the objectives stated within these European strategic documents, it is clear that the European port sector has an important role to play. Similarly, the role of the nautical tourism sector and the so-called small port/marinas should not be neglected. Overall, the boating industry, with a turnover of 566 billion euros and which employs 3.5 million people, is a significant contributor to the European economy. Furthermore, there are over 6 million boats in the European boat park and 10,000 marinas, which provide over 1 million berths both inland and in coastal areas, which make Europe one of the most competitive destinations globally (EBI, 2020).

Therefore, acknowledging the importance of the boating industry sector, it is thus of extreme importance to think about the implementation of green solutions and innovations in nautical ports. Also, it is important to bear in mind that the port sector is forging ahead with numerous studies which are highlighting the importance of key performance indicators and the measurement of ports' environmental performance. The complexity of the problem is reflected in the fact that ports interface with both sea and land, and therefore serve as a connection between marine and terrestrial interactions (Green Port, 2015).

Therefore, this paper aims to confirm the adequacy of multi-criteria analysis for the evaluation of the most viable investments as part of the green port management concept and energy-efficient mobility. To fulfill the research aim, a model that includes criteria for energy-efficient mobility selection is set. This paper analyses which of the proposed development concepts is the most suitable for the two selected case study areas. The criteria model and methodology used are developed as part of the DEEP-SEA project – "Development of Energy Efficiency Planning and Services for the Mobility of Adriatic MARINAs" (DEEP-SEA, 2020).

This paper uses the developed model criteria and tests them on marinas that are not engaged in project partnership. The secondary goal of this study is to demonstrate the possible application of the developed methodology in other areas and locations. The case study areas considered include two privately managed ports which are within close vicinity to each other (Marina Kaštela and Marina and Yacht Service Center Trogir).

The structure of the paper is as follows. After the Introduction section, a *Background* section on the green port management concept in marinas is presented. This section also deals with the pressures of nautical tourism on the environment, and provides the best port practices and policies in nautical port management and their possible implementation in small ports. The next section, *Methodology*, includes a short overview of the application of multi-criteria analysis and the theoretical background of the PROMETHEE method implemented. To carry out the multi-criteria analysis process in this research, the Visual PROMETHEE 1, Academic Edition, software was used. The next two sections are the central parts of the paper, where the *Model for the evaluation and comparison of energy efficient mobility in nautical ports* section presents a model for the evaluation and comparison of energy-efficient mobility in nautical ports. Meanwhile, *The application of MCA for the evaluation of energy efficient mobility actions in nautical ports* section brings the results of the application of MCA for the evaluation of energy-efficient mobility actions in the selected study area. The final section, *Conclusions*, provides a discussion and the concluding remarks for the applied method and obtained results.

Background: green port management concept in marinas

Both types of nautical ports, public ports open for international traffic and private marinas, share the same responsibility to achieve acceptable management standards. The term "green port" relates to sustainability in the context of the maritime industry. Adoption of green initiatives represents a decisive role in the further evolution of the sustainable port concept (Beškovnik & Bajec, 2014).

In general, this term means the production of a long-term strategy for the sustainable and climate-friendly development of the port's infrastructure (Pavlic et al., 2014). However, in practice, a green port is a synonym for the responsible behavior of all stakeholders in the port business, from the individual employees, port managers, port users and the local population. According to The World Association for Waterborne Transport Infrastructure (PIANC), the concept of a green port and a green energy policy means a "shift of thinking", moving away from a reactive approach, and towards a proactive approach with a focus on the long-term vision rather than on short-term thinking.

The key elements part of the green port management concept are (PIANC, 2014):

- A long-term vision towards an acceptable footprint on the environment and nature;
- Transparent stakeholder participation and stakeholder approved strategies;
- Shift from sustainability being a legal obligation to an economic driver;
- Active sharing of knowledge with other ports and stakeholders;
- Continuous striving towards innovation in processes and technology.

One of the key issues of this concept is energy efficiency, or the process of shifting from fossil fuels towards clean fuel sources and renewable energy sources. This influences different players in the nautical tourism sector to act accordingly, namely: Port authorities (including local and/or regional administrations which act as a port authority) – to make a shift from traditional to proactive green port and green energy approaches; Public authorities – to recognize the need of port managing authorities and to support the change; Marina operators – to plan and incorporate sustainable design principles and technologies in development projects and innovative energy-efficient services; Financial institutions – to support the development of green port infrastructure and green services in marina development projects; NGOs – to disseminate the idea and validate implemented results; Researchers – to share the knowledge on innovative technologies, their application, and benefits for the community.

Ports that aim to achieve a "green port" status should establish a system for monitoring energy consumption as well as the overall environmental quality monitoring. Sustainable development also requires a change or upgrade in current port policies and strategies to understand new opportunities, such as the exploitation of alternative fuels and renewable energy sources, can benefit the port. The joint effort of all port and marina stakeholders, as well as the local community, is crucial for the adoption of these changes. Implementation of green-port concepts and practices must be followed by the implementation of energy and Environmental Management Systems (EMS) to enable a port's management to follow accepted decisions, adopt the implementation strategies, and monitor performance (Pavlic et al., 2014).

To improve environmental and energy performance in ports, the European Sea Ports Organization (ESPO) laid down group of actions structured on a "5E" framework which includes following: exemplifying (setting a good example in the port community when managing own operations); enabling (providing conditions for facilitating port users and improving environmental performance within the port area); encouraging (providing incentives to greener port users); engaging (sharing knowledge, means and skills between port users and/or competent authorities); enforcing (using mechanisms to enforce effective environmental practices by port users and ensuring compliance). These pillars may also be used as a guideline for small public nautical ports and marinas as well (ESPO, 2012).

Pressures of the nautical tourism sector and response measures

Generally, the maritime industry generates about 3% of worldwide CO_2 emissions. Boats, yachts, other pleasure crafts and cruisers, as well as maritime tourism activities, contribute to these emissions to some extent. The pressure on coastal areas of the Adriatic Sea is extensive during the summer season. Consequently, reducing Greenhouse gas (GHG) emissions and dependences on fossil fuels, as well as shifting to renewable energy sources is big challenge for the sector. Marinas and nautical public ports are isolated in this matter and should follow common strategies for reducing their impact.

The major issues for this matter are two-fold: 1) how to reduce energy consumption and energy costs while also increasing the efficiency of port activities, and 2) how to develop long-term renewable energy sources. Marine activities have seasonal characteristics, with peak-traffic and energy consumption demands during the summer months. Furthermore, renewable energy sources like solar and wind are unlikely to provide a continuous and secure energy supply. Developing smart grid networks with buffers such as energy storage utilities, can contribute to efficient energy production and bring flexibility in balance between energy supply and demand.

To cope with these challenges, it is necessary to understand what the response options from a port's management perspective are. These options include actions that contribute to better environmental and energy management, and actions to take advantage of available technologies and services.

Where management is concerned, it is necessary to set-up good information sources based on the identification of GHG emissions and energy consumption sources, and their quantities. Then, measurement and control systems should be established. Some ports prepare so called inventories on emissions and fuel consumption as part of their first action for achieving their goals. Another area of action on the management level may be the improvement of port traffic management. Where the reduction of boat speed, reduction of waiting time for boat services, control of inbound and outbound traffic and introduction of smart berth management systems, may contribute to efficient use of energy and less air pollution. Furthermore, an Energy Management Plan should be prepared and adopted, acting as roadmap for implementation of the green port strategies to achieve an energy efficient port system.

Overview of green port initiatives in marina industry

Implementation of different environmental initiatives have proved beneficial for the development of further ports. Some of the initiatives are easily adopted, and some of them require significant investment, but all the initiatives can be divided into the following groups (Beškovnik & Bajec, 2014):

- Green shipping, with the use of green ships;
- Energy consumption and recycling processes;
- Water and land quality;
- Sustainable and clean manipulation and internal transport;
- Sustainable hinterland transport;
- Sustainable accompanying actions in port development, such as dredging, maintenance, etc.;
- Improvements in community and environmental involvement.

Furthermore, to monitor adopted initiatives by the ports, different certified measures can be used, such as: ISO9001 (Quality Management System); ISO 14001 (Environmental Management System). ISO26000 (Social Sustainability); SDM – Self Diagnosis Method; PERS – Port Environmental Review System, which incorporates the general requirements from the ISO14001 standard but adapted to the port management needs and port objectives; EMAS – European Union's Eco-Management and Audit Scheme; Port-Index – developed by ESPO (Adams et al., 2009).

Besides general quality standards and certification systems targeting impacts of activities, there are business driven initiatives which aim to evaluate the quality of operation and services of the marina industry. Compliance with such schemes is optional and involves various quality standards (e.g. water quality, safety and services, tranquility, respect of the environment, energy consumption, etc.). Participation in certification and quality labels increases the number of port visitors and helps distinguish a marina from others by ensuring that its services or locations are of a particular quality.

One of the initiatives of quality labels which exist in the marina industry, and challenges local authorities to achieve higher standards in predefined criteria, is The Blue Flag Program. The Program defines the criteria and requirements for its implementation, covering water quality, environmental management, environmental education and information, safety and services, which a marina needs fulfil in order to be awarded with the Blue Flag certification (Blue Flag, 2020). All Blue Flag marinas can only obtain certification for one season at a time, where for example, in 2019, 27 Croatian marinas were awarded with the Blue Flag. This award indicates that the sea water is clean, the marina has an environmental management plan, it performs certain activities to raise environmental awareness, it has the equipment to meet these needs, and it ensures users' safety. Therefore, obtaining the Blue Flag certification is now characterized as a brand, or an "Eco-Label" (Font, 2002).

Furthermore, the Gold Anchor scheme is another initiative, which provides a template for a customer friendly marina. The link between the Blue Flag, ISO standards and Gold Anchor Scheme is to provide all environmental aspects of a marina's activities, using a logical objective methodology to rank such aspects

by their impact on the environment (Gold Anchor, n.d.).

Other programs such as The Blue Star Marina Certification and ADAC Ship's Wheel marina rating system are also used to indicate the quality of certified marinas and services.

Methodology

Ports and marinas are striving for new renewable solutions to improve their services. Each marina has different investment needs and priorities, depending on various factors, such as: how developed the port and its infrastructure is; the need for the improvement of the services for end-users. The in-sight analysis of marinas, which are involved in the DEEP-SEA project identified the need for marinas to make investments regarding energy savings, environmental protection, nautical capacities and infrastructure, and the improvement of the services for end-users. The analysis of investment needs and investment priorities of marinas point out the focus on several sustainability issues: energy resources, environment protection, and sustainable mobility. As part of these needs and priorities, regarding energy resources, marinas are prioritizing investments in energy-saving devices (microgrid, e-charges, LED, solar power…). Meanwhile, for their sustainable mobility goals, getting more e-bikes, e-boats, e-vehicles are a priority (DEEP-SEA, 2020). On top of this, marinas would like to improve their infrastructure and provide more services for users. All these aforementioned measures are decisive in order for marinas to become "Green Marinas".

To implement energy-efficient actions, marinas require a clear, defined strategy and a scenario development is needed. As part of the planning for the sustainable development of energy mobility actions it is necessary to estimate the impacts of each action that would need to be carried out. Within the DEEP-SEA project, these actions were defined during pilot site testing and considered the following activities: investment in facilities, equipment, and e-mobility services. As a result, this paper aims to confirm the adequacy of multi-criteria analysis as a suitable tool to be used as an ex-ante evaluation of the opportunity and impacts estimated by the stakeholders and marina experts.

The application of Multi-Criteria Analysis

Multi-Criteria Decision Analysis, or Making (MCDA/MCDM), is a branch of operation research models and a well-known field of decision making. According to (Belton & Stewart, 2002), MCDA is "an umbrella term to describe a collection of formal approaches which seek to take explicit account of multiple criteria in helping individuals or groups explore decisions that matter". Multi-criteria analysis is a method that is used to solve complex problems, which in most cases consist of contradictory criteria, and different, quantitative and qualitative measures (Deluka-Tibljaš, Karleuša & Dragičevič, 2013; Vilke, Krpan & Milković, 2018).

In the area of multi-criteria decisions, there are two main categorizations of multi-criteria problems (Mendoza & Martins, 2006; Deluka-Tibljaš, Karleuša & Dragičevič, 2013):

- Multi-Attribute Decision Making (MADM), or Multi-Criteria Analysis, which is suitable for so-called "ill-structured problems". In these problems, the objectives are very complex, often unclearly formulated with numerous uncertainties, and the nature of the observed problem is gradually changing over its resolution. MCA functions via the use of a limited amount of previously known alternatives that have to be evaluated and ranked. The problem is solved by finding the best variant, or a set of good variants, concerning the defined attributes/criteria and their weight;
- Multi-Objective Decision Making (MODM) is suitable for well-structured problems. Calculation of a set of unlimited feasible alternatives gives an optimal solution. Unlike predetermined alternatives in MADM, the alternatives in MODM are a set of functions that are optimized according to certain conditions.

To summarize, MCA can be defined as a decision model which contains (Hajkowicz & Collins, 2007):

1) A set of decision options (variants are ranked and scored by the decision maker(s));
2) A set of criteria (typically consisting of multi-dimensional criteria which can only be measured and evaluated in different units);
3) A set of performance measures, which represents the scores for each decision option against each criterion.

MCA/MCDM has been implemented across various application areas solving a wide range of problems like selection, sorting, and ranking (Mladineo, Jajac & Rogulj, 2016).

As energy issues and the sustainable development of energy supply systems are usually complex and involve dealing with uncertainty and different stakeholders, multi-criteria decision analysis represents a suitable decision tool (Løken, 2007;

Braune, Pinkwart & Reeg, 2009). Furthermore, another important aspect of energy planning also regards both ecological and social criteria. These types of criteria are difficult to measure, so, through relative scales, expert opinions can be quantified and included in the decision process (Braune, Pinkwart & Reeg, 2009). The most common multi-criteria decision methods used in energy planning literature are: Analytic Hierarchy Process (AHP), Weighted Sum model (WSM), PROMETHEE, ELECTRE, MAUT, fuzzy methods and decision support systems (DSS) (Pohekar & Ramachandran, 2004). These methods can handle both quantitative as well as qualitative criteria and analyze the conflict between criteria and decision makers.

The theoretical background of the PROMETHEE method

The PROMETHEE (Preference Ranking Organization METHod for Enrichment Evaluations) method, developed by J.P. Brans and B. Mareschal in 1983, represents one of the most noteworthy methods for MCA (Mareschal, Brans & Vincke, 1984).

The main input of the PROMETHEE method, for a multi-criteria ranking, is a matrix which consists of a set of potential alternatives (actions), A, where each element of A has its own evaluation, f (a). The PROMETHEE I method allows the partial ranking of variants, where the different variants can have the same rating, which allows the utilization of certain ranks.

Because this method allows both the partial and complete ranking of a large number of alternatives, the PROMETHEE II method is mostly used in practice, due to concern when a larger number of criteria are involved. The PROMETHEE II method ranks the actions according to a complete ranking; i.e. each variant is ranked in dependence on the function of preference (Mladineo, Jajac & Rogulj, 2016; Vilke, Krpan & Milković, 2018).

For each solution $a \in A$, the net flow is:

$$\phi(a) = \phi^{+}(a) - \phi^{-}(a) \tag{1}$$

and for the solution ranking, it could be applied that:

- a has a higher rank than b:

$$(aP^{(2)}b) \quad \text{if} \quad \phi(a) > \phi(b) \tag{2}$$

- a is indifferent to b:

$$(aI^{(2)}b) \quad \text{if} \quad \phi(a) = \phi(b) \tag{3}$$

According to (Yu, Chen & Ji, 2019), "as the PROMETHEE is very easy and transparent, it can be easily understood by decision-makers. The method can offer reasonable ranking of all alternatives. Therefore, they are widely adopted in energy projects regional tourism competitiveness, and airport location selection".

Model for the evaluation and comparison of energy efficient mobility in nautical ports

Multi-criteria analysis requires decision-makers to consider different impact areas for certain solutions. The impact area of the green port management concept is represented by thematic groups of criteria. To set up a model for the evaluation and comparison of energy-efficient mobility solutions to be implemented into the green port management concept, the criteria group and sub-criteria have to be defined.

The impact area (i.e., the criteria groups for the evaluation and comparison of energy-efficient mobility solutions) in this study, was divided into four thematic groups that are divided into less complex components or sub-criteria. The model for energy-efficient mobility solutions, that include the thematic groups of the criteria and sub-criteria for evaluation, is shown in Table 1.

As seen, the defined sub-criteria for evaluation and comparison of different solutions are divided into four criteria groups or impact areas: environmental, economic, technical, and social. The economic group of criteria comprises six sub-criteria, while the other three thematic groups include four sub-criteria which are relevant for the solution evaluation. A description and explanation for each of the sub-criteria is also presented in Table 1.

In the second phase, the defined model must be evaluated by experts in the management of nautical ports. In this phase, the experts thus settle the importance of the thematic criteria and sub-criteria groups by assigning weighting coefficients (i.e., coefficients of importance). According to the information obtained from experts, the importance of the criteria groups is mutually compared. Meanwhile, the weighting coefficients for these groups are normalized so that their sum amounts to 100%. Furthermore, the weighting coefficients of the sub-criteria within a certain group are also normalized so that the total possible sum within each group is also 100%.

By analyzing the potential solutions to be assessed, and to ensure the implementation of the green port management concept, four possible actions for energy-efficient mobility were selected. Each of them

Table 1. Criteria group and sub-criteria explanation for the evaluation and comparison of energy efficient mobility solutions (prepared by authors – developed within DEEP SEA project)

Criteria group	Sub-criteria	Abb	Description
Environmental	GHG emission reduction	ER	Criteria reflect on the potential of CO_2 emissions reduction as a result of the implementation of a specific action. It analyses the difference in the emissions level before and after the action has been implemented.
	Noise reduction	NR	Criteria reflect on the reduction of noise as the result of the action, mostly caused by maritime or road traffic and operations.
	Spatial impact	SI	Criteria express the impact of the action on land usage, layout occupancy requirement, space limitation, conflict with other activities, and similar issues that may complicate the implementation of the action.
	Reduction in energy consumption	CR	Criteria consider the reduction in energy consumption as the result of the action, mostly as the result of the implementation of the new source of energy or savings resulted from the implementation of new technologies in energy production.
Economical	Cost levels	CL	Criteria consider the overall costs required for the construction and implementation of a specific action. It focuses on cost levels to be estimated according to the expectation and complexity of the investment.
	Cost effectiveness	CE	Criteria is evaluated according to the relationship between monetary inputs and the expected outcome concerning the specific objectives.
	Seasonal dependency	SD	Criteria measures the seasonal dependency of the action. It is generally better that the benefits are equally distributed throughout the year and not limited to the seasonal period.
	Development of business activities	BA	Criteria express the possibility of the expansion of economic activities in the nearby zone as a result of the action.
	Profitability levels	PL	Criteria estimate the profitability levels resulting from the action, or to what extent the action may result in an increment of the profit.
	Funding opportunities	FO	Criteria aim at considering the potential to support the action with a feasible source of funding. If the indicator is low then the action may have financial constraints.
Technical	Mobility benefit	MB	Criteria measure the benefits of improved mobility resulting from the action. It may be improved by introducing new services or by facilitating traffic movements.
	Quality of service impact	QS	Different impacts on service quality may result from the implementation of the action. The target groups are a nautical tourist and other marina end-users.
	Technical feasibility	TF	Criteria consider the technical aspects of the action, where it is assumed that the feasibility is in co-relation with the complexity of the investment, less complex action means higher technical feasibility.
	Implementability	IM	Criteria refer to the capacity of the stakeholders involved in the implementation of the action. It considers potential difficulties, barriers, or conflicts that may occur during the implementation of the action.
Social	Contribution to local/ regional development	RD	Criteria focus on the effect on local and regional socioeconomic life activities. It aims at considering the change of dynamics and the potential increase for socio-economic growth in the future.
	Stakeholder acceptance	SA	Criteria reflect the overview of opinions related to the energy-efficient systems and e-services by the local stakeholders and expectations from the action.
	Social consciousness	SC	Criteria measure the opportunity to change the social awareness toward energy efficiency and e-services resulting from the action.
	Enforceability	LE	Criteria focus on the legal basis for enforcement of the implemented action. It aims to evaluate whether the action is supported by an existing legal framework and whether there is an authority responsible for implementing the action.

is defined by the criteria groups, sub-criteria, and weighting coefficients. The four actions chosen for multi-criteria analysis are:

1. Electric charging stations (ECS) for boats/vessels;
2. Electric charging stations (ECS) for cars;
3. E-mobility & sharing services;
4. Micro-grid systems.

It must be also kept in mind that any other alternative solutions for improving the energy efficiency and mobility services in a nautical port may also be added and evaluated through this multi-criteria optimization method, depending on the interest of port stakeholders. The purpose of the multi-criteria analysis is to show the opportunity and direction of the

solutions for improving the green port management concept, rather than to choose only one solution with the best result. Furthermore, the most valuable result is achieved when the score is analyzed against different weighting values concerning the strategy and objectives of the nautical port operator.

The application of MCA for the evaluation of energy efficient mobility actions in nautical ports

To optimize the evaluation of energy-efficient actions a process of a multi-criteria ranking of the variants was applied via the so-called PROMETHEE II method, using a computer program for multi-criteria programming, named "Visual PROMETHEE".

Through the use of this software, the multi-criteria analysis for the evaluation and comparison of energy-efficient mobility actions was conducted in four phases in the following order:

1. the determination of the actions for energy-efficient mobility,
2. the evaluation of the actions in accordance with the criteria group and sub-criteria,
3. the comparison and ranking of the options, i.e. the evaluation of the defined actions,
4. the decision-making for the optimal solution for the nautical port.

For the application of the MCA optimization method in this study, two nautical ports were chosen: marina Kaštela and marina Trogir. Each nautical port compares the defined actions to the defined criteria groups. To perform the optimization method for the evaluation and comparison of energy-efficient mobility actions, each criteria group as well as each sub-criterion should be evaluated by assigning weighting coefficients, as explained in the previous section.

In the last step, to evaluate the performance of the action, all the defined criteria in each group explained in Table 1. have to be evaluated by marinas according to a qualitative scale. The evaluator uses the qualitative scale of indicators with ratings from 1 to 5, where 1 is the lowest value and 5 is the highest value.

Description of study areas: Marina Kaštela and Service Center Trogir-Marina Trogir

Marina Kaštela, the first case study considered, is a privately managed marina situated on the south east side of Kaštela Bay, which is shielded from the north by Kozjak Mountain and guarded by the Marjan Peninsula and the Čiovo Peninsula on the bay's southern side. The marina has an outstanding geographical position in the central Adriatic with great connections by air, railroad, bus, and ferry. Marina has 420 berths, each with electricity and water supplies (depth from 2.5 to 8 meters – 8 to 26 feet inside the marina, 10 meters – 33 feet on the outer side of the peer for mega yachts), and 200 dry berths for ships on land. Except for general services, an affiliated charter company is situated in the marina (Marina Kaštela, 2020).

Regarding the second case study marina, Service Center Trogir-Marina Trogir is located in the central part of the Adriatic coast, in a protected bay which is surrounded by numerous islets and walls of the ancient town of Trogir. The marina offers 260 sea berths for all types of vessels ranging from 10 m to 60 m in length. During the winter months, the marina has 20,000 m^2 at its disposal for storing 150 vessels (10–50 m length). Except for general services, Service Center Trogir provides complete and high-quality outboard motor servicing for all types of vessels. The Marina's business activities are certified by ISO 9001 and ISO 14001 standards (Service Center Trogir, 2020).

By using computer software, and the aforementioned case studies, an optimal solution regarding the green port management concept was selected.

To select the optimal action from the four proposed solutions, the values of the criteria obtained from the marina management interview were entered in the computer program "Visual PROMETHEE". Furthermore, the values of the importance of certain criteria groups and the criteria evaluated have also been included. Where, the importance of a certain criteria group, the sub-criteria, and the values of the attributes of individual criteria for the four defined actions will be used as input data.

Results

The results from the interviews show that both marinas give the greatest impact to the economic criteria group (value of 50%). In second place is the environmental criteria group (value of 30% for the Marina Trogir and value of 35% for Marina Kaštela). For the social impact criteria group, both marinas gave the same results (value of 10%), while for the technical group there was a slight difference (Marina Kaštela scores with 5% of impact and Marina Trogir with 10%). This shows that in this scenario, private port operators give the majority of the importance to the economic impact. To further assess this outcome,

Rank	Car	Phi	Phi+	Phi−
1	ECS cars	0.1700	0.3650	0.1950
2	E-mobility/sharing	0.0267	0.2283	0.2017
3	ECS boats	−0.0067	0.2167	0.2233
4	Micro-grid systems	−0.1900	0.1833	0.3733

Rank	Car	Phi	Phi+	Phi−
1	ECS cars	0.1600	0.3650	0.2050
2	E-mobility/sharing	0.0267	0.2317	0.2050
3	ECS boats	0.0033	0.2267	0.2233
4	Micro-grid systems	−0.1900	0.1867	0.3767

Figure 1. An overview of the result of the multi-criteria analysis for the evaluation of energy efficient mobility actions in the nautical port Kaštela (left) and marina Trogir (right)

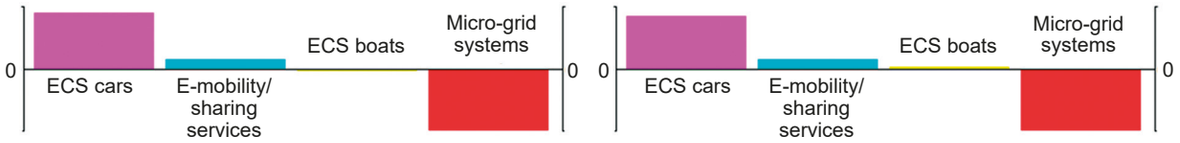

Figure 2. An overview of the multi-criteria analysis for the evaluation of energy efficient mobility actions in the nautical port Kaštela (left) and marina Trogir (right)

a sensitivity analysis could be performed for port strategies and development objectives.

The multi-criteria optimization method PROMETHEE I calculated the Phi values of two preference flows (Phi+ and Phi−) (i.e., the relations of the dominance of certain pairs of actions). The PROMETHEE II gave the final rankings for the actions based on the net preference flow (Phi).

In Figure 1, the obtained results for each individual energy-efficient mobility action and their positive and negative values of Phi are shown. Figure 2 brings a graphic overview of the numerical values of net flows.

From the above-presented results, the ranking of analyzed energy-efficient mobility actions is similar for both marinas. The Electric charging stations (ECS) for cars, with a value of the net flow of 0.17 (Kaštela) and 0.16 (Trogir), is the most highly ranked action; while E-mobility and sharing services take second place, with a net flow ranking of 0.0267 for both marinas. The differences between marinas is highlighted for the action which can in third place. While the results for Marina Trogir for the Electric charging stations (ECS) for boats were close to zero (0.0033), but positive, the results for Marina Kaštela expressed negative results with a net flow of −0.0067. The final action (micro-grid systems), expressed negative values for both marinas, with a net flow of −0.1900. From the elaborated results, the most suitable action (for both marinas), which presents no weaknesses with respect to the other actions, is the electric charging stations (ECS) for cars. Where, of course, the final choice according to the set goals is dependent on the decision-maker.

To provide detailed insight into the problem of choosing an appropriate energy-efficient mobility action, the GAIA ("Geometrical Analysis for Interactive Aid") plane was used as a descriptive complement to the PROMETHEE rankings. It functions via a standard two-dimensional GAIA plane, and a direct interpretation of a multiple-criteria analysis in a "u, v" can be made. Also, on the plane, both, the actions and criteria are visible, and so an analysis of the conflicting criteria can be carried out significantly faster. Each criterion is represented by an axis drawn from the center of the GAIA plane. Criteria that express similar preferences are grouped together with each other, while the conflicting criteria are in opposite directions (dispersed). The same applies to the actions (i.e., actions with similar numerical characteristics will be closer to each other).

Again, and as seen in Figure 3, the best results are shown for the "ECS for cars" action for both marinas. This was largely as a result of the higher weighting of the economic criteria, which includes cost-effectiveness, development of business activities, profitability levels, funding opportunities, investment and operation cost level, and seasonal dependency; where as seen previously both marinas prioritized the economic criteria group. Similarly, the "ECS for cars" option also scored the highest for the environmental section (second highest weighting) for the Marina Trogir results.

The direction of the majority of the "ECS cars action" criteria vectors for both marinas, implies its dominance over the other energy-efficient mobility actions. Also, the direction of the decision axis (red vector) for both marinas, prioritizes "ECS cars action" over the other options. It must also be noted that the vector axes of individual criteria are dispersed (i.e., they influence the respective action with different intensities). Where, the closing or conflicting sub-criteria equally affect the respective action.

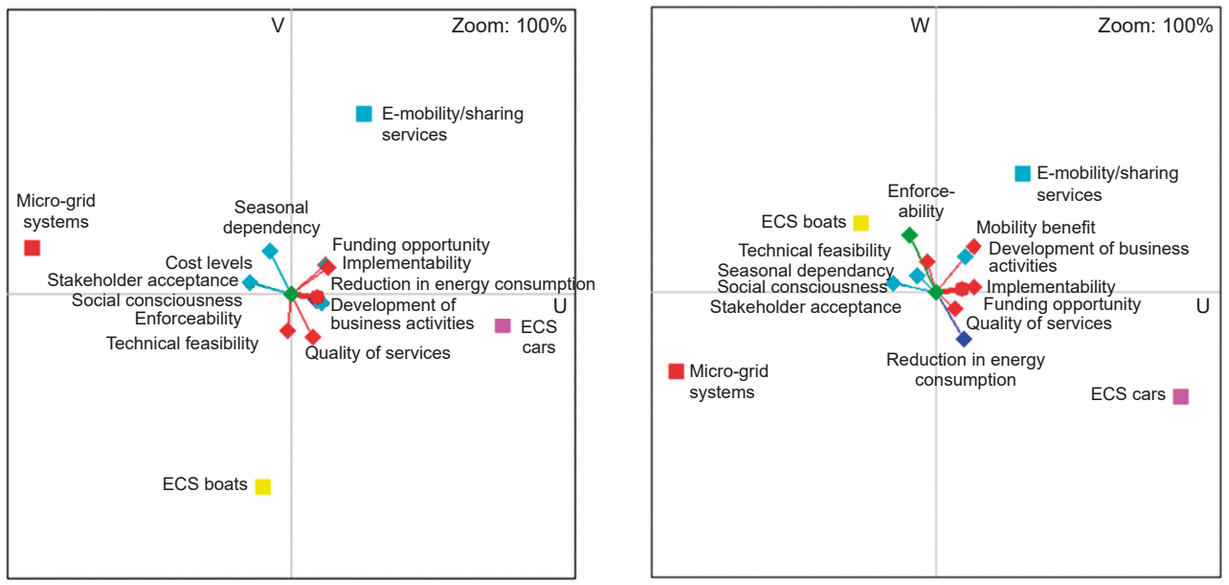

Figure 3. An overview of the multi criteria analysis in the GAIA plane for the Marina Kaštela (left) and Marina Trogir (right)

Conclusions

Many port authorities are now implementing Environmental Management Systems (EMS) to systematically and sustainably manage their seaports. A major, current priority for the environmental management of marina infrastructures is to minimize consumption, especially of water and electricity, and prevent water and air pollution; without compromising user comfort. As a result, the basic requirements of EMS for marinas are typically based on standards, such as ISO 14001, EMAS, and the PERS methodology.

Port development strategies are one of the key issues involved in their management planning. And when the "greening" concept is included as part of a port's strategic development, its effectiveness and success depend on the tools adopted by the port authorities and/or administrations. According to (Lam & Notteboom, 2014) each management authority may choose one or several tools among the following: charging and pricing; monitoring and measuring; market access control; environmental standard regulation.

Different modes of marina management and diversity in marina establishment and organization impose differences in objectives, functions, market position, competencies, and investment capabilities. That is also a case with environmental and energy considerations, depending on the specific location and characteristics of each marina.

As marinas are decisive in their goal to become "Green Marinas", further investments regarding energy saving and environmental protection are needed. To properly invest in energy-efficient solutions it is necessary to estimate the impacts of the actions which need to be carried out. As part of this, the evaluation of the energy-efficient mobility actions can be done with Multi-Criteria Analysis, as confirmed in the present study. As part of this study, the defined criteria groups for the MCA evaluation and the comparison of energy-efficient mobility solutions have been done based on the information collected for the case studies considered, including from representatives of the two case study marinas, experts, scientific researchers, and other relevant stakeholders in the marina industry. Analyzing the obtained MCA results, for the introduction of the energy-efficient mobility actions in nautical ports, both marinas gave priority to electric charging stations (ECS). These results were derived from the higher-weighted economic criteria in the model developed, which includes cost-effectiveness, development of business activities, profitability levels, funding opportunities, investment and operation cost level, and seasonal dependency considerations. This study also provides a characteristic scenario for private port operators; who give major importance to the economic impact of green port management practices.

A multi-criteria-based optimization model, such as the one used in this study, which includes criteria for energy-efficient mobility selection, can also be applied in other nautical ports where new solutions are needed to improve energy efficiency and mobility services. This model can assist decision-makers in

port authorities and marina administrations in planning and finding the best scenario for the development of energy-efficient systems and services. The background goal of the paper, which included the testing of the model on more than one study area, was also achieved.

Finally, it is important to highlight that both types of nautical ports (public ports and private marinas) share the same responsibility to achieve acceptable management standards. This means that both business and industry growth targets, and social and environmental acceptability, should be achieved through sustainable development. Ports are not just service providers, but also energy consumers and potential energy production centers.

Acknowledgments

The submitted paper was prepared within the framework of the project Development of Energy Efficiency Plan and SErvices for the mobility for the Adriatic MARINAs (DEEP SEA), No. 10047821. The Interreg HR-ITA 2014/2020 is the Program's main coordinator.

References

1. Acciaro, M., Ghiara, H. & Cusano, M.I. (2014) Energy management in seaports: A new role for port authorities. *Energy Policy* 71, pp. 4–12; doi: 10.1016/j.enpol.2014.04.013.
2. Adams, M., Quinonez, P., Pallis, A.A. & Wakeman, T.H. (2009) Environmental issues in port competitiveness. Working Paper No. 7 of the Atlantic Gateway Working Paper series. Dalhousie University, Centre for International Trade and Transportation, Halifax, Canada, January.
3. Belton, V. & Stewart, T.J. (2002) *Multiple Criteria Decision Analysis*. Springer: Boston, MA; doi: 10.1007/978-1-4615-1495-4.
4. Beškovnik, B. & Bajec, P. (2014) Determination of environmental initiatives and measures for port systems: The case of Koper Port. *Scientific Journals Maritime University of Szczecin, Zeszyty Naukowe Akademia Morska w Szczecinie* 39 (111), pp. 16–24.
5. Blue Flag (2020) *Blue Flag marina criteria and explanatory notes 2020*. [Online] Avaliable from: https://www.blueflag.global/criteria [Accessed: December 09, 2020].
6. Braune, I., Pinkwart, A. & Reeg, M. (2009) *Application of multi-criteria analysis for the evaluation of sustainable energy systems – A review of recent literature*. In Proceedings of 5th Dubrovnik Conference on Sustainable Development of Energy, Water and Environment Systems.
7. DEEP-SEA (2020) *Development of Energy Efficiency Planning and Services for the Mobility of Adriatic MARINAs*. [Online] Avaliable from: https://www.italy-croatia.eu/web/deep-sea [Accessed: December 09, 2020].
8. Deluka-Tibljaš, A., Karleuša, B. & Dragičevič, N. (2013) Pregled primjene metoda višekriterijske analize pri donošenju odluka o prometnoj infrastrukturi. *Gradjevinar* 65, 07, pp. 619–631; doi: hrcak.srce.hr/106196.
9. EBI (2020) *European Boating Industry*. [Online] Avaliable from: https://www.europeanboatingindustry.eu/ [Accessed: December 09, 2020].
10. ESPO (2012) Annex 1: Good practice examples in line with the 5 Es. In *ESPO Green Guide: Towards excellence in port environmental management and sustainability*. [Online] Avaliable from: https://www.espo.be/publication/espo-green-guide-towards-excellence-in-port-enviro [Accessed: December 09, 2020].
11. ESPO (2019) *EcoPortsinSights 2019*. ESPO Environmental Report 2019. [Online] Avaliable from: https://www.espo.be/media/Environmental%20Report-2019%20FINAL.pdf [Accessed: December 09, 2020].
12. EU (2002) Directive 2002/49/EC of the European Parliament and of the Council of 25 June 2002 relating to the assessment and management of environmental noise – Declaration by the Commission in the Conciliation Committee on the Directive relating to the assessment and management of environmental noise. *Official Journal of the European Union* L 189.
13. EU (2005) Directive 2005/35/EC of the European Parliament and of the Council of 7 September 2005 on ship-source pollution and on the introduction of penalties for infringements. *Official Journal of the European Union* L 255/11.
14. EU (2009) Directive 2009/28/EC of the European Parliament and of the Council of 23 April 2009 on the promotion of the use of energy from renewable sources and amending and subsequently repealing Directives 2001/77/EC and 2003/30/EC. *Official Journal of the European Union* L 140/16.
15. EU (2014) Directive 2014/94/EU of the European Parliament and of the Council of 22 October 2014 on the deployment of alternative fuels infrastructure. *Official Journal of the European Union* L 307/1.
16. EU (2015) Regulation (EU) 2015/757 of the European Parliament and of the Council of 29 April 2015 on the monitoring, reporting and verification of carbon dioxide emissions from maritime transport, and amending Directive 2009/16/EC. *Official Journal of the European Union* L 123/55.
17. EU (2016) Directive (EU) 2016/802 of the European Parliament and of the Council of 11 May 2016 relating to a reduction in the sulphur content of certain liquid fuels. *Official Journal of the European Union* L 132/58.
18. EU (2019) Directive (EU) 2019/883 on port reception facilities for the delivery of waste from ships. *Official Journal of the European Union* L 151/116.
19. Font, X. (2002) Environmental certification in tourism and hospitality: Progress, process and prospects. *Tourism Management* 23, 3, pp. 197–205; doi: 10.1016/S0261-5177(01)00084-X.
20. Gold Anchor (n.d.) *Gold Anchor. General Infomation and Application Form*. [Online] Avaliable from: https://www.marinas.net.au/documents/item/7 [Accessed: December 09, 2020].
21. Green Port (2015) *KPIs and measuring environmental performance*. [online] Avaliable from: https://www.greenport.com/news101/Projects-and-Initiatives/kpis-and-measuring-environmental-performance-at-ports-and-terminals [Accessed: December 09, 2020].
22. Hajkowicz, S. & Collins, K. (2007) A review of multiple criteria analysis for water resource planning and management. *Water Resources Management* 21, pp. 1553–1566.

23. Lam, J.S.L. & Notteboom, T. (2014) The Greening of Ports: A Comparison of Port Management Tools Used by Leading Ports in Asia and Europe. *Transport Reviews* 34 (2); doi: 10.1080/01441647.2014.891162.
24. Løken, E. (2007) Use of multicriteria decision analysis methods for energy planning problems. *Renewable and Sustainable Energy Reviews* 11, 7, pp. 1584–1595; doi: 10.1016/j.rser.2005.11.005.
25. Longo, F., Padovano, A., Baveja, A. & Melamed, B. (2015) *Challenges and opportunities in implementing green initiatives for port terminals*. 3rd International Workshop on Simulation for Energy, Sustainable Development and Environment, SESDE 2015.
26. Mareschal, B., Brans, J.P. & Vincke, P. (1984) *Prométhée: a new family of outranking methods in multicriteria analysis.* ULB Institutional Repository 2013/9305, ULB – Universite Libre de Bruxelles.
27. Marina Kaštela (2020) *Marina Kaštela official web page*. [Online] Avaliable from: https://www.marina-kastela.hr/ [Accessed: December 09, 2020].
28. Mendoza, G.A. & Martins, H. (2006) Multi-criteria decision analysis in natural resource management: A critical review of methods and new modelling paradigms. *Forest Ecology and Management* 230, 1–3, pp. 1–22; doi: 10.1016/j.foreco.2006.03.023.
29. Mladineo, M., Jajac, N. & Rogulj, K. (2016) A simplified approach to the PROMETHEE method for priority setting in management of mine action projects. *Croatian Operational Research Review CRORR* 7 (2), pp. 249–268; doi: 10.17535/crorr.2016.0017.
30. Pavlic, B., Cepak, F., Sucic, B., Peckaj, M. & Kandus, B. (2014) Sustainable port infrastructure, practical implementation of the green port concept. *Thermal Science* 18, 3, pp. 935–948; doi: 10.2298/TSCI1403935P.
31. PIANC (2014) *Sustainable Ports – A Guide for Port Authorities*. *Raport No. 150*. The World Association for Waterborne Transport Infrastructure.
32. Pohekar, S.D. & Ramachandran, M. (2004) Application of multi-criteria decision making to sustainable energy planning – A review. *Renewable and Sustainable Energy Reviews* 8, 4, pp. 365–381; doi: 10.1016/j.rser.2003.12.007.
33. Sdoukopoulos, E., Boile, M., Tromaras, A. & Anastasiadis, N. (2019) Energy efficiency in European ports: State-of-practice and insights on the way forward. *Sustainability* 11(18), 4952; doi: 10.3390/su11184952.
34. Service Center Trogir (2020) *Service Center Trogir – Marina Trogir*. [Online] Avaliable from: https://sct.hr/ [Accessed: December 09, 2020].
35. UNCTAD (2018) *Review of Maritime Transport 2018*. [Online] Avaliable from: https://unctad.org/system/files/official-document/rmt2018_en_pdf [Accessed: December 09, 2020].
36. Vilke, S., Krpan, L. & Milković, M. (2018) Application of the multi-criteria analysis in the process of road route evaluation. *Tehnicki Vjesnik* 25, 6, pp. 1851–1859; doi: 10.17559/TV-20170530085451.
37. Yu, X., Chen, H. & Ji, Z. (2019) Combination of probabilistic linguistic term sets and PROMETHEE to evaluate meteorological disaster risk: Case study of southeastern China. *Sustainability* 11 (5), 1405; doi: 10.3390/su11051405.

Cite as: Ukić Boljat, H., Vilke, S., Grubišić, N. & Maglić, L. (2021) Application of multi-criteria analysis for the introduction of green port management practices: an evaluation of energy efficient mobility in nautical ports. *Scientific Journals of the Maritime University of Szczecin, Zeszyty Naukowe Akademii Morskiej w Szczecinie* 65 (137), 72–83.

Maritime University of Szczecin

The Maritime University of Szczecin (MUS) continues the tradition of marine-related education at Szczecin's maritime schools that was established in 1947. Since then, it has developed dynamically and maintained the highest standards in all areas of research and education.

MUS is recognized by the maritime industry as an important research centre developing marine engineering, navigation, transportation engineering and many other fields. MUS provide research services by ***Green Energy*** **– laboratory of wind power plants,** ***Marine Fuel and Lubricating Oils Laboratory*****,** ***Maritime Risk Analysis Center*** **and** ***Marine Power Plants Laboratory*****.**

Experts at the University develop innovative concepts like the LNG terminal in Świnoujście. The **European LNG Training Centre** (at MUS) provides the necessary training and awards the required qualifications for operating the terminal LNG equipment and LNG tankers.

The Baltic Fishing Training Centre in Kołobrzeg is a new MUS unit, established in June 2013. There are plans to set up a European Maritime Education Centre in co-operation with other universities of the Baltic states. This project involves two MUS training units, the Marine Traffic Engineering Centre and the Marine Rescue Centre. These units, equipped with several state-of-the-art simulators, will be run a broad training courses for Polish and foreign seafarers of all ranks.

The Marine Rescue Training Centre, one of the largest and best equipped centers of its type in Poland, offers training courses covering areas such as safety, life rescue, health security and environment protection. Participants are trained to respond in extreme emergency situations.

The Training Centre for Marine Officers runs training qualifications and specialized courses for merchant and fishing fleets officers.

The education of mariners calls for thorough onboard seamanship training. Part of this training takes place aboard the modern research-training vessel **Nawigator XXI**.

MUS graduates, with an excellent academic background of theoretical knowledge and practical skills, become specialists recognized in Europe and internationally. At present, students can choose a program at one of our five faculties, all conferring bachelor, master in Polish, or in English (selected programs). Doctoral studies are possible at two faculties: Faculty of Marine Engineering and Faculty of Navigation.

There are five faculties at the Maritime University of Szczecin:

1. **Faculty of Computer Science and Telecommunication**
   The following field of study is available:
   - Computer Science
2. **Faculty of Engineering and Economics of Transport Engineering**
   The Faculty of Engineering and Economics of Transport Engineering offers courses in four major fields:
   - Management and Production Engineering
   - Transport
   - Logistics
   - Management
3. **Faculty of Marine Engineering**
   The following field of study is available:
   - Mechanical Engineering
4. **Faculty of Mechatronics and Electrical Engineering**
   The following field of study is available:
   - Mechatronics
5. **Faculty of Navigation**
   The Faculty of Navigation offers courses in four major fields:
   - Navigation
   - Transport
   - Geodesy and Cartography
   - Naval Architecture

Maritime University of Szczecin provides education to professionals who succeed in finding jobs on the sea and in land. Our graduates are well prepared to meet the requirements of the employment market – English-speaking and equipped with modern knowledge.

Our education programmes comply with requirements of STCW Convention. Our training centres provide continuing education on safety and professional development.

Maritime University of Szczecin
1–2 Wały Chrobrego St., 70-500 Szczecin, Poland
tel. +48 91 4809400, www.am.szczecin.pl

Centrum Innowacji Akademii Morskiej w Szczecinie

The MUS Innovation Centre is a company established by the Maritime University of Szczecin and it was founded in August 2013. We were established in response to growing interest in solutions that arise at the Maritime University of Szczecin – one of leading maritime universities in the world.

Our main goal is to provide these solutions to the market. As an independent company, but working closely with the University, we are your first and last stop on the way to use the knowledge and skills of the university faculty.

Our main task is to commercialize the **results of scientific research and inventions**. We also offer the opportunity to benefit from our **modern laboratories**, **research facilities and highly qualified staff (R&D).**

We are especially interested in collaborations in the following areas:

- **Research, expertise, analysis, opinions, training**
- **Sale of licenses (exclusive and non-exclusive)**
- **Establishing a new company with or without VC/seed involved (spin off, spin out)**
- **Other kinds of IPR sale**
- **Joining consortia with other public and private bodies**
- **Project implementation**

If you have any questions please do not hesitate to contact us. More information about our services can be found on www.innoam.pl.

9/102 Teofila Starzyńskiego St.
70-506 Szczecin, Poland
Tel. +48 531980949

Share capital:
641,000 zł

NIP: 851-317-13-20
REGON: 321422451

Bank account:
79 2490 0005 0000 4600 5640 3049

info@innoam.pl
www.innoam.pl

View publication stats